NASA Electronic Parts and Packaging (NEPP) Program

NEPP Task:

Reliability of Solid Tantalum Capacitors

Alexander Teverovsky

Perot Systems
Code 562, NASA GSFC, Greenbelt, MD 20771

Alexander.A.Teverovsky@nasa.gov

December 2008

Table of Contents

Overview

The NEPP report on reliability of tantalum capacitors published in 2007 was focused on surge current breakdown voltages (VBR_SCT), specifics of the measurement technique, probability of occurrence under multiple surge conditions, and factors affecting distribution of VBR_SCT in different lots. In this year's report, scintillation breakdowns (VBR_scint) and their relation to surge current breakdowns have been analyzed to better understand the breakdown phenomena and their mechanisms and significance for reliability of tantalum capacitors. It has been shown that failures in tantalum capacitors can be considered as time-dependent dielectric breakdowns, and that the failure acceleration factor (AF) depends on the ratio between the operational and breakdown voltages. This provides a physical explanation of the relationship between reliability and rated voltages in tantalum capacitors, and indicates the necessity to have an acceptable level of safety margins between the rated voltage and minimum breakdown voltages in the lot. The effects of environment, including soldering simulation tests, thermal cycling, and humidity testing, have been evaluated using both VBR_SCT and VBR_scint measurements to assess the robustness of tantalum capacitors to environmental stresses and to suggest appropriate test conditions for reliability qualification of the parts. Deficiencies of the existing screening and qualification system per MIL-PRF-55365 have been discussed, and recommendations for improvements have been suggested.

Experiments in this work were performed using various commercial and military-grade solid chip tantalum capacitors. The majority of the parts were leftovers from design and development of space instruments, and the author appreciates the help of NASA Goddard Space Flight Center (GSFC) projects for providing samples for testing.

Part I. Scintillation Breakdowns in Chip Tantalum Capacitors

I.1. Introduction.

Scintillations in solid tantalum capacitors are momentary local breakdowns terminated by self-healing or conversion to a high-resistive state of the manganese oxide cathode. This conversion effectively caps the defective area of the tantalum pentoxide (Ta_2O_5) dielectric and prevents short-circuit failures. Typically, this type of breakdown has no immediate catastrophic consequences and is often considered as a nuisance rather than a failure. Scintillation breakdowns likely do not affect failure of parts under surge current conditions [1], and so-called "proofing" of tantalum chip capacitors, which is a controllable exposure of the parts after soldering them to voltages slightly higher than the operating voltage to verify that possible scintillations are self-healed, has been used to improve the quality of the parts [2]. However, no in-depth studies of the effect of scintillations on reliability of tantalum capacitors have been performed to date. Kemet is using scintillation breakdown testing as a tool for assessing process improvements and comparing quality of different manufacturing lots. Nevertheless, the significance of scintillation breakdowns and their relationship to failures is not clear, and this test is not considered suitable for lot acceptance testing [3].

Military documents and manufacturers' data sheets do not specify breakdown voltages of tantalum capacitors, but it is assumed that the rated voltage (VR) is chosen to be far below the breakdown range. Typically, VR is a portion of maximum formation voltage (VF), which determines the thickness of anodically grown Ta_2O_5 dielectrics and their electrical strength. It is often assumed that VF corresponds to the maximum electrical strength of the part [4], and, respectively, the formation ratio, n = VF/VR, indicates the margin for the operating conditions. However, the value of n varies from manufacturer to manufacturer; depends on the materials and processes used; and steadily decreases over the years, reducing from 4 for parts manufactured more than 20 years ago to ~2.5 for parts manufactured in 2005 [5]. This might be partially due to improvements in the quality of the dielectric, but the wish of manufacturers to increase performance of their product by decreasing the margin is also possible. In any case, the result is uncertainty of the significance of VR, which is determined differently for similar parts manufactured by different vendors, and even for different part types manufactured by the same vendor. This difference in defining VR might explain the fact that in spite of using similar materials and processes, different manufacturers of tantalum capacitors are using different acceleration factors to predict reliability of their product.

Quality and reliability of tantalum capacitors strongly depends on the safety margin between the operating and breakdown voltages. It has been shown that screening out parts with potentially low breakdown voltage (VBR) results in significant reduction of life test failures [6]. Uncertainty in the meaning of VR and its relation to VBR casts some doubt upon the results of reliability estimations. This also reduces the effectiveness of derating, which might be excessive in some cases and insufficient in others. Obviously there is a need in evaluation of breakdown characteristics of tantalum capacitors to assure their quality, especially for high-reliability applications.

Failures of tantalum capacitors can be considered as time-dependent dielectric breakdowns (TDDB) that are caused by field and temperature accelerated degradation of the electrical strength of the Ta_2O_5 dielectric. When a local breakdown occurs, it might create a spike in power supply

lines and thus cause a faulty signal in sensitive detecting systems. In low-impedance applications, the scintillation can be sustained by the power supply, thus preventing self-healing and resulting in a catastrophic failure of the part. TDDB in Ta_2O_5 has been studied using metal-insulator-metal (MIM) and metal-insulator-semiconductor (MIS) structures for dynamic random-access memory (DRAM) applications [7-10] and has been observed in tantalum capacitors [11, 12]. However, the TDDB model has not been used yet to predict failures in chip tantalum capacitors.

In this work, scintillation breakdowns in different military-grade and commercial tantalum capacitors were characterized and related to the rated voltages and to life-test failures. A model for assessment of times to failure based on distributions of breakdown voltages and the thermochemical model of time-dependent breakdowns is discussed.

I.2. Techniques.

Two methods can be used to determine scintillation breakdown voltages in tantalum capacitors. One is based on application of a constant current stress (CCS) while the voltage across the part is monitored. This method has been described in several publications by J. Primak and co-authors, Kemet [3, 13], and is referred to below as the V-t technique. During scintillation, the capacitor discharges momentarily and a voltage drop is observed on the V-t curve. The scintillation breakdown voltage is determined as amplitude of the voltage spike.

Another method, which is essentially a constant voltage step-stress technique, is based on application of a constant, incrementally increasing voltage and monitoring leakage current during a certain period of time. The scintillation event manifests as a current spike on the I-t curve, and VBR is the voltage at which the first current spike is detected. This method is referred below as the I-t technique. Details of the benefits and drawbacks of these techniques are described below.

I.2.1. V-t technique.

When a charging current, I_{ch}, is applied to a capacitor C, having a leakage current I_L, the voltage across the part increases with time:

$$V(t) = \frac{1}{C} \times \int_0^t [I_{ch} - I_L(t)] \times dt \qquad (1)$$

When $I_{ch} >> I_L$, V(t) is a linear function of time: $V(t) = I_{ch} \times t/C$ and the slope of the V-t curve can be used to calculate the value of capacitance C. When charging current is comparable with the leakage current, the V-t curve becomes sublinear and leakage current can be estimated as:

$$I_L(t) = I_{ch} - C \times \frac{dV(t)}{dt} \qquad (2)$$

Figure I.1.a shows typical results of V-t testing for parts having multiple scintillations during the test. For a 15 µF 10 V capacitor, a secondary scintillation occurs at a higher voltage than the first one, Vsc2 > Vsc1, and the electrical strength of the dielectric increases as a result of the first scintillation. For a 100 µF 16 V capacitor, the secondary scintillation occurs at a lower voltage, Vsc2 < Vsc1, and the part apparently degrades after the first scintillation. As no catastrophic failures occur, both parts manifest self-healing, although of different degrees. In the second case the part remains damaged, self-healing is not complete, and the secondary breakdown obviously develops at the same site as the first one.

It should be noted that even when Vsc2 > Vsc1, it is conceivable that the secondary scintillation occurred at the same site as the first one because other sites of the dielectric might have breakdown voltages even greater than Vsc2. In this case, the first scintillation also should be considered as damaging. However, for practical purposes it is important to discriminate among these cases, and in the following analysis such scintillations are considered as non-degrading.

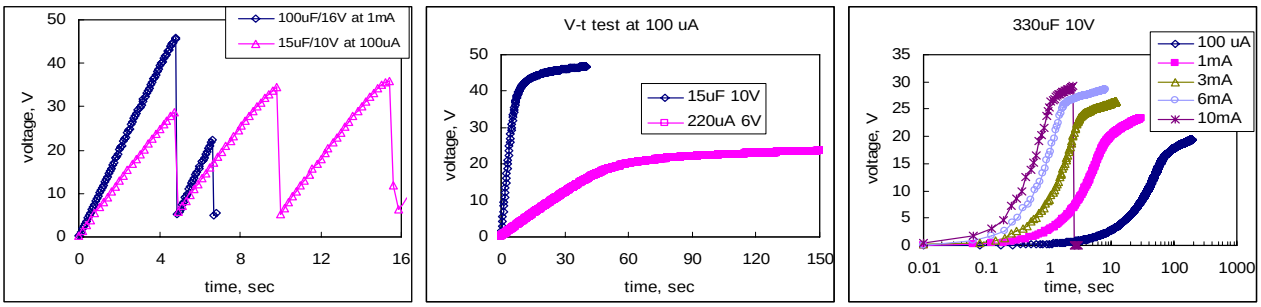

a) b) c)

Figure I.1. Examples of V-t scintillation breakdown testing. Two cases of multiple scintillations, one (15 µF 10 V) with increasing VBR (non-degrading oscillations), and another (100 µF 16 V) with decreasing VBR (degrading oscillations), are illustrated in Figure a). Figure b) shows two parts where scintillations were not observed because the charging current (100 µA) was close to the leakage currents of the parts. Figure c) shows that in high-leakage capacitors the breakdown conditions can be reached eventually with increased charging currents.

If the charging current is not sufficient, breakdown does not occur, and the voltage stabilizes at a certain level as shown in Figure I.1.b. In this case $I_L(t) = I_{ch}$, dV/dt = 0, and the voltage does not increase with time. By carrying out this test at increased charging currents, the breakdown can be reached eventually as shown in Figure I.1.c.

Capacitance calculated as a slope of V-t curve exceeds the value measured using AC signals typically on 10% to 20%, and the leakage current calculated per Eq. (2) can be much greater than the one measured after 5 minutes at VR (dielectric leakage current [DCL]) as required per military specifications. Figure I.2 shows a correlation between AC and DC measurements of capacitance for 33 µF 10 V and 15 µF 10 V parts and an increase in capacitance of 22 µF 35 V parts as the rate of charging decreases from 300 µA DC to 10 µA DC.

An increase of capacitance and DCL obtained during V-t measurements compared to the standard methods is due to a substantial amount of charge absorbing on electron traps inside the Ta_2O_5 dielectric. Measurements of polarization/depolarization currents (see Section II.7 of this report) showed that the concentration of traps is very high, ~1E19 cm^{-3}. The difference between C_AC and C_DC and between DCL and the current calculated per Eq. (2) can be also used for rough estimations of the concentration of electron traps and their characteristic times.

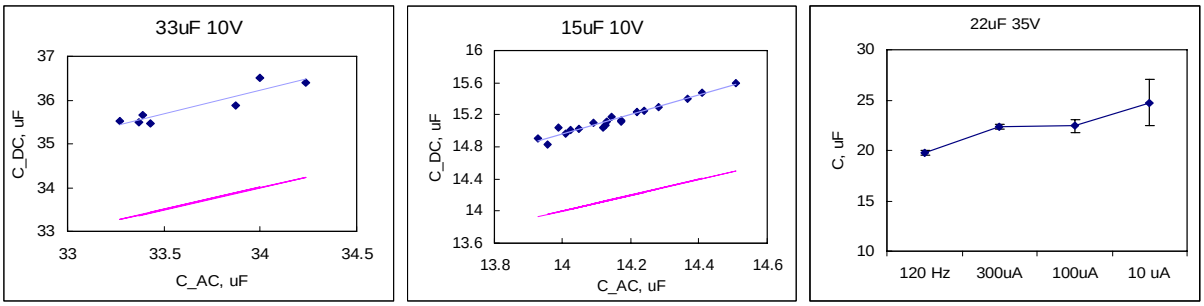

a) b) c)

Figure I.2. Correlation between AC (120 Hz) and DC measurements of capacitance for 33 µF 10 V (a) and 15 µF 10 V (b) parts. Lines in Figures a) and b) indicate no-change values. Figure c) shows variations of capacitance with charging current for 22 µF 35 V parts compared to measurements at 120 Hz.

I.2.2. I-t technique.

Typical results of I-t measurements are shown in Figure I.3. During these tests the voltage increased typically in 2 V or 3 V increments every 100 seconds. As a rule, breakdown does not occur right after voltage application, and it takes from a few seconds to a few dozen seconds for the scintillation to develop. Note that in the case shown in Figure I.3.a the currents almost completely recovered after the scintillation spikes, whereas in the case shown in Figure I.3.b the current remained higher. This indicates a full recovery of the part in the first case and remaining damage in the second case.

Obviously, this technique is more time consuming compared to the V-t technique and has worse voltage resolution; however, it is more sensitive to possible scintillation-induced damage and degradation. Besides, the necessity to vary charging currents depending on the value of capacitance and leakage current for the V-t technique might complicate comparison of test results for different part types.

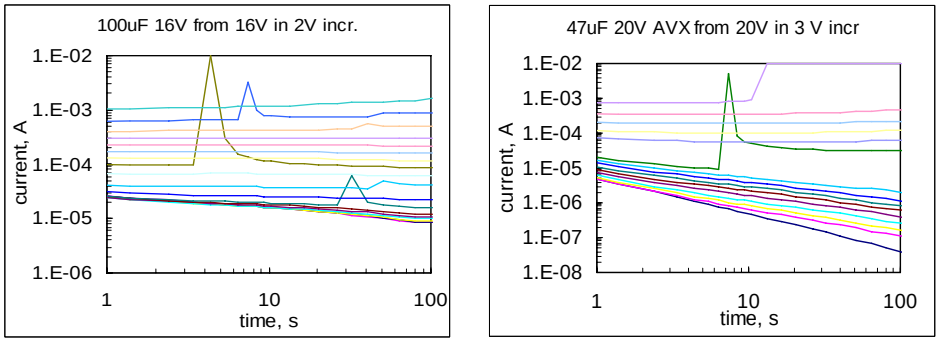

a) b)

Figure I.3. Examples of scintillation I-t testing for 100 µF 16 V (a) and 47 µF 20 V (b) parts. I-t variations were recorded during 100 seconds starting VR with 2 V (a) and 3 V (b) increments. The first scintillation (current spike) was observed at 34 V after 32 sec. in case a) and at 50 V after 8 sec. in case b).

I.2.3. Comparison of V-t and I-t techniques.

Groups of 10 to 42 samples of four different part types were tested using both V-t and I-t techniques. Weibull distributions of the breakdown voltages are shown in Figure I.4 and indicate that both methods produce similar results. However, on average, VBR determined using the I-t method was slightly lower (by 3% to 10%) compared to the V-t method. This might be explained considering that the scintillation breakdowns in tantalum capacitors are time dependent. A typical time to breakdown during V-t tests (seconds) is approximately 10 times less than during I-t testing.

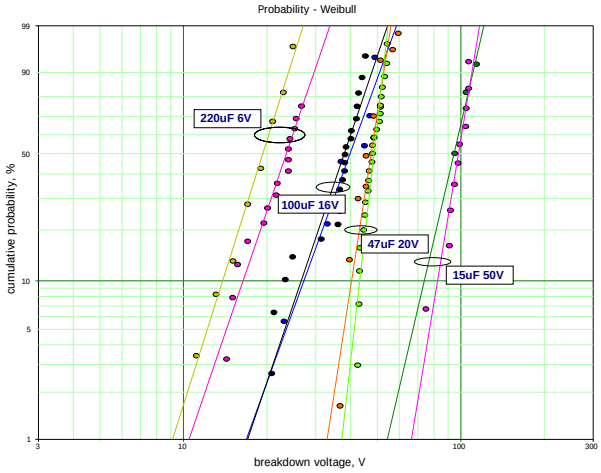

Figure I.4. Weibull distributions of first scintillations for four part types obtained using V-t and I-t techniques.

I.3. Distributions of VBR for different part types.

Scintillation breakdowns were measured on 16 different types of commercial (seven types) and military-grade (nine types) solid chip tantalum capacitors. Note that all high-CV parts were commercial products. One part type, CWR11FH156KB, a 15 µF 15 V capacitor, was presented by three lots with different date codes, thus allowing evaluation of the lot-to-lot reproducibility of VBR. In most cases two-parameter Weibull distributions were used to characterize scintillation breakdowns in the parts, as shown in a probability plot in Figure I.5. However, in some cases bi-modal distributions provided a better fit to experimental data.

Table I.1 displays major statistical characteristics of the distributions, the shape factor, β, characteristic breakdown voltage, η, the rated characteristic breakdown voltage, η /VR, and the probability of failure at VR, P_{VR}. The value of P_{VR} varies in a wide range from 0.12% to less than 10^{-11} %. It is reasonable to assume that $P_{VR} > 10^{-3}$ % corresponds to poor-quality lots and should not be used in high-reliability applications.

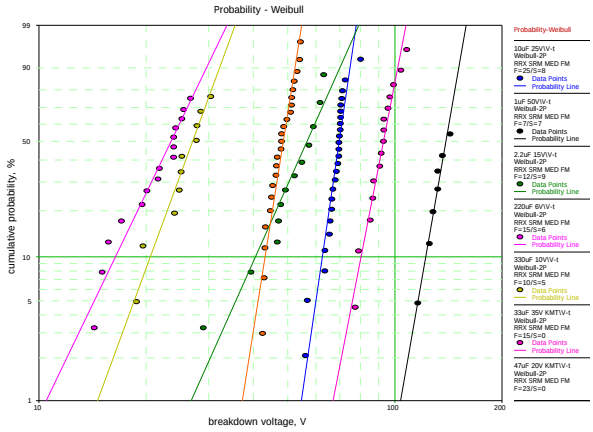

Figure I.5. Weibull distributions of first scintillation breakdowns for seven different part types.

Based on these distributions, another important parameter, breakdown margin, M, can be calculated. This parameter indicates a relative safety margin between the rated voltage and the minimum breakdown voltage of the population. For practical purposes it can be assumed that VBR_{min} corresponds to 1% of the distribution. In this case $M = (V_1 – VR)/VR \times 100$, where V_1 is the breakdown voltage at probability 1%.

The characteristic breakdown voltage exceeds VR by 3.4 times on average, and there is a trend of decreasing this ratio with VR as shown in Figure I.6. However, the spread of η/VR is large, from 2 to 5.4, and the margin varies from 6.4% to more than 220%. This indicates that generally VR is not a reliable indicator of the electrical strength of tantalum capacitors, and each lot should be characterized to assess the electrical strength of the parts. Interestingly, some lots had a significant proportion of parts exceeding the rated voltage by more than four times, thus indicating that breakdown voltages might exceed the formation voltage of solid tantalum capacitors.

Table I.1. Statistical characteristics of scintillation breakdowns in capacitors.

Part	Type	Qty.	β	η	M, %
10 µF 25 V	CWR09	33	17.25	71.28	118
100 µF 16 V	Commercial	39	5.57	39.65	6.4
15 µF 50 V	Commercial	10	10.84	101.49	32
1 µF 50V Mfr. V	CWR06	14	8.07	154.46	74
1 µF 50 V Mfr. A	CWR09	12	31	149	120
2.2 µF 15 V	CWR06	21	5.65	60.44	78
220 µF 6 V	Commercial	21	20.8	15.43	74
22 µF 6 V	CWR11	15	6.7	29.25	145
22 µF 20 V	CWR09	16	19.5	57.66	110
3.3 µF 10 V	CWR09	33	14.73	30.01	135
330 µF 10 V	Commercial	15	6.89	28.5	46
33 µF 10 V	CWR11	15	8.98	53.68	222
33 µF 35 V	Commercial	15	12.96	95.57	91
22 µF 35 V	Commercial	34	11.21	90.74	72
47 µF 20 V	Commercial	23	15.98	49.72	101
15 µF 10 V DC0017	CWR11	25	5.82	31.73	44
15 µF 10 V DC0026	CWR11	23	9.41	35.48	117
15 µF 10 V DC0038	CWR11	31	10.91	49.65	226

An average margin for military-grade parts (126%) is substantially greater than for commercial parts (60%), and both have a trend of decreasing with VR as shown in Figure I.6.b. This might be used as an indication of a higher overall quality of military parts compared to commercial parts. However, a relative spread of this parameter is also greater for military parts (standard deviation 55% compared to 36% for commercial parts). Due to a large spread of the data, some commercial lots might have quality even higher than the military parts. Note also that high-CV capacitors are not available in a military-grade version, so this comparison might be not accurate.

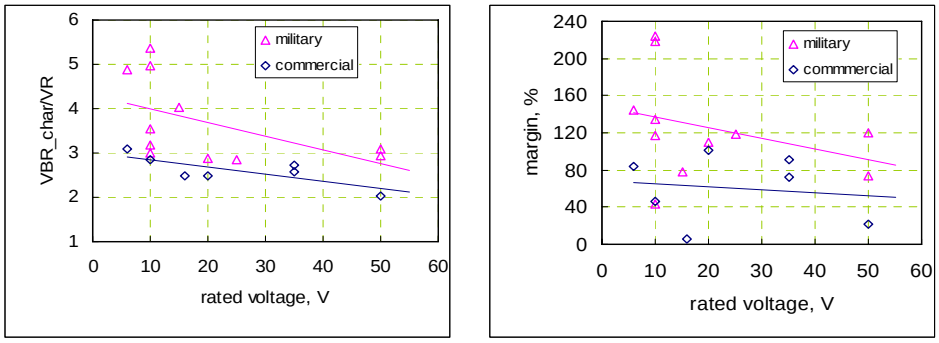

a) b)

Figure I.6. Variations of the ratio of the characteristic breakdown voltage to VR (a) and margin (b) with the rated voltages for different commercial and military-grade parts.

Having a distribution of VBR for a given lot of parts, the rated voltage can be determined as the voltage at which the margin exceeds a certain acceptable level. Considering the range of M variations for different lots, it is reasonable to accept a 50% safety margin as a minimum standard value for a high-reliability lot of capacitors. In this case, VR = V_1/1.5, and the probability of failure at VR will be several orders of magnitude lower than 1%.

Figure I.7 shows substantial lot-to-lot variation of the electrical strength for CWR11FH156KB capacitors. The characteristic values of VBR in these lots varied from 31.7 V to 49.6 V. Although VBR in all parts exceeded VR, the margin varied by more than three times, from 51% to 163%, thus indicating substantial variations in the quality and reliability of the parts from different batches.

The data presented above describe distributions of the first scintillation breakdowns. An important question regarding the scintillations is whether they result in complete self-healing or whether some damage remains in the part, resulting in degradation of its electrical strength and reliability. By continuing V-t measurements after the first scintillation occurred, the breakdown voltages of the secondary scintillations, V_{sc2}, were measured for some parts. The quantity of parts tested to multiple scintillations and the proportion of parts with damaging scintillations, P_{ds} (proportion of parts with $V_{sc2} < V_{sc1}$), are shown in Table I.2 and Figure I.8.

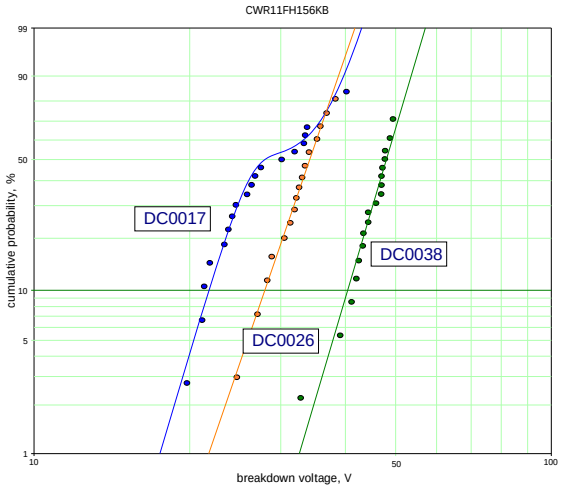

Figure I.7. Weibull distributions of breakdown voltages for three different lots of CWR11FH156KB capacitors. Note that the lot with DC0017 had a bimodal distribution, thus indicating the presence of two subgroups in this batch.

Table I.2. Proportion of damaging scintillations.

Part	Qty.	P_{ds}, %
10 µF 25 V	12	25.0
100 µF 16 V	14	35.7
15 µF 50 V	10	40.0
1 µF 50 V Mfr. V	7	57.1
2.2 µF 15 V	12	41.7
220 µF 6 V	17	35.3
22 µF 6 V	14	14.3
3.3 µF 10 V	10	20.0
330 µF 10 V	10	*
33 µF 10 V	7	28.6
33 µF 35 V	15	0.0
47 µF 20 V	20	15.0
15 µF 10 V DC0017	25	36.0
15 µF 10 V DC0026	7	14.3
15 µF 10 V DC0038	17	58.8
1 µF 50 V Mfr. A	12	*
22 µF 20 V	8	25
22 µF 35 V	29	24.1

*All parts failed catastrophically.

On average, the first scintillation was damaging in approximately one-third of the cases, P_{ds_avr} = 29.4%, and there was no significant difference between commercial parts and military parts. The spread of this proportion varied from 0% to 100%, suggesting that in many cases the self-healing was not complete, and electrical strength of the parts had degraded. For this reason, a scintillation event should be considered as an indicator of potential failure, and a distribution of scintillation breakdown voltages can be used to characterize quality of the lot. Note also that experiments showed that scintillations in high-CV parts might cause explosion and ignition of the capacitors

due to high energy stored in the part and released quickly during scintillation. In these cases failures are similar to the surge current events (see Figure I.8.b).

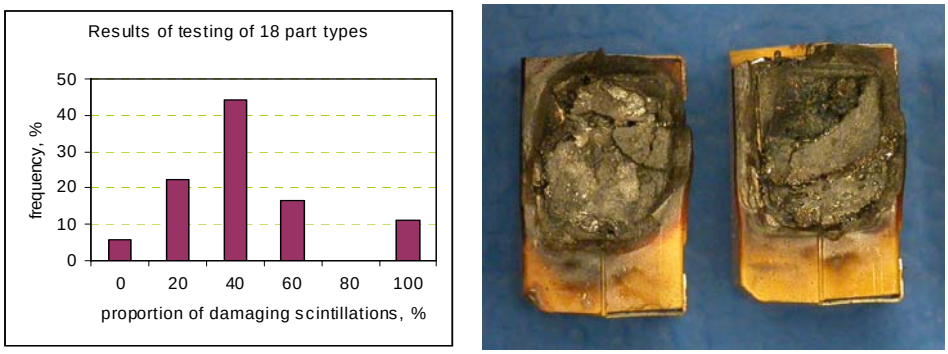

a) b)

Figure I.8. Distribution of damaging scintillations for 18 part types (a) and example of 330 µF 10 V capacitors that failed after scintillation testing (b).

I.4. Scintillation breakdowns during long-term testing.

As mentioned before, scintillations require some time to develop, and during I-t testing they often occur after a few seconds following application of the breakdown voltage. To prove that similar events might happen even after long-term operation under bias, monitoring of leakage currents was carried out on parts at room temperature and 125 ^{o}C at voltages varying from 1.5×VR to 3×VR.

Figure I.9 shows examples of long-term current variations in 47 µF 20 V, 2.2 µF 15 V, and 100 µF 16 V capacitors. In all cases the breakdown appeared as a sharp current spike occurring with time ranging from seconds to dozens of hours. Note that one 47 µF 20 V and one 100 µF 16 V capacitor shown in Figures I.9.a and I.9.b had two scintillations. The repeat scintillation occurred after a few hours of operation, thus confirming that parts experiencing scintillations have a higher probability of failure with time. Figure I.9.d shows variations of leakage currents in four 100 µF 16 V parts having scintillations after 6 to 20 hours of operation at 125 ^{o}C, 24 V. Here one of the four parts also had a repeat scintillation.

In the experiments described above, leakage currents were recorded every 20 seconds by measuring voltage across limiting 1 kOhm resistors. This allowed only relatively powerful and damaging scintillations resulting in increased leakage currents to be observed. Obviously, scintillations not causing a substantial increase in the leakage current could be easily skipped because their duration is typically in the millisecond range. Also, the presence of resistors might limit the available current and energy of scintillations, thus limiting damage to the dielectric.

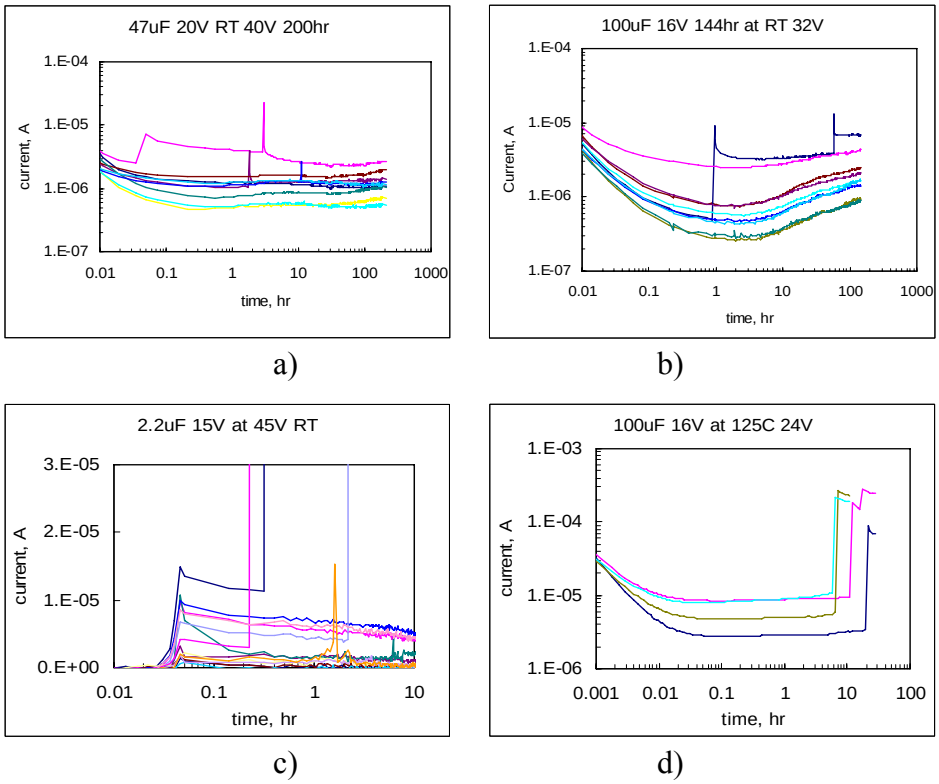

Figure I.9. Examples of scintillations observed during long-term I-t measurements in 47 µF 20 V (a), 100 µF 16 V (b, d), and 2.2 µF 15 V (c) capacitors at room temperature (a, b, c) and 125 °C (d). Parts presented in Figures a), b), and d) were tested with 1 kOhm resistors connected in series. Parts in Figure c) were tested with 1 Ohm 125 mA fuses. For this testing the voltage was gradually increased from 0 V to 45 V during the first 5 min., resulting in increased currents at the beginning of the test. A sharp increase of currents to more than 3E-5 A corresponds to the fuse blowing.

Replacing limiting resistors with fast-acting fuses potentially allows all scintillations to be revealed, and by recording the time to the fuse blowing, a distribution of times to failure can be obtained. Figure I.9.c shows results of experiments with 20 capacitors, 2.2 µF 15 V, stressed at room temperature and 45 V for more than 10 hours. All parts had 125 mA fuses connected in series. The cold resistance of the fuses was 1.7 Ohms, and measurements of voltages across the fuses allowed for estimations of the leakage currents in capacitors (starting from a few microamperes) and detection of the times to failure. Three failures, ranging from 0.2 hour to 2 hours, were recorded during these experiments, but in two cases the scintillations that occurred without blowing the fuses were also observed. This indicates that even relatively low-current fuses might be insufficient for detecting all scintillation events in tantalum capacitors, and more sophisticated electronic systems are required.

During highly accelerated life testing (HALT) described in [1], five different lots of commercial capacitors were tested at 125 °C for 100 to 200 hours at 1.5 VR. To reveal failures, 125 mA fuses were connected in sequence to each of the parts. Electrical measurements after life testing showed that out of 63 life test failures (parts with blown fuses), only three had high leakage currents exceeding the specified limits. This behavior can be explained considering that in most cases scintillations do not degrade the part to the level at which they exceed the specified limits of DCL.

I.5. Discussion.

According to the thermochemical model developed by McPherson and co-workers [8, 14], electrical breakdown in oxides occurs when the local electrical field weakens polar molecular bonds to the level at which thermal energy is sufficient to cause the breakage. This model also predicts that the time-dependent dielectric breakdown follows the E-model, so the time to failure can be expressed as:

$$TF = t_o \times \exp\left(-\gamma E + \frac{\Delta H}{kT}\right), \tag{3}$$

where ΔH is the activation energy required for displacement of ions from their normal bonding environment, γ is the field acceleration parameter, and t_o is a constant. For Ta_2O_5 dielectric ΔH is in the range from 1.7 eV to 2 eV.

Equation (3) is a special case of a more general Eyring E-model that is based on thermodynamic free-energy considerations [15] and is often used to describe time-dependent breakdown when the effective activation energy depends on the applied field. Similar equations were used by Goudswaard and Driesness from Phillips [12]; Loh from Hughes Aircraft [16]; and Khanin from Positron, Russia [17] to describe voltage and temperature dependencies of times to failure for solid tantalum capacitors. However, their estimations of the activation energy were lower: 1.2 eV in [12] and 1.45 eV in [17].

McPherson's model predicts that the breakdown field, EBR, decreases with the dielectric constant as $\varepsilon^{0.5}$, and the field acceleration parameter, γ, increases with ε, so that their product does not depend on the dielectric constant and can be presented as:

$$\gamma \times E_{BR} = \frac{\Delta H}{kT} \tag{4}$$

When (3) is used in conjunction with (4), the time to failure can be expressed via the breakdown voltage:

$$TF = t_o \times \exp\left(\frac{\Delta H}{kT}\right) \times \exp\left(-\frac{\Delta H}{kT} \times \frac{V}{V_{BR}}\right) = t_o \times \exp\left[\frac{\Delta H}{kT} \times \left(1 - \frac{V}{V_{BR}}\right)\right] \tag{5}$$

Assuming that VBR is related to the rated voltage that corresponds to the forming voltage of the dielectric, it can be expressed via VR: VBR = n×VR, where n = (2.5 - 3.5) is the formation ratio, and Eq. (5) can be presented as:

$$TF = t_o \times \exp\left(\frac{\Delta H}{kT} \times \left(1 - \frac{V}{n \times V_R}\right)\right) \tag{6}$$

A voltage acceleration factor (AF) at constant temperature, T, can be presented as follows:

$$AF_V = \frac{TF(V_R)}{TF(V)} = \exp\left(\frac{\Delta H}{nkT} \times \left(\frac{V}{V_R} - 1\right)\right) = \exp\left(-\frac{\Delta H}{nkT}\right) \times \exp\left(\frac{\Delta H}{nkT} \times \frac{V}{V_R}\right) = A \times \exp\left(B \times \frac{V}{V_R}\right), \tag{7}$$

where A = exp(-B) and B = ΔH/nkT.

The acceleration factor, which is used for Weibull grading test in MIL-PRF-55365, also varies exponentially with voltage:

$$AF = 7.03\times10^{-9}\times\exp\left(18.77\frac{V}{V_R}\right) \quad (8)$$

Note that *AF(VR) = 1* and *exp(-18.77) = 7.05×10-9.* This means that expressions (7) and (8) are identical if parameter B is constant and equal to 18.77. However, according to the thermochemical model, this parameter, and respectively the voltage acceleration factor, depends on the relationship between the breakdown voltage and rated voltage. Assuming that VBR is close to the formation voltage, the AF value depends on parameter n that is assigned by manufacturers depending on their experience and internal guidelines that varies from vendor to vendor. In the absence of relationship between VBR and VR the applicability of Eq. (8) is limited to specific and unpredictable cases only. This might make reliance on the reliability level calculated during Weibull grading testing misleading.

Figure I.10 shows temperature variations of parameter B for ΔH in the range from 1.5 eV to 2 eV and the formation ratio of 2.5 and 3.5. For military-grade parts the Ta_2O_5 dielectric is likely formed at relatively high voltages, so n = 3.5. At 1.75 eV < ΔH < 2 eV and T = 85 °C, the agreement between the values of B calculated using the thermochemical model (16.5 < B < 19.2) and the value used in MIL-PRF-55365 (B = 18.77), which was obtained based on empirical data during extensive life testing of solid tantalum capacitors in 1970s [18], can be considered as reasonably good. However, due to exponential dependence on B, even these relatively minor variations might cause changes in AF by more than 40 times. Variations of n and ΔH might cause much more substantial variations of B and AF, resulting in erroneous reliability estimations.

Considering that for a given lot, the distribution of breakdown voltages can be described using a Weibull function with a characteristic breakdown voltage η and shape parameter β, the breakdown voltage can be expressed via the probability, p, of the part to have a certain level of VBR:

$$V_{BR} = \eta\times\left[-\ln(1-p)\right]^{1/\beta} \quad (9)$$

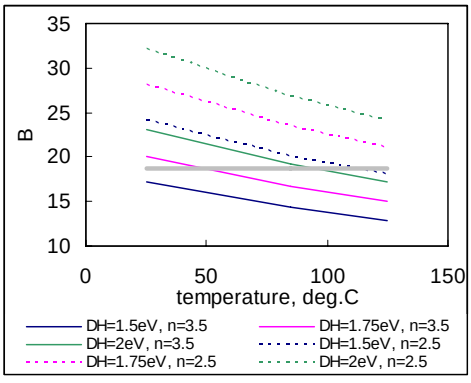

Figure I.10. Variations of parameter B with temperature for n = 2.5 and 3.5 and activation energies ΔH = 1.5 eV, 1.75 eV, and 2 eV. A horizontal line corresponds to the value of B used in MIL-PRF-55365.

Using Eq. (5) and (9), the corresponding times to failure can be calculated, thus allowing numerical modeling (Monte Carlo simulation) of life testing. Table I.3 shows results of simulation of life testing performed for three part types for T = 125 ^{o}C and V= 1.5 VR.

Table I.3. Parameters of VBR distributions and time-to-failure model per Eq. (5).

Parameters		100 µF 16 V	47 µF 20 V	33 µF 35 V
VBR Distribution	**η, V**	40.2	49.1	94.8
	β	5.8	10.1	12.5
Life Model	**ΔH, eV**	1	1	2.5
	t_0, hr.	1E-3	1.5E-3	2E-12
Simulated TF	**η, hr.**	86.6	241	5562
	β	0.25	0.49	0.29

Figure I.11 shows comparison of experimental and calculated per Eq. (5) and Eq. (9) distributions of times to failure during highly accelerated life testing for three types of capacitors. By adjusting parameters ΔH (in the range from 1 eV to 2.5 eV) and t_0 (from 1E-3 to 2E-12 hr.) experimental data can be adequately approximated by Eq. (5). Note also that in all cases the shape factor of the time-to-failure distributions, β, was below 1, suggesting infant mortality (IM) failures. Typically, similar failures are associated with manufacturing defects and occur during early stages of operation. For a typical electronic part, the rate of failures decreases with time and remains low during the so-called useful life period until it increases eventually due to wear-out mechanisms. Variations of the failure rate with time form the famous "bath-tub" curve. However, for tantalum capacitors the IM period continues even when more than 50% of the parts failed. This indicates that most of the failures in these parts are caused by defects (sites with low electrical strength) in the Ta_2O_5 dielectric. These defects are likely due to a large and irregular surface area of the oxide that is electrochemically grown on pellets made of sintered tantalum powder and can be considered as intrinsic for this technology.

Although the thermochemical model provides a good qualitative agreement with experimental data and allows for reliability predictions, parameters ΔH and t_o derived for Ta_2O_5 dielectrics based on measurements of breakdown fields cannot be used and need to be adjusted empirically. The reason for this is likely related to the presence of a high concentration of electron traps and oxygen vacancies in Ta_2O_5 films. Redistribution of oxygen vacancies and charging of electron traps with time might substantially change electrical field in the dielectric and affect the probability of breakdown. The thermochemical model does not account for these changes that are specific to electrochemically grown Ta_2O_5 dielectrics and additional analysis that would take into account these variations is necessary. The effect of traps is discussed in more detail in Part II of this report.

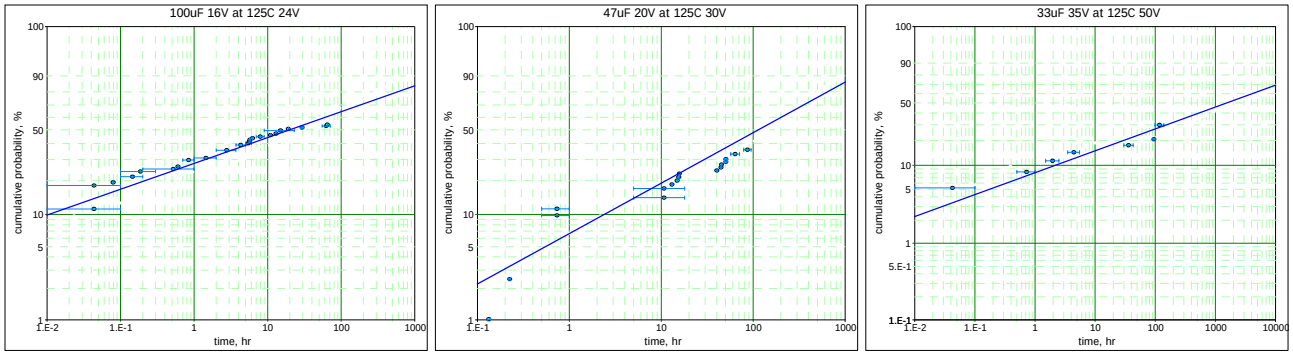

a) b) c)

Figure I.11. Experimental (marks) and calculated (lines) distributions of times to failure during HALT at 125 °C and 1.5 VR for three part types.

The time-to-failure model allows also for demonstration of the significance of the rated voltage and safety margin. Assuming that parts are tested at a rated voltage and VBR at 1 percentile of the distribution is V_1, the minimum time to failure that corresponds to the minimal breakdown voltage in the group can be calculated as:

$$TF_{\min} = t_o \times \exp\left[\frac{\Delta H}{kT} \times \left(1 - \frac{VR}{V_1}\right)\right] = t_o \times \exp\left[\frac{\Delta H}{kT} \times \left(\frac{M}{M+1}\right)\right] \qquad (10)$$

The margin-related acceleration factor AF_M can be defined as a ratio of TF_{min} at a given margin to TF_{min} at M = 0. Figure I.12 shows variations of AF with the margin calculated for three values of activation energy: 1 eV, 1.5 eV, and 2 eV. At relatively small M (below ~50%), Eq. (10) predicts exponential increase of time to failure with the safety margin. Note that assuming M = 50% as a minimal acceptable limit, the corresponding acceleration factors are significantly greater than 1E6.

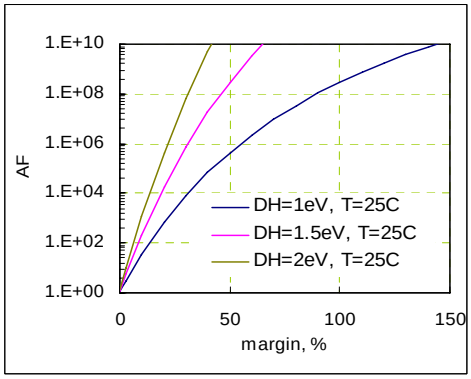

Figure I.12. Variations of acceleration factors with the margin calculated per Eq. (10) at room temperature and ΔH in the range from 1 eV to 2 eV.

I.6. Conclusions.

1. Scintillation breakdowns in solid chip tantalum capacitors have been characterized using constant current stress (V-t) and constant voltage step-stress (I-t) techniques. Both techniques gave similar results.
2. Measurements of breakdown voltages in 16 commercial and military-grade part types show poor correlation between VBR and rated voltage. This means that VR is not a reliable indicator of the electrical strength of the parts and does not assure the necessary safety margin.
3. Analysis of distributions of scintillation breakdown voltages shows that the safety margin for different part types varies in a wide range from 6% to 230%, and there is a trend of decreasing margin with the rated voltage.
4. Because of uncertainty in relationship between VBR and VR, the effect of derating on reliability of tantalum capacitors might be either excessive or insufficient even for lots with the same VR.
5. Scintillation breakdowns were found damaging (reducing electrical strength of capacitors and/or increasing leakage currents) on average in 30% of cases and up to 100% in some lots, and for this reason they should be considered as a reliability hazard.
6. Failures of tantalum capacitors operating at steady-state conditions can be considered as time-dependent breakdowns and can be simulated based on the distribution of breakdown voltages and thermochemical model of TDDB. Adjusting parameters of the model allows for a reasonable agreement with the results of highly accelerated life testing.
7. Measurements of scintillation breakdowns provide important information regarding quality and reliability of tantalum capacitors, allow for assessment of the safety margin, and should be used to qualify parts for high-reliability applications.

I.7. References to Part I.

[1] A. Teverovsky, "Effect of surge current testing on reliability of solid tantalum capacitors," Proceedings of the 28th Symposium for Passive Components, CARTS'08, Newport Beach, CA, 2008, pp. 293-310.

[2] J. Primak, P. Blais, B. Long, A. Ifri, and E. Jones, "Alternate methods of defining dielectric quality using step stress surge testing and scintillation testing," Proceedings of 2008 Components for Military and Space Electronics Conference, San Diego, CA, 2008, pp. 323-347.

[3] J. D. Prymak and M. Prevallet, "Scintillation testing of solid electrolytic capacitors," Proceedings of 26th Symposium for Passive Components, CARTS'06, Orlando, FL, 2006, pp. 395-406.

[4] J. Hossick-Schott, "Prospects for ultimate energy density of oxide-based capacitor anodes," Proceedings of CARTS Europe, Barcelona, Spain, 2007, pp. 15-24.

[5] Z. Sita, M. Biler, T. Karnik, J. Sikula, and V. Sedlakova, "Dielectric improvement in NbO capacitors," Proceedings of CARTS Europe, Barcelona, Spain, 2007, pp. 123-130.

[6] Y. Freeman, R. Hahn, P. Lessner, and J. Prymak, "Reliability and critical applications of tantalum capacitors," Proceedings of CARTS Europe, Barcelona, Spain, 2007, pp. 193-204.

[7] K. H. Allers, R. Schwab, W. Walter, M. Schrenk, and H. Korner, "Thermal and dielectric breakdown for metal insulator metal capacitors (MIMCAP) with tantalum pentoxide

dielectric," Proceedings of IEEE International Integrated Reliability Workshop Final Report, 2002, pp. 96-101.

[8] J. W. McPherson, J. Kim, A. Shanware, H. Mogul, and J. Rodriguez, "Trends in the ultimate breakdown strength of high dielectric-constant materials," *IEEE Transactions on Electron Devices*, vol. 50, 2003, pp. 1771-1778.

[9] C. Chaneliere, J. Autran, R. Devine, and B. Balland, "Tantalum pentoxide (Ta_2O_5) thin films for advanced dielectric applications," *Material Science and Engineering*, vol. R22, 1998, pp. 269-322.

[10] A. Inani, V. Koldyaev, and S. Graves, "Accelerated testing for time dependent dielectric breakdown (TDDB) evaluation of embedded DRAM capacitors using tantalum pentoxide," *Microelectronics Reliability*, vol. 47, 2007, pp. 1429-1433.

[11] L. Howard and A. Smith, "Dielectric breakdown in solid electrolyte tantalum capacitors," *IEEE Transactions on Component Parts,*, vol. 11, 1964, pp. 187-193.

[12] B. Goudswaard and F. J. J. Dreisens, "Failure mechanism of solid tantalum capacitors," *Electrocomponent Science and Technology*, vol. 3, 1976, pp. 171-179.

[13] B. Long, M. Prevallet, and J. D. Prymak, "Reliability effects with proofing of tantalum capacitors," Proceedings of the 25th Symposium for Passive Components, CARTS'05, Palm Springs, CA, 2005, pp. 167-172.

[14] L. McPherson, J. Kim, A. Shanware, H. Mogul, and J. Rodriguez, "Proposed universal relationship between dielectric breakdown and dielectric constant," Proceedings of Digest International Electron Devices Meeting, IEDM '02, 2002, pp. 633-636.

[15] M. Kimura, "Field and temperature acceleration model for time-dependent dielectric breakdown," *IEEE Transactions on Electron Devices*, vol. 46, 1999, pp. 220-229.

[16] E. Loh, "Development of a model for voltage degradation of various dielectric materials," *IEEE Transactions on Components, Packaging, and Manufacturing Technology*, vol. 4, 1981, pp. 536-544.

[17] S. D. Khanin, "Electrical destruction of amorphous tantalum and niobium oxide films," Proceedings of the 4th International Conference on Conduction and Breakdown in Solid Dielectrics, 1992, pp. 528-532.

[18] J. N. Burkhart, "Use of accelerated testing techniques in military specification MIL-C-39003," Proceedings of CARTS, Phoenix, AZ, 1983, pp. 111-117.

Part II. Comparison of Scintillation and Surge Current Breakdown Voltages in Chip Tantalum Capacitors

II.1. Introduction.

Depending upon test conditions, two types of electrical breakdowns are observed in solid tantalum capacitors: scintillation breakdowns, in which the voltage increases relatively slowly (characteristic times are more than a second), and surge current breakdowns, in which the voltage increases instantly (characteristic times are from microseconds to hundreds of microseconds depending on the parameters of the part). Scintillation breakdown voltages (VBR_CCS) are measured using a constant current stress (CCS) technique, and surge current breakdown voltages (VBR_SCT) are measured using a step stress surge current testing (3SCT) technique. The latter technique includes charging of a large bank capacitor, imitating a low-impedance power source, to incrementally increasing voltages, and then discharging it onto a device under test. Charging of capacitors at a high voltage rate, dV/dt, creates substantial current spikes, $I_{sp} = C \times dV/dt$, reaching dozens to hundreds of amperes [1]. The failure often occurs as an explosion with dramatic acoustic and sparking effects and in many cases causes melting of the tantalum pellet and ignition of the molding compound.

Scintillations are local momentary breakdowns of tantalum pentoxide dielectric, and typically during testing and/or high-impedance applications they do not degrade parameters of the parts to the degree exceeding the specified limits. For this reason scintillations are often considered as nuisances rather than failures. However, our studies (see Part I) showed that scintillations can cause degradation of breakdown voltages and compromise reliability of parts [2]. A relatively benign characteristic of the scintillation breakdown is attributed to a so-called self-healing mechanism in tantalum capacitors with manganese cathodes. The self-healing is due to the capability of a conductive manganese oxide (MnO_2) to convert into high-resistive forms (Mn_2O_3, Mn_3O_4, MnO) when heated to a relatively low temperature of ~500 ^oC [3]. This conversion insulates the damaged area of the dielectric and prevents short-circuit failures. However, the area of manganese cathode that is decomposed is typically smaller than the area of damaged or fractured Ta_2O_5 dielectric [3], and a large proportion of parts after scintillations have greater leakage currents and lower breakdown voltages [2, 4].

Contrary to scintillations, during surge current breakdowns self-healing of the manganese does not occur because the destruction of the dielectric occurs much faster than the heating of the cathode at the breakdown site. This causes short-circuit failures of the part and might result in catastrophic consequences for the whole system. Multiple attempts have been made to explain turn-on failures in solid tantalum capacitors since their introduction to the market in the 1960s. However, the physical nature of surge current breakdowns is still not understood completely and there is a lack of experimental data on factors affecting VBR_SCT, and in particular, the effect of temperature. Also, the relationship between scintillation and surge current breakdowns voltages has not been studied yet.

Different hypotheses were discussed in relevant literature in an attempt to explain surge current failures in tantalum capacitors. These hypotheses can be combined in five groups as follows:

1. Electrical oscillations in circuits. At low limiting resistances and relatively high inductances of the circuit, oscillations might occur during turning on of the power supply. These

oscillations might increase the voltage across the capacitor up to two times and result in breakdown [5-7]. However, at a proper control over inductance, in particular over the length of connecting conductors, the circuit is overdamped and the probability of voltage overshooting can be eliminated [8]. Nevertheless, surge current failures occur even in the absence of oscillations.

2. Local overheating of the cathode. It is assumed that high inrush currents in a capacitor can cause formation of "hot spots" either in the dielectric by the current directed through a weak area of Ta_2O_5 dielectric [9], or in locations of manganese cathode with increased resistance and/or poor thermal contact to a heat sink [9, 10]. In either case temperature increases locally and either directly reduces the breakdown strength of the Ta_2O_5, or converts amorphous Ta_2O_5 dielectric into a crystalline phase [7, 11, 12] and then the increased electrical field over the converted area causes breakdown. However, the presence of the weak sites in the dielectric can be revealed by increased leakage currents, but no correlation between DCL and VBR_SCT is typically observed. Currents flowing along the manganese layer would rather bypass high-resistive areas and be unlikely to cause their overheating. Possible overheating of cathode sites with poor thermal contacts might not overheat the underlying dielectric because of the high thermal resistance. E. Reed from Kemet showed that surge current testing does not cause any substantial temperature increase in chip tantalum capacitors [13]. A significant increase in VBR_SCT for parts rated to the same voltage but having Ta_2O_5 dielectric formed at higher voltages was reported by Gill [9]. Increased forming voltages corresponded to greater thicknesses of the dielectric but did not change the possibility of local overheating in the manganese layer, so thermal effects are likely not the prime cause of the turn-on failures.

3. Mechanical damage to tantalum pentoxide dielectric. High values of capacitance in tantalum capacitors are due to employment of very thin (typically from 40 nm to 200 nm) Ta_2O_5 dielectric layers, which operate under high electrical fields (~2E6 V/cm) and respectively experience high compressive mechanical pressures (up to ~3 MPa [11]). Considering that a manganese cathode has fine MnO_2 crystals with sharp edges, it is possible to imagine that these edges impair the dielectric either directly due to the electrostatic pressure, or due to distortion and friction caused by high inrush currents [3, 11, 12]. However, the electrostatic pressure does not depend on the rate of voltage variations, and there is no experimental or theoretical evidence of friction under high inrush currents. Note also that tantalum capacitors with polymer cathodes, which do not have sharp crystals, are also vulnerable to the turn-on failures. A direct effect of mechanical stresses on VBR_SCT was shown in our previous work [14] and was explained by stress-induced electron trap generation. This mechanism still remains a hypothesis, and the effect of mechanical stresses on VBR_SCT needs more experimental work and analysis.

4. Sustained scintillation breakdown. This model assumes that a surge current breakdown occurs when the electrical field in the tantalum pentoxide dielectric exceeds its electrical strength and a scintillation breakdown is initiated. With high current available from a low-impedance power supply, the breakdown process develops so rapidly that the self-healing does not occur and the scintillation transfers into a destructive mode. It is generally assumed that soldering of tantalum capacitors during assembly onto a board can damage the dielectric, and a part that would not fail in as-received condition fails during first turn-on of the assembly [15-17]. To eliminate the possibility of these failures, J. Primak and co-workers suggested a so-called "proofing" technique, which is a slow-rate, controllable exposure of the part after soldering to

voltages slightly higher than the operating voltage to verify that possible scintillations are self-healed [16, 18]. Currently, some manufacturers of DC-DC converters are using this technique to assure reliable operation of tantalum capacitors used in the output circuits of the hybrid converters. However, our results reported below show that VBR_CCS is substantially higher than VBR_SCT, so the absence of scintillations might not guarantee that turn-on failures would not occur.

5. Polarization delay. E. Reed from Kemet observed a decrease of the surge current breakdown voltages with the resistance of the test circuit within the range of resistances from 0.1 Ohm to 10 Ohms [19]. The effect was explained by a polarization delay in Ta_2O_5 dielectrics. He speculated that an instant application of a high electric field to a capacitor results in distortion of atomic bonds, which in the absence of polarization might be strong enough to rupture and cause a breakdown. If the rate of the voltage increase is low, polarization would catch up to the applied field, reduce the stress, and increase breakdown voltage. However, no details of the polarization delay mechanism were provided. Besides, the thermochemical model [20] that relates polarization to the breakdown field (E_{BR}) in dielectrics predicts a decrease of E_{BR} at increased times of the electrical stress.

Unfortunately, no adequate experimental evidence and/or theoretical analysis were presented to support these hypotheses, and the physical nature of surge current breakdowns in chip tantalum capacitors still remains to be explained.

In this work, scintillation and surge current breakdown voltages were measured using constant-current-stress and step-stress-surge-current techniques. Distributions of breakdown voltages and safety margins were analyzed for 30 different lots of commercial and military-grade capacitors. Results of measurements of temperature dependencies of VBR_CCS and VBR_SCT were analyzed and the effectiveness of the proofing technique was evaluated. To explain the observed data, a concentration of electron traps in Ta_2O_5 dielectrics was estimated using measurements of polarization and depolarization currents. The physical nature of breakdowns in tantalum capacitors is discussed. The suggested model explains both the scintillation and surge current breakdowns as a result of electron impact ionization and avalanche breakdowns. It is shown that the specific feature of anodic Ta_2O_5 dielectrics is a very high concentration of electron traps, which might exceed 1E19 cm^{-3}. Charges trapped in the dielectric during a slow voltage increase result in raising of the barrier at the cathode/dielectric interface and enhancing scintillation breakdown voltages compared to surge current breakdown voltages.

II.2. Experiment.

The surge current breakdown voltages, VBR_SCT, were measured using a technique compliant to MIL-PRF-55365 and described in [21]. To simulate the worst-case conditions, no current-limiting resistors were used. Monitoring of the surge current oscillograms and measurements of current spike amplitudes were used to verify that no oscillations occurred during testing and to assure reproducibility of test results. A constant current stress technique detailed in [4, 22] was used to measure scintillation breakdown voltages, VBR_CCS.

Seventeen commercial and 13 military-grade lots of tantalum capacitors were used in this study (see Table II.1). Several part types had the same values, but were manufactured by different vendors, and three part types had two to three lots with different date codes and were used to evaluate the consistency of their quality. Two groups of samples, from 12 to 35 parts each, were

selected for scintillation and surge current breakdown measurements for each lot. Analysis of the data was carried out using Weibull-7 software available from ReliaSoft.

Table II.1. Tantalum chip capacitors used for testing.

Part Number	Military/ Commercial	C, μF	VR, V	EIA Size/ Case Size	Comment
	M	15	10	6032	DC0017
CWR11FH156KB	M	15	10	6032	DC0038
	M	15	10	6032	DC0126
CWR06HC225KBA	M	2.2	15	Case A	Coated
CWR09FC335KBA	M	3.3	10	6032, Mfr. A	Mfr. A
CWR06FH335KPA	M	3.3	10	case A	Mfr. V
CWR11DH226KD	M	22	6	6032	6032
TPSD476K020R0100	C	47	20	7343	Mfr. A
T495X476K020ASE150	C	47	20	7343	Mfr. K
T495X227K006AS	C	220	6	7343	DC0532
	C	220	6	7343	DC0101
T510X337K010AS	C	330	10	7343	DC0038
	C	330	10	7343	DC0718
TPSD336K035R0200	C	33	35	7343	Mfr. A
T495X336K035AS	C	33	35	7343	Mfr. K
T495X107K016AS	C	100	16	7343	
T495D226K015DS	C	22	15	7343	
CWR11FH336KD	M	33	10	7343	
CWR09KC106KBA	M	10	25	6032	
CWR09JC226KB	M	22	20	6032	
CWR09NC105KB	M	1	50	6032	Mfr. A
CWR06NC105KCA	M	1	50	case D	Mfr. V
T495156M035AHE225	C	15	35	7343	
T495X156M050AS	C	15	50	7343	
T491D226M035AS	C	22	35	7343	
TAJB475K010R	C	4.7	10	6032	
293D686X901602	C	68	16	7343H	
CWR11HH106KD	M	10	15	6032	
T491D336K016AS	C	33	16	7343	
T491C335K035AS	C	3.3	35	7343	

II.3. Analysis of distributions.

Typical examples of distributions of scintillation and surge current breakdown voltages for four part types are shown in Figure II.1. Several conclusions can be made based on analysis of these and similar data obtained for different part types:

1. In most cases both VBR_CCS and VBR_SCT can be described accurately enough using unimodal Weibull distributions and be characterized by two parameters: η, the characteristic breakdown voltage, and β, the shape factor.
2. Scintillation breakdown voltages are significantly greater than surge current breakdown voltages.

3. In Weibull plots, the probability lines approximating scintillation and surge current breakdown voltages are parallel, indicating similar shape factors and a resemblance in the mechanisms of breakdowns.
4. Distributions of breakdown voltages for CWR06- and CWR09-style 1 µF 50 V capacitors were similar (Figure II.1.b). This indicates that packaging of the part is not a critical factor and the breakdown voltages are determined by the quality of the pellet and manganese cathode assembly, which were likely similar for these part types.
5. Both VBR_SCT and VBR_CCS for the parts presented on Figure II.1.a were greater than the rated voltage (VR). However, more than 50% of 1 µF 50 V capacitors manufactured by two vendors had VBR_SCT below VR, suggesting that even military-grade parts can fail in the as-received condition at voltages below the rated one.

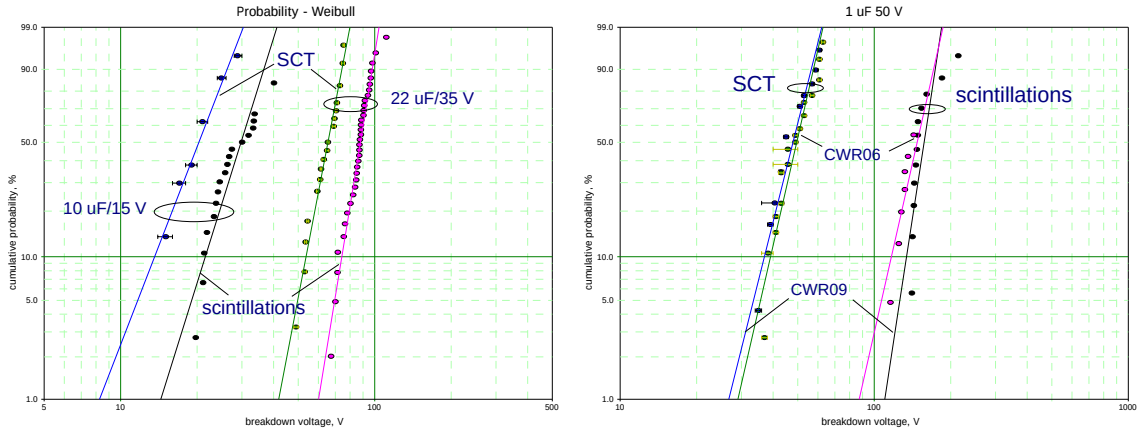

a) b)

Figure II.1. Weibull distributions of surge current (data with error bars) and scintillation breakdown voltages for 10 µF 15 V, 22 µF 35 V (a), and 1 µF 50 V (b) capacitors. Note that Figure b) shows similar results for different styles (CWR06 and CWR09) capacitors having the same values of capacitance and rated voltage.

Comparison of parameters of scintillation and surge current breakdown distributions for all tested parts is shown in Figure II.2. There is clearly a correlation between η_SCT and η_CCS. However, in all cases η_CCS > η_SCT and the ratio of the characteristic breakdown voltages, η_CCS/η_SCT, varies from 1.08 to 2.47 for commercial parts and from 0.97 to 3.22 for military-grade parts. On average, scintillation breakdown voltages exceed surge current breakdown voltages by 50% (an average ratio η_CCS/η_SCT = 1.51, STD = 0.47). In spite of the observed correlation, the spread of the data is large, so it is not possible to predict surge current breakdown voltages based on VBR_CCS accurately enough.

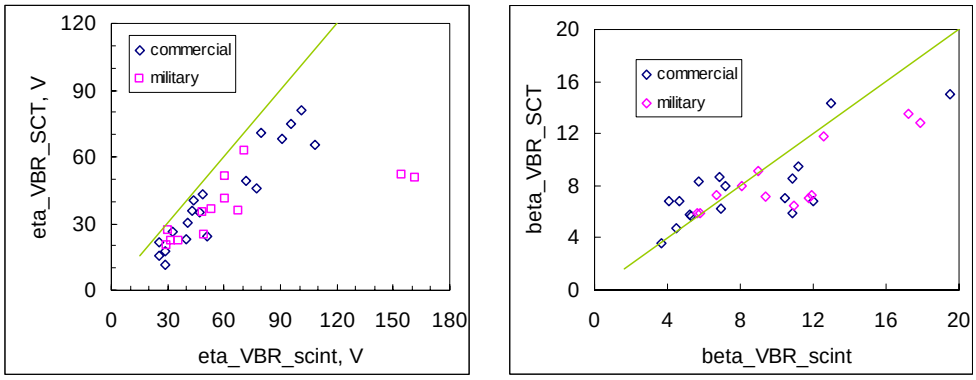

a) b)

Figure II.2. Correlations between characteristic breakdown voltages (a) and shape factors (b) of distributions of scintillation and surge current breakdown voltages for commercial and military-grade parts. Green lines correspond to no-change values.

A similarity of the shape parameters for scintillation and surge current breakdown distributions for the four parts shown in Figure II.1 is confirmed for all tested capacitors in Figure II.2.b. The range of β_CCS is from 3.6 to 19.5, which is close to the range of β_SCT, from 3.6 to 15, and the average ratio β_CCS/ β_SCT = 1.1 at a standard deviation of 0.33.

In reliability applications, the value of β is considered sensitive to the physical processes causing failures, and close values of β for distributions obtained for different stress levels are regarded as a proof of similarity in the failure mechanisms. Considering SCT and CCS as tests with different levels of electrical stress, a close correlation of β over a wide range of values implies that the same physical processes control failures in both tests.

For commercial parts, on average, the characteristic breakdown voltage for scintillation breakdowns exceeds the rated voltage by 3.38 times (STD = 1.32) and for surge current breakdowns by 2.38 times (STD = 0.89). For military-grade parts η_CCS/VR = 3.73 (STD = 1.2) and η_SCT/VR = 2.49 (STD = 0.8). Note that in all cases the standard deviations were rather large and the spread of data, from 32% to 39%, was virtually the same for commercial and military-grade parts. This suggests that there is no significant difference between the quality of these two groups of parts.

Figure II.3 shows that there is a trend of decrease in the rated characteristic breakdown voltages (η_CCS/VR and η_SCT/VR) with the nominal rated voltage of the parts. This ratio for scintillation breakdowns decreases on average from 4 for parts rated to 6 V, to 2.1 for 50 V parts. For surge current breakdowns this ratio decreases from 3 to 1.2 for 6 V and 50 V rated parts, respectively. However, the spread of the ratio is large. For example, for parts rated to 10 V, η_CCS/VR varies from 2.84 to 7.73 and for η_SCT/VR the variation is from 1.15 to 4.61. It is assumed sometimes that the maximum breakdown voltage in dry tantalum capacitors is identical to the maximum forming voltage (VF) during anodization [23]. However, the forming ratio (VF/VR) is typically in the range from 2 to 4.5, so the capacitors having VBR/VR more than 5 would have VBR substantially exceeding VF.

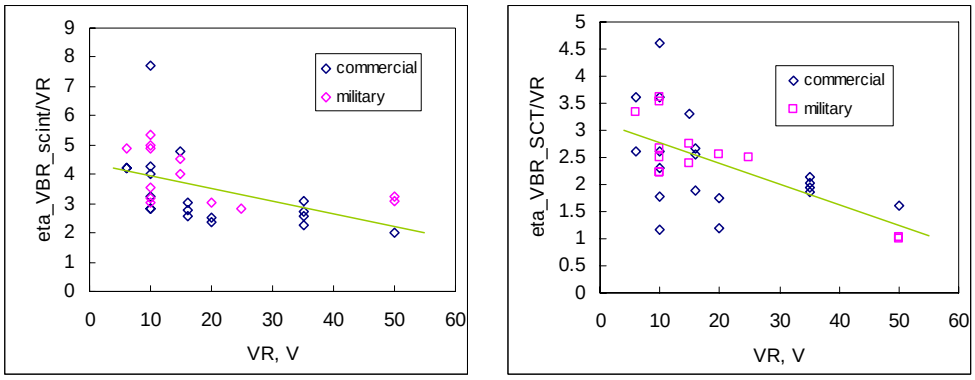

a) b)

Figure II.3. Variations of the rated characteristic breakdown voltages with the nominal rated voltage of the parts for scintillation (a) and surge current (b) breakdowns.

The results indicate that the quality of tantalum capacitors on average decreases with the rated voltage. However, variations between different part types rated to the same voltage are substantial, and hence VR is not a reliable indicator for the capability of parts to operate at high voltages. A poor correlation between VR and breakdown voltages for solid tantalum capacitors was also indicated in [24].

Obviously, the probability of having a defective area with a low electrical strength in a dielectric increases with the surface area of the capacitor. This explains a trend of decreasing breakdown voltages with the value of capacitance shown in Figure II.4. For capacitors rated to 10 V, the values of η_CCS decrease on average from 46 V for 3.3 µF capacitors to 28 V for 330 µF capacitors. For surge current breakdown voltages this decrease was from 31 V to 15 V for 3.3 µF and 330 µF parts, respectively. Note that this trend is more evident for commercial parts mostly because high CV values are not available for military-grade parts. On the other hand, this trend might explain the difficulties of assuring military-level quality of the parts with high capacitance and/or rated voltage.

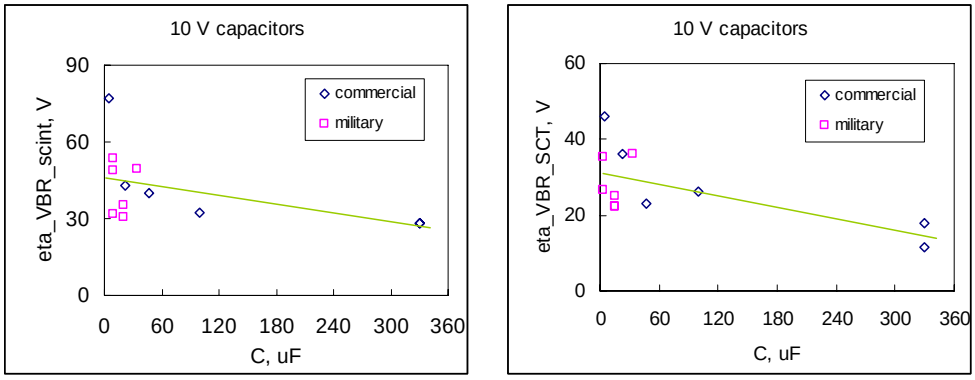

a) b)

Figure II.4. Variations of the scintillation (a) and surge current (b) characteristic breakdown voltages with capacitance for tantalum capacitors rated to 10 V.

II.4. Safety margin.

A comparison between the characteristic breakdown voltages and VR does not provide a reliable estimation of the quality of the parts. Capacitors with the same values of η but different slopes of Weibull distributions might have significantly different proportions of low voltage, and potentially defective devices. These low-breakdown-voltage parts are of the most concern regarding reliability, and the screening and qualification system used to assure the necessary quality of military and space-grade capacitors should be focused on elimination of these parts.

To characterize the quality of capacitors, a margin between the minimal breakdown voltage in the lot and VR should be estimated. Considering a typical sample size of a group used for analysis of breakdown distributions (15 to 25 samples), it is reasonable to use a voltage corresponding to 1 percentile of the distribution, V_1, as an estimation of the minimal breakdown voltage in the lot. Using this value, a breakdown safety margin, which is a ratio of the difference between V_1 and VR to VR, and is expressed as a percentage, can be calculated for scintillation (M_{scint}) and surge current (M_{SCT}) breakdown voltages:

$$M_{scint} = (V_{1\_scint} - VR)/VR \times 100;\ M_{SCT} = (V_{1\_SCT} - VR)/VR \times 100.$$

Average values of the safety margins and their standard deviations are shown in Table II.2. The safety margin for scintillation breakdowns was significantly greater than for surge current breakdowns (by 4.7 times for commercial parts and by 3.6 times for military-grade parts). Both scintillation and surge current breakdown margins were on average approximately two times greater for military parts than for commercial parts. However, the spread of the data was large and roughly the same for commercial and military parts (from 45% to 65%). Analysis using a Student t-test shows that at a confidence level of 95% there is no difference between M_{SCT} for military and commercial parts. Note that lower margins for commercial parts compared to military-grade parts might be related to higher CV values available for commercial capacitors.

Figure II.5 shows variations of the safety margin for different part types vs. the rated voltage. For both M_{SCT} and M_{scint} there is a trend of decrease of the margin with VR. Only one commercial lot had a negative value of M_{scint}, whereas margins for surge current breakdown voltages were much lower, and 3 out of 13 military lots and 8 out of 17 commercial lots had $M_{SCT} < 0$. This means that the probability of having surge current breakdown failure at the rated voltage is more than 1% for approximately 30% of the lots. A high probability of SCT failures at VR could be due to insufficient control over the testing during manufacturing or due to relatively high-value limiting resistors used in testing setups for SCT screening during manufacturing. In either case such lots are not acceptable for high-reliability applications.

Table II.2. Safety margins for commercial and military-grade parts.

Part		Surge Current Testing		Scintillation Testing	
	Qty.	$M_{_SCT}$_avr, %	STD	$M_{_scint}$_avr, %	STD
Commercial	17	15.7	45.4	75.3	65.6
Military	13	39.8	52.3	143.6	66.4

A large spread of the safety margin values indicates insufficient control over the quality of the product both for military and commercial parts. The uncertainty in the electrical strength of the part is likely a major reason forcing manufacturers to suggest a significant voltage derating (up to 50% and more) to their customers. The purpose of derating is to create an additional margin to increase reliability of the part compared to the rated conditions. Most high-reliability original equipment manufacturers (OEM) employ rigorous derating programs to decrease the level of stress that the parts experience during operation and thus guarantee the necessary reliability of the product. It is typically assumed that the military-grade components have high reproducibility and uniformity of characteristics, so the same derating conditions are applied for different lots. Obviously, it might be not so for tantalum capacitors.

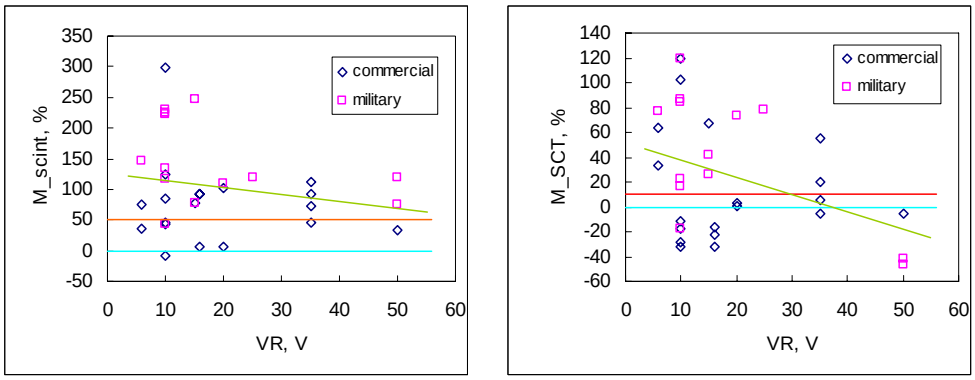

a) b)

Figure II.5. Variations of the safety margin with the rated voltage for scintillation (a) and surge current (b) breakdowns. Blue lines indicate zero levels of margin, red lines indicate acceptable levels, and green lines indicate trends.

For tantalum capacitors, the stress depends mostly upon the operating voltage, and derating is determined as a portion of the rated voltage. However, when the significance of the nominal level of VR is uncertain, derating might be unjustifiably severe for some lots and not sufficient for others. By utilizing a safety margin verification testing for screening and qualification of tantalum capacitors, the meaning of VR and its relation to quality and reliability becomes more apparent and derating can be made in a more rational and effective way.

It was shown in our previous work [1] that to assure reliability of the parts under surge current conditions, the SCT screening should be carried out at 1.1×VR. This sets a minimum level of acceptable safety margin to 10%. Considering that the average scintillation breakdown margin is roughly five times greater than the surge current margin, it is reasonable to set the acceptable limit for M_{scint} to 50%. The relevant testing procedures are discussed in Part IV of this report and should be included for screening and qualification of capacitors for space applications. The space-grade-quality lots should be also able to demonstrate that the safety margins remain within the required limits after environmental stress testing including soldering simulation, temperature cycling, and humidity testing.

II.5. Effect of the vendor and date code.

Table II.3 displays average values for breakdown voltages measured on tantalum capacitors of the same value, but manufactured by different vendors. Analysis of the data using a Student t-test at a 95% confidence level showed that only 1 μF 50 V capacitors had the same breakdown characteristics, whereas in other cases the difference was significant.

Table II.3. Effect of vendors.

Part	Mfr.	Surge Current Testing			Scintillation Testing		
		Qty.	VBR_avr	STD	Qty.	VBR_avr	STD
47 μF 20 V Commercial	A	23	33	4.7	13	43.7	8.85
	K	38	40.6	4.3	28	49.5	3.15
33 μF 35 V Commercial	A	17	66.5	8.5	-	-	-
	K	28	72.2	6.17	15	91.8	8.64
3.3 μF 10 V Military	A	15	25.7	2.44	23	29.5	2.04
	V	20	33.1	5.52	16	46.6	4.8
1 μF 50 V Military	A	16	47.2	7.65	12	155.2	15.85
	V	25	48.9	7.3	14	145.5	21.42

The effect of lot date codes for the same part types of tantalum capacitors is shown in Table II.4. Statistical analysis suggests a significant difference for both surge current (for 330 μF 10 V and 220 μF 6 V capacitors) and scintillation (for 15 μF 10 V capacitors) breakdown voltages.

As expected, breakdown voltages in same-value tantalum capacitors are vendor and lot related. This is true for both commercial and military-grade parts, and indicates the necessity of verification of the relationship between VBR and VR for each lot of capacitors for space and military applications.

Table II.4. Effect of date codes.

Part	Date Code	Surge Current Testing			Scintillation Testing		
		Qty.	VBR_avr	STD	Qty.	VBR_avr	STD
330 μF 10 V Commercial	0038	26	10.9	1.63	15	26.6	4.54
	0718	15	16.5	3.23	12	27.1	3.05
220 μF 6 V Commercial	0532	53	20.0	4.02	21	23.2	5.09
	0101	20	14.6	2.5	15	22.8	6.27
15 μF 10 V Military	0017	12	20.1	4.87	25	29.3	5.85
	0038	23	23.2	4.22	31	47.4	5.25
	0126	17	20.7	3.42	23	33.7	4.29

II.6. Temperature dependence of breakdown voltages.

Temperature dependencies of breakdown voltages were measured on eight lots of capacitors at temperatures varying from -196 ^{o}C (liquid nitrogen conditions) to +150 ^{o}C. A test matrix is shown in Table II.5. The measurements in the range of temperatures from -55 ^{o}C to +150 ^{o}C were carried out in a temperature chamber, and at -196 ^{o}C in a Teflon cell immersed in a dewar with liquid nitrogen. In the latter case, a temperature sensor was used to assure that the temperature was stabilized at the required level.

Table II.5. Test matrix for temperature dependence of breakdown voltages.

	Surge Current Test					Scintillation Test			
Part	-196 ^{o}C	-55 ^{o}C	25 ^{o}C	85 ^{o}C	125 ^{o}C	-196 ^{o}C	25 ^{o}C	125 ^{o}C	150 ^{o}C
3.3 µF 10 V	X		X		X	X	X	X	
15 µF 10 V DC0017							X	X	X
15 µF 10 V DC0038	X		X		X		X	X	X
22 µF 6 V	X		X		X	X	X		
220 µF 6 V	X	X	X	X	X	X	X	X	
10 µF 25 V	X		X		X	X	X	X	
100 µF 16 V	X		X		X	X	X	X	
47 µF 20 V		X	X	X					
15 µF 50 V	X	X	X		X				
22 µF 15 V						X	X	X	

Typical results of measurements at -196 ^{o}C, +25 ^{o}C, and +125 ^{o}C for two part types are shown in Figure II.6 and indicate that both scintillation breakdowns and surge current breakdowns decrease with temperature. In an attempt to characterize VBR(T) dependence, the results were approximated using ALTA-PRO software from ReliaSoft with Arrhenius and Eyring models. Analysis showed that the Eyring relationship provides a much better fit than the Arrhenius model. For this reason, the results presented in Figure II.6 were approximated using the Eyring model:

$$\eta_{BR}(T) = \frac{1}{T} \times \exp\left(-A + \frac{B}{T}\right), \quad (1)$$

where A and B are constants.

This equation is similar to the Arrhenius relationship and is often used to describe temperature dependence of time-dependent dielectric breakdowns when activation energy depends on the electrical field [25]. Using substitutions $E_a = -k \times B$ and $D = exp(-A)$, where E_a is activation energy and D is a constant, Eq. (1) can be rewritten in the Arrhenius-like form:

$$V_{BR}(T) = \frac{D}{T} \times \exp\left(-\frac{E_a}{kT}\right) \quad (2)$$

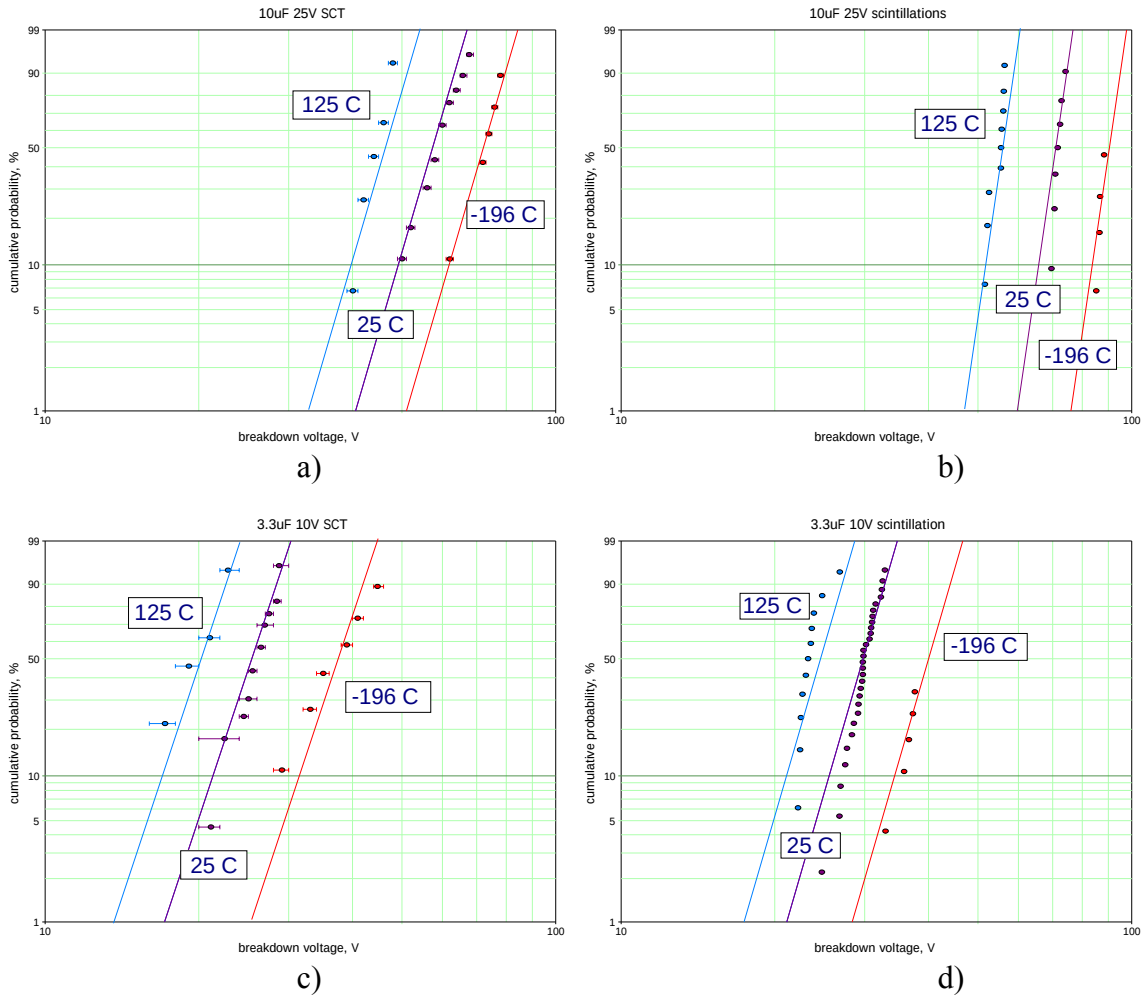

Figure II.6. Weibull plots for surge current (a, c) and scintillation (b, d) breakdown distributions measured for 10 μF 25 V (a, b) and 3.3 μF 10 V (c, d) capacitors at three temperatures. The data were approximated using an Eyring model.

To calculate parameters in Eq. (1) and (2), the slopes of Weibull distributions were assumed to be the same at each temperature, while the characteristic breakdown voltages were approximated using a maximum likelihood model. Results of calculations for five part types are shown in Table II.6. Parameters A and activation energies for scintillation and surge current breakdowns are close. The values of E_a are low and vary from 0.004 eV to 0.014 eV for scintillation breakdowns and from 0.006 eV to 0.01 eV for surge current breakdowns.

Table II.6. Parameters of Weibull/Eyring distributions.

Part	Test	Qty.	Beta	A	B	Ea, eV
3.3 µF 10 V	SCT	33	10.75	-9.30	-97.27	8.1E-03
	Scint.	58	12.28	-9.50	-110.29	9.2E-03
100 µF 16 V	SCT	73	6.29	-9.55	-122.28	1.0E-02
	Scint.	31	7.52	-9.67	-45.50	3.8E-03
10 µF 25 V	SCT	31	12.20	-10.17	-117.14	9.8E-03
	Scint.	26	24.38	-10.33	-112.95	9.4E-03
22 µF 6 V	SCT	42	6.53	-8.99	-77.45	6.5E-03
	Scint.	21	8.44	-9.45	-110.38	9.2E-03
10 µF 15 V DC0038	SCT	41	6.88	-9.17	-71.12	5.9E-03
	Scint.	57	10.66	-10.16	-167.24	1.4E-02

The effect of temperature on characteristic breakdown voltages for all lots tested in this work is shown in Figure II.7. In all cases, both VBR_CCS and VBR_SCT had similar and relatively weak temperature dependencies. Some decrease of VBR_SCT (on ~11%) at liquid nitrogen temperatures was observed for 15 µF 50 V capacitors only and might be due to high sensitivity of these parts to thermomechanical stresses. For all other capacitors, VBR decreased monotonically as the temperature increased from -196 °C to +150 °C. At this temperature range, a decrease of VBR_CCS was from 1.3 to 1.7 times and of VBR_SCT from 1.4 to 2.6 times. Estimations for the operating temperature range, from -55 °C to +85 °C, showed that the changes of surge current and scintillation breakdown voltages are similar and vary from 10% to 35% for different lots.

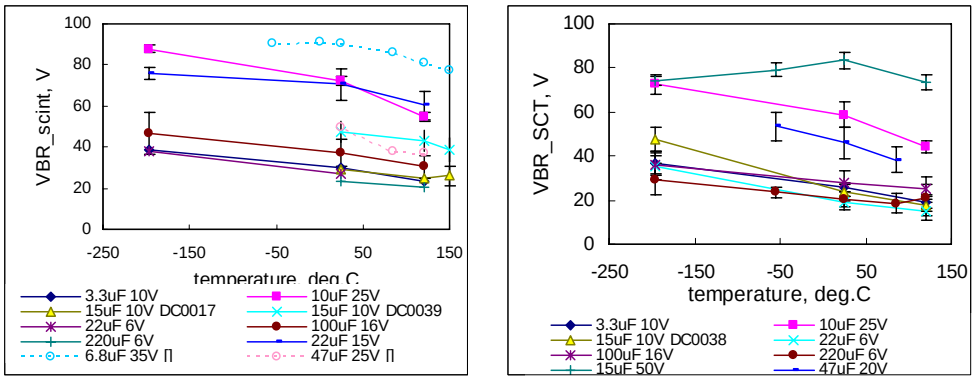

a) b)

Figure II.7. Temperature dependencies of scintillation (a) and surge current (b) breakdown voltages. Dashed lines in Figure a) show data presented for 6.8 µF 35 V capacitors by Howard and Smith [26] and for 47 µF 25 V capacitors by Franklin [5].

Our results correlate with the data reported in relevant literature. Klein [27] observed a two-fold increase (from 160 V to 80 V) during 10-second breakdown voltage measurements in Ta-Ta_2O_5-Au capacitors when temperature decreased from 360 K to 200 K. No significant variations in the breakdown behavior of thin (3 nm to 4 nm) anodic tantalum oxide films were observed in [28]. Howard and Smith [26], in 1964, published data for 6.8 µF 35 V solid tantalum capacitors tested at temperatures between -55 °C and +165 °C showing a decrease of breakdown voltages on ~22%.

Their data, together with results presented by Franklin [5] for 47 μF 25 V capacitors, are plotted in Figure II.7.a for comparison and indicate similar temperature dependencies as in our experiments.

Variations of the conductivity of manganese cathode layers with temperature probably play an important role in the observed VBR(T) dependencies. Manganese is a semiconductor with a low activation energy of ~40 meV [29], and its conductivity increases with temperature approximately two times over the operational range of temperatures, from -55 ^{o}C to +85 ^{o}C.

It has been well established by multiple studies [30] that the scintillation breakdown voltage during electrolytic formation of tantalum pentoxide layers decreases as the conductivity of the electrolyte increases:

$$VBR = a + b \times log\,(\rho), \qquad (3)$$

where a and b are constants and ρ is the specific resistivity of the electrolyte. This dependence is explained by enhanced electron emission from electrolytes having increased conductivity. Assuming that this is true for the systems with manganese cathodes and allowing for a three-fold increase in the conductivity of manganese as temperature increases from -55 ^{o}C to +85 ^{o}C, a decrease of VBR should be much less than three-fold, which is in agreement with our results.

Considering that scintillations are local events and occur in very small areas, likely a few micrometers in size, the resistivity of manganese cathode can also affect the breakdown voltage by limiting the current flowing through the breakdown site. Assuming that the size of the breakdown area is d, the constriction resistance can be estimated as $R_c = \rho_{MnO2}/d$. At ρ_{MnO2} = 1 Ohm*cm and d = 1 μm, R_c = 10,000 Ohms. Even at a scintillation current of 1 mA and larger values of d (~10 μm), the constriction resistance remains high (~1 kOhm), so the voltage drop (~1 V) would still limit the current and prevent breakdown. Obviously, a decrease of ρ_{MnO2} with temperature would decrease the voltage drop, facilitate the rate of delivery of energy to the breakdown site, and thus decrease the breakdown voltage.

Surge current breakdown voltages are also dependent on the resistivity of the manganese layer. Due to a highly developed surface area of tantalum capacitors, there is a relatively large time delay (~dozens of microseconds) for a voltage, which is instantly increased at the terminals of the capacitor, to propagate into internal areas of the tantalum pellet. This delay can be explained by presenting a schematic of the capacitor as a distributed R-C ladder [31, 32] and is responsible for a so-called roll-off effect (a decrease of capacitance with frequency). Considering that surge current breakdowns typically occur after dozens to hundreds of microseconds, the surface area of the capacitor where the voltage has reached the applied level and the breakdown might happen should be much less than the total surface area of the part. For this reason, to improve surge current behavior of tantalum capacitors, some manufacturers are forming a dielectric shell at the outer anode surface by increasing the thickness of the oxide at peripheral areas of the pellet [33].

A decrease of ρ_{MnO2} with temperature would allow for faster distribution of the signal and increase the effective area, where the breakdown might occur. This increases the probability of having a defective site in the dielectric, and thus decreases VBR_SCT. An increase in conductivity of manganese with temperature might decrease surge current breakdown voltages also because lower ESR values allow for a faster voltage rise, which as shown below is a prime factor affecting VBR.

It is possible that the effect of resistance of cathode materials on breakdown voltages is partially responsible for the difficulties with developing high-voltage and low-ESR tantalum capacitors. This problem is especially apparent in the case of capacitors with polymer cathodes [34].

II.7. Electron traps in tantalum capacitors.

As shown in the discussion section below, the difference between VBR_CCS and VBR_SCT is mainly attributed to the presence of a high concentration of electron traps in the anodic Ta_2O_5 dielectric in tantalum capacitors. To estimate the concentration of the traps, two techniques were used. The first one, a polarization/depolarization (PD) technique, consists of cycles of consequential measurements of polarization (at $V = V_p$) and depolarization (at $V = 0$) currents with time while V_p is incrementally increasing after each cycle. Integration of depolarization currents (I_d) allows for calculation of the total charge trapped in the dielectric:

$$Q_d = \int I_d \times dt \qquad (4)$$

If the thickness (h) and surface area (S) of the dielectric are known, then the concentration of the traps can be calculated as $N_t = Q_d/(e \times h \times S)$. The capacitance related to charging of the traps can be determined as a ratio of Q_d to polarization voltage: $C_t = Q_d/V_p$.

The thickness of oxide can be estimated using a formation voltage (VF), and considering that the rate of electromechanical oxidation, β, is approximately 1.7 nm/V to 2.2 nm/V. For estimations, the formation factor $m = VF/VR$ can be assumed to be equal to 3. With these assumptions, the thickness and the effective surface area of the oxide film in a capacitor can be calculated as $h = \beta \times m \times VR$ and $S = h \times C/(\varepsilon \times \varepsilon_0)$, where ε is the dielectric constant of tantalum pentoxide (ε = 27) and $\varepsilon_0 = 8.85\ 10^{-12}$ F/m is the permittivity of free space.

The second technique is a variation of the first one and is based on measurements of thermally stimulated depolarization currents (TSD), which are currents measured at 0 V and linearly increasing temperature after the sample has been polarized, typically at high voltages and temperatures. In addition to estimation of the total trapped charge per Eq. (4), this technique allows for assessment of the location of traps in the forbidden energy gap of the dielectric.

Typical results of measurements of polarization/depolarization currents for a 47 µF 20 V capacitor at 85 °C are shown in Figure II.8. During polarization, the absorption currents decrease gradually due to electron injection from the manganese cathode and filling up the traps located below the conduction band of Ta_2O_5 near the MnO_2/Ta_2O_5 interface. When the capacitor is shorted during depolarization, the charges are released from local states creating a reverse, depolarization current.

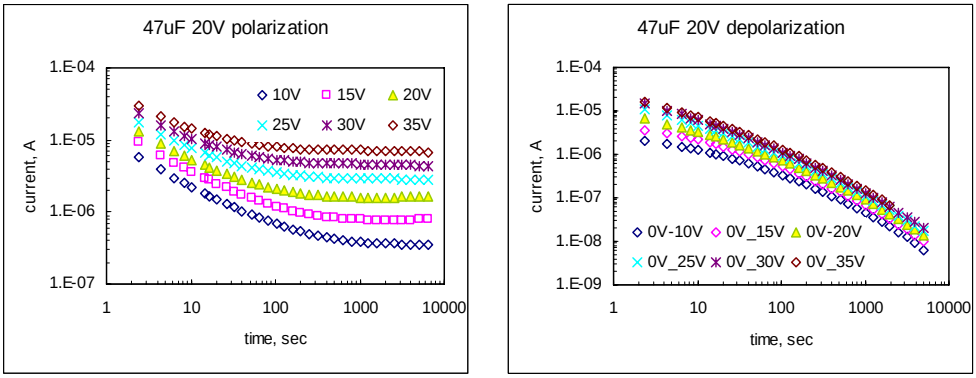

a) b)

Figure II.8. Typical polarization (a) and depolarization (b) currents in a 47 µF 20 V capacitor at 85 °C and voltages incrementally increasing from 10 V to 35 V. The legends show polarization voltages. Note that polarization and depolarization currents have different polarity.

Figure II.9 shows variations of the trapped charge with polarization voltages measured for different samples and at different temperatures. The results were reproducible for all samples and indicate capacitance of the traps Ct = 30 µF. Temperature variations in the range from 85 °C to 125 °C did not change the amount of trapped charges substantially, thus indicating that trapping is likely due to the tunnel effect. This is consistent with our previous results, in which it was shown that polarization currents remain within the same order of magnitude at room and liquid nitrogen temperatures [32].

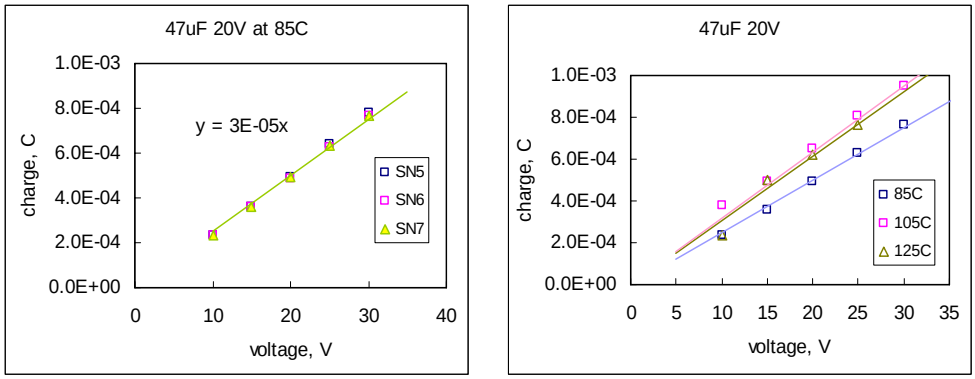

a) b)

Figure II.9. Variations of the accumulated charges, calculated as integrals of depolarization currents in Figure II.8.b, vs. polarization voltage for three samples at 85 ^{o}C (a) and for SN6 at temperatures of 85 ^{o}C, 105 ^{o}C, and 125 ^{o}C. The slope of the lines indicates capacitance of electron traps of ~30 µF.

Assessments of the thickness and surface area of the dielectric for 47 µF 20 V capacitors yields h = 140 nm and S = 270 cm^2. At V_p = 30 V, Q_t = 7.6E-4 C and N_t = 1.3E18 cm^{-3}. As Figure II.9 shows, the trapped charge does not saturate with polarization voltage even at V_p = 30 V. Note also that the trapped charge is not evenly distributed in the volume of the dielectric, but mostly accumulated near the cathode surface. This means that the global trap concentration is much greater than the estimated value, and probably exceeds 1E19 cm^{-3}.

Results of TSD measurements for three types of capacitors, 47 µF 20 V, 15 µF 50 V, and 3.3 µF 10 V, are shown in Figure II.10. Estimations of the global trap concentration gave more than 1E18 cm^{-3} for 47 µF 20 V and 3.3 µF 10 V capacitors, and 3.1E17 cm^{-3} for 15 µF 50 V capacitors, respectively. For 47 µF 20 V and 3.3 µF 10 V capacitors, the results of TSD measurements correspond to the results of the PD technique.

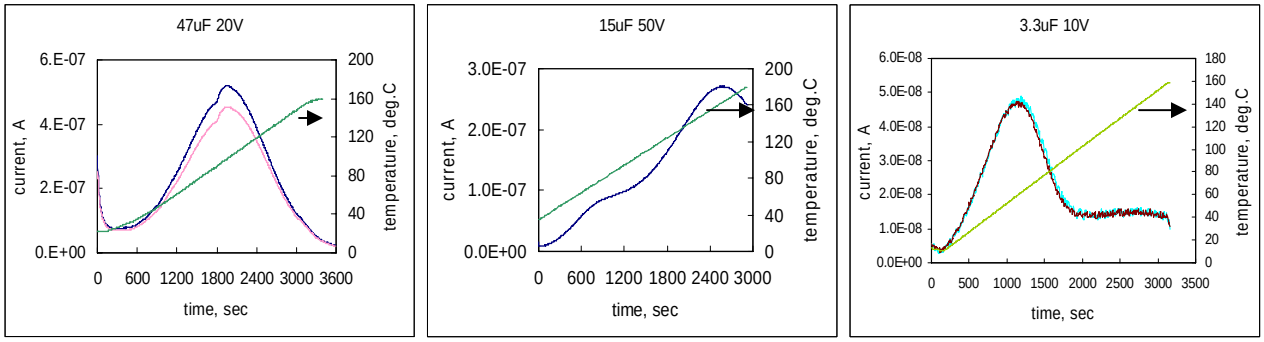

a) b) c)

Figure II.10. TSD currents in two 47 µF 20 V capacitors at polarization conditions: 20 min. at 20 V and 120 °C (a), in a 15 µF 50 V capacitor at polarization conditions: ramp at 3 °C/min. up to 175 °C at 50 V (b), and in two 3.3 µF 10 V capacitors at polarization conditions: ramp at 3 °C/min. up to 160 °C at 15 V (c). The temperature ramp during TSD measurements is 3 °C/min.

Estimations showed the presence of two energy levels, 0.25 eV and 0.45 eV below the conduction band, for the traps in 15 µF 50 V capacitors. Low-energy traps are typically associated with fast electron states in the dielectric, and as shown below, are likely responsible for the difference in scintillation and surge current breakdown voltages. The presence of fast and slow states with different energies for Ta_2O_5 dielectrics was also observed in [35].

TSD currents were measured for two types of 47 µF 20 V capacitors manufactured by different vendors. Results of these measurements are shown in Figure II.11 and indicate the presence of electron states with three distinctive energy levels in the Mfr. K parts, whereas in parts manufactured by Mfr. A only one type of trap was prevailing. Most likely, concentrations and distributions of the traps depend on the specific technological processes used and can be used to characterize quality of the oxide. However, more analysis is necessary to establish correlations between TSD spectrums, manufacturing process specifics, and breakdown voltages.

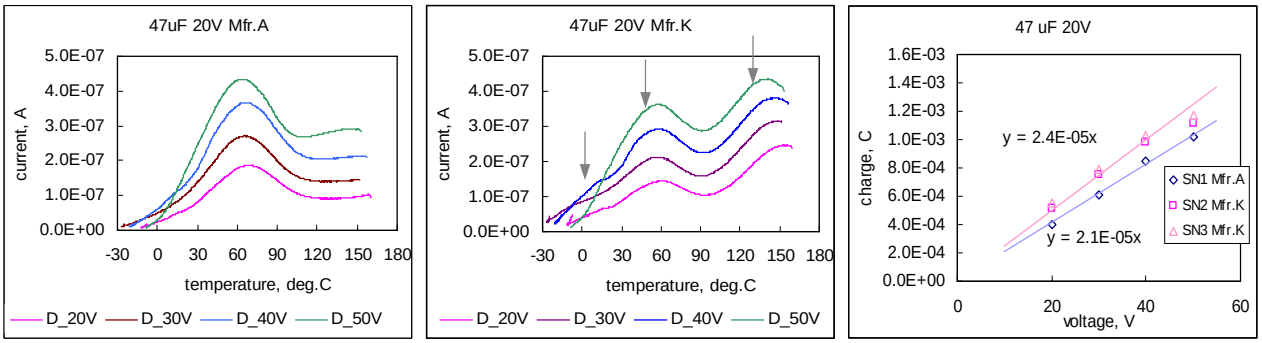

a) b) c)

Figure II.11. TSD currents at a temperature rate of 3 °C/min. in 47 µF 20 V capacitors manufactured by two vendors (a, b) after thermo-stimulated polarization at voltages from 20 V to 50 V. Arrows indicate peaks corresponding to different energy levels of the traps. Figure c) shows variations of a depolarization charge with polarization voltage. Slopes of the lines indicate capacitances of 21 µF and 24 µF.

Figure II.12 shows kinetics of depolarization currents and variations of the accumulated charge with V_p for four types of capacitors tested at room temperature. Results of calculations based on these and previously reported data are summarized in Table II.7. In all cases the concentration of traps was very high and exceeded 1E18 cm^{-3}. Assuming that N_t = 1E19 cm^{-3} and considering that the concentration of Ta_2O_5 molecules in the dielectric is ~1E23 cm^{-3}, one trap exists in every 10,000 molecules. The average distance between these traps is ~30 Å, which is still more than an order of magnitude greater compared to the length of Ta-O bond (~2.1 Å).

Note that for a 500-nm-thick Ta_2O_5 dielectric thermally grown at 500 ^oC, the density of trapping centers was much lower, from 1E15 cm^{-3} to 1E16 cm^{-3} [36]. In high-quality thermally grown SiO_2 layers, the concentration of traps is very low (below 1E11 cm^{-3}), but increases by several orders of magnitude (to 1E18 cm^{-3} – 1E19 cm^{-3}) with time under high electrical fields due to field-induced trap generation [25, 37] prior to time-dependent dielectric breakdown (TDDB).

Table II.7. Trap concentration in capacitors.

Capacitor	d, nm	S, cm^2	C_t, µF	N_t	N_t_TSC
47 µF 20 V	140	270	30	1.3E18	1.1E18
22 µF 6 V	42	39	8	9.5E18	
22 µF 15 V	106	97	5	1.4E18	
33 µF 10 V	70	97	4	1.0E18	
3.3 µF 10 V	70	9.7	0.8	1.5E18	4.5E18
15 µF 50 V	320	270	-	-	3.1E17

Electron traps in Ta_2O_5 dielectrics are typically associated with oxygen vacancies and broken or stressed atomic bonds. A high concentration of electron traps observed in all tested tantalum capacitors indicates a much more disordered structure of electrochemically grown Ta_2O_5 dielectrics compared to the thermally grown oxides.

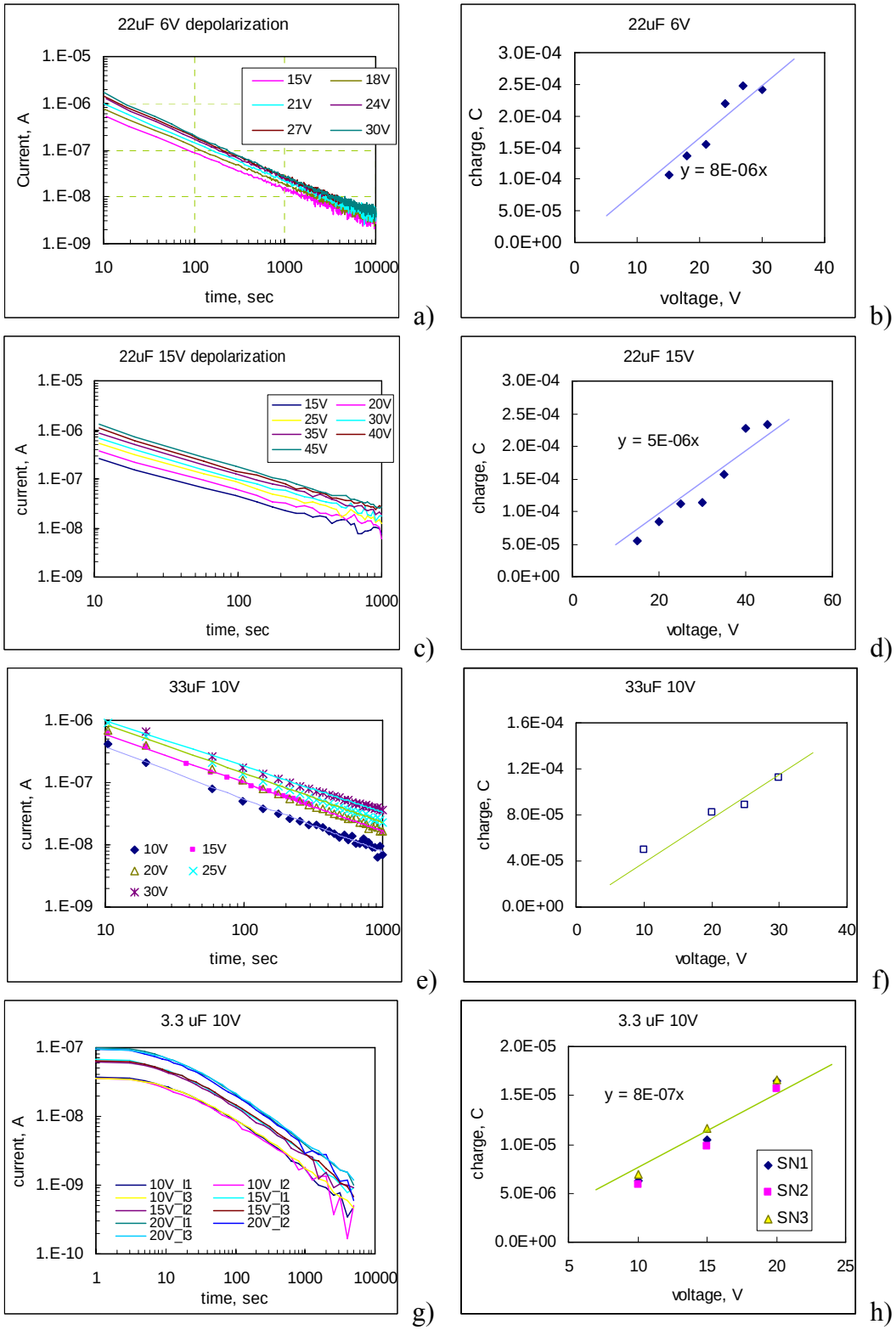

Figure II.12. Depolarization currents (a, c, e, g) and variations of trapped charges with polarization voltage (b, d, f, h) for 22 µF 6 V (a, b), 22 µF 15 V (c, d), 33 µF 10 V (e, f), and 3.3 µF 10 V (g, h) capacitors. The legends show polarization voltages and serial numbers of the samples.

II.8. Is proofing technique effective?

If surge current failures occur at the same defective sites of the Ta_2O_5 dielectric as scintillation breakdowns and a surge current breakdown can be imagined as a sustained scintillation, then CCS testing of capacitors should change results of surge current testing. Assuming that the self-healing after scintillation is complete, VBR_SCT measured on the post-scintillation-tested parts should be greater compared to surge current breakdown voltages measured on virgin parts. In this case, the probability of turn-on failures would be decreased. This assumption originates from the basis of the proofing technique suggested to improve reliability of solid chip tantalum capacitors after soldering them onto a board [16, 18]. Obviously, if the self-healing is not complete and scintillation testing results in degradation of breakdown voltages, then the distribution of VBR_SCT would shift towards low voltages and proofing would increase the probability of turn-on failures.

To evaluate the effect of CCS testing on VBR_SCT, a comparative step stress surge current testing (3SCT) was carried out on virgin capacitors and post-CCS capacitors from 15 different lots. Results of these tests are shown in Figure II.13 and suggest that scintillation testing did not change characteristic breakdown voltages and/or slopes of the distributions compared to the virgin parts. This means that scintillation events do not affect the probability of surge current failures and that the proofing technique is not justified.

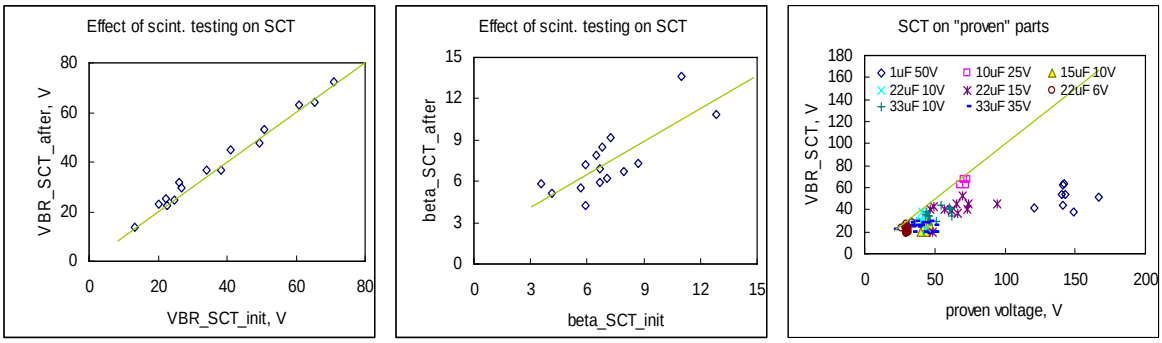

a) b) c)

Figure II.13. Correlation between characteristic values (a) and slopes (b) of distributions of surge current breakdown voltages measured on 15 lots of virgin capacitors and capacitors after scintillation breakdown testing. Figure c) shows results of SCT on eight lots, which had no scintillations below the proven voltage.

To confirm this conclusion further, from five to 12 samples from eight different lots of capacitors were "proven" by increasing voltage during the CCS test to a voltage V_{pr}, which was chosen to be equal approximately to the median of the relevant VBR_CCS distribution. Parts that did not exhibit scintillations were used for 3SCT to determine the value of VBR_SCT. Note that this procedure allows for selection of parts with VBR_CCS exceeding the proven voltage. Correlation between VBR_SCT and V_{pr} is shown in Figure II.13.c and suggests that the surge current failures occur at voltages significantly lower than the proven voltage.

II.9. Discussion.

Electrical breakdowns in dielectrics might be caused by a variety of alternative mechanisms including impact ionization, electromechanical, thermal, or thermochemical processes. Literature analysis shows that different aspects of failures and breakdowns in anodic Ta_2O_5 films are mostly explained using thermochemical, field-induced crystallization, and electron impact ionization models. Below is a brief description of these models and analysis of their applicability for scintillation and surge current breakdowns in tantalum capacitors.

II.9.1. Thermochemical model.

According to the thermochemical model developed by McPherson and co-workers [20, 38], electrical breakdown in oxides occurs when a local electrical field weakens bonds in polar molecules to the level at which thermal energy is sufficient to cause the breakage. A local electric field, which distorts the bonds, is a superposition of an external field and the Lorentz-Mossotti fields, and for dielectrics with high dielectric constants (ε) it might substantially exceed the external field (E). As molecular bonds break, a conductive pass is formed, and conditions for a thermal breakdown develop. This model also predicts that the time-dependent dielectric breakdown follows the E-model, and the time to failure can be expressed as:

$$TF = t_o \times \exp\left(-\gamma E + \frac{\Delta H}{kT}\right), \tag{5}$$

where ΔH is activation energy required for displacement of ions from their normal bonding positions, γ is the field acceleration parameter, and t_o is a time constant. Note that this equation is a form of a general Eyring model, which is often used to describe TDDB in dielectrics [39, 40] or times to failure in tantalum capacitors [41, 42].

The value of γ depends on the dielectric constant and dipole moment of the molecule (p_0):

$$\gamma = \frac{p_0\left(\frac{2+\varepsilon}{3}\right)}{kT} \tag{6}$$

Assuming that an instant breakdown occurs at TF = t_0, a substitution to Eq.(5) allows for calculation of the breakdown field:

$$E_{BR} = \frac{\Delta H}{p_0\left(\frac{2+\varepsilon}{3}\right)} \tag{7}$$

For Ta_2O_5 dielectrics, ΔH is in the range from 1.7 eV to 2 eV and p_0 varies from 5 e-Å to 13 e-Å. At these conditions the value of E_{BR} calculated per Eq. (7) varies from 1.3 MV/cm to 4 MV/cm, which is close to the experimental data reported in relevant literature, from 2 MV/cm to 7 MV/cm [27, 28, 43].

As was shown in Part I of this report, the thermochemical model, with some adjustment of parameters γ and ΔH caused by the trapping effects, can likely describe TDDB in Ta_2O_5 at long time durations and might be used to predict failures in tantalum capacitors. However, it predicts an increase of VBR at shorter time durations, which does not agree with the results of our experiments.

II.9.2. Field-induced crystallization.

A field-induced growth of TaO_2 crystals is believed to be a mechanism of failures specific to tantalum capacitors. A review of works carried out mostly on wet tantalum capacitors before 1961 is given by Young [44]. A review of existing literature as applicable to crystallization in solid tantalum capacitors was published by Tripp and Freeman in 2008 [45].

The field-induced crystallization model assumes that tantalum oxide crystals are growing with time of operation under the amorphous anodic tantalum pentoxide dielectric and eventually disrupt the amorphous layer, causing a breakdown. Until the moment of disruption, the integrity of the dielectric is not compromised and no changes in leakage currents are observed. Tantalum oxide crystals and fractured dielectric layers were observed on the surface of wet and solid tantalum capacitors after high-voltage electrical stresses. However, Ikonopisov [30] suggested that the formation of crystals is a result of breakdown, rather than their prime cause. It is well established that at high temperatures, more than 500 ^{o}C, amorphous Ta_2O_5 crystallizes, so high local temperatures at scintillation breakdown sites might stimulate a fast conversion of the amorphous dielectric into a crystal. A correlation between the probability of crystallization and failures in tantalum capacitors during high-temperature testing was studied recently by Zednichek and co-workers [46]. Their results indicate that field crystallization may not be the only or even the main driving process responsible for failures. In our experiments, we observed a substantial rise of leakage currents (DCL) with time in chip tantalum capacitors at voltages exceeding VR by two to three times. Most importantly, these changes of DCL were reversible, and leakage currents decreased substantially after annealing. These data, as well as observed changes in I-V characteristics in post-high-voltage-stress capacitors, are indicative to the field-induced trap generation or ion charge instability mechanisms rather that to the crystal growth.

Field crystallization might be responsible for time-dependent breakdowns, likely in high-voltage capacitors and at high temperatures [46], but this mechanism cannot explain the difference between scintillation and surge current breakdowns.

II.9.3. Electron impact ionization.

Classical theories (Von Hippel, Frohlich) [47] ascribed breakdowns in dielectric films to electron avalanches produced by impact ionization. The avalanche breakdown is followed by a thermal runaway resulting in destruction of the dielectric. These so-called intrinsic breakdown events occur uniformly in the whole specimen and do not vary with time of voltage application.

Klein [27] suggested a model of time-dependent avalanche breakdowns in insulations and in Ta_2O_5 dielectrics in particular. According to this model, electrons injected in a conduction band of the dielectric cause impact ionization and produce a finite avalanche of free electrons, leaving behind nearly immobile positive charges. These electrons are swept out in picoseconds, while positive charges drift to the cathode slowly (microseconds to milliseconds). The positive charges temporarily enhance the electrical field at the cathode, create a positive feedback, and greatly increase the rate of electron injection. At high enough fields, further avalanching occurs, resulting in local instability, current runaway, and destructive breakdown at a small spot on the surface. However, at lower fields, in most cases the positive charge clusters leave the insulator without further effects, and no breakdown occurs. Many harmless avalanches might happen under electrical stress until at one spot the chance event of a succession of avalanches leads to an instability and breakdown. The enhancement of the electric field increases the chance of injected electrons hitting the cluster and reduces the time to instability. For the thermoionic injection that

occurs at the cathode of Ta_2O_5 dielectrics, the time to instability is an exponential function of the field, $\tau \sim exp(-b \times E^{0.5}/kT)$. However, the electron impact model cannot adequately account for the TDDB phenomena occurring over a long period of time [40].

According to this mechanism, similar to the thermochemical model, breakdown voltages in dielectrics should decrease with time of testing. However, this model also predicts a substantial variation of VBR due to formation of space charges near the cathode. Processes such as trapping of injected electrons or drifting of ions and relevant redistributions of charges in the oxide would cause distortion of the electrical field near the cathode and enhance or decrease the probability of breakdown.

II.9.4. Mechanism of scintillation breakdowns.

It is generally accepted that scintillation breakdowns during electrochemical oxidation of tantalum are due to electron impact ionization and avalanching. It is reasonable to assume that scintillation breakdowns in solid tantalum capacitors are caused by the same physical mechanism. Electron conduction in Ta_2O_5 films is related to the mechanism of breakdown, and its analysis can provide additional information regarding the physical nature of scintillation events.

Multiple studies have shown that the electron transport in Ta_2O_5 is due either to a bulk-limited Poole-Frenkel (PF) mechanism or surface-barrier-limited Schottky mechanisms [36, 48, 49]. Figure II.14 illustrates these mechanisms of conductivity.

The current density for PF conduction depends on the energy level of the traps, U_t, through which electrons are hopping:

$$J_{PF} = C_t E \exp\left(-\frac{U_t}{kT}\right)\exp\left[\frac{1}{kT}\left(\frac{q^3 E}{\pi\varepsilon\varepsilon_0}\right)^{1/2}\right], \quad (8)$$

where C_t is a trap-density-related constant, E is the electric field, q is the charge of electron, k is the Boltzmann constant, and T is the absolute temperature; and ε_0 is the permittivity of the free space, and ε is the high-frequency dielectric constant for Ta_2O_5.

According to the Schottky mechanism the current is limited by a surface barrier, $q\Phi_B$, and the current density is also an exponential function of $E^{1/2}$:

$$J_{Sch} = C_{RD} T^2 \exp\left(-\frac{q\Phi_B}{kT}\right)\exp\left[\frac{1}{kT}\left(\frac{q^3 E}{4\pi\varepsilon\varepsilon_0}\right)^{1/2}\right], \quad (9)$$

where C_{RD} is the Richardson-Dushman constant.

The similarity of J(E) and J(T) characteristics described by Eq. (8) and (9) makes discrimination of the PF and Schottky mechanisms a rather challenging task. This is especially true for tantalum capacitors having large surface areas and non-uniform thickness of the dielectric.

Nevertheless, detailed analysis of I-V curves and calculation of parameters of PF and Schottky models for capacitors with relatively small surface areas showed that both mechanisms are present. At low fields (below ~0.8 MV/cm) Schottky emission dominates, whereas at higher fields the process is controlled by the PF mechanism [50]. This is also in agreement with the results reported in [43, 51].

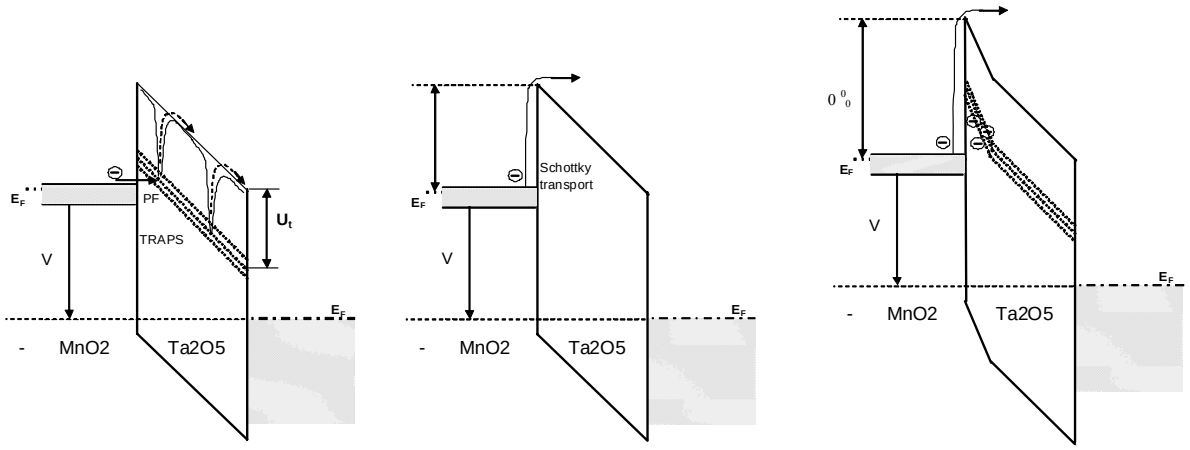

a) b) c)

Figure II.14. Energy diagram of a tantalum capacitor with manganese cathode illustrating Poole-Frenkel conduction (a), Schottky conduction (b), and Schottky conduction after electron trapping (c). Figure b) corresponds with conditions for surge current and Figure c) for scintillation breakdowns.

The fact that at high fields the PF mechanism is prevailing apparently contradicts the electron impact model of the scintillation breakdown. Obviously, at a high trap concentration, short distances between the traps (~30 A) do not allow for accumulation of sufficient energy to cause impact ionization and avalanche breakdown. However, both mechanisms coexist and contribute to the current in tantalum capacitors [43]. This means that Schottky emission still occurs at high fields, and hence injection of electrons into conduction band of Ta_2O_5 can cause avalanching and scintillation breakdown.

II.9.5. Mechanism of surge current breakdowns.

The following experimental facts indicate that scintillation and surge current breakdowns have the same physical nature.

1. The slopes of Weibull distributions for scintillation and surge current breakdown voltages are similar.
2. Both types of breakdowns have similar, relatively weak, temperature dependencies.
3. Typically, a dramatic acoustic effect is observed during explosions caused by surge current breakdowns. Less known is that a short pulse of light emission occurs prior to the explosion. This emission was observed in our experiments when breakdown events in tantalum capacitors soldered onto an FR4 board were filmed (see Figure II.15). This emission is ascribed to recombination processes of carriers produced by impact ionization and is a characteristic of avalanche breakdowns [27]. This suggests that similar to scintillation breakdowns, electron avalanching also accompanies surge current events.

Figure II.15. Three consecutive shots made during filming of the surge current breakdown events in tantalum capacitors soldered onto a board. The picture in the middle shows a light emission from the capacitor under test.

Typically, the faster the voltage increase the greater the breakdown voltage of a dielectric is, and VBR measured using short pulses is normally greater than VBR measured at quasi-DC conditions, when voltage increases slowly. This is not the case for chip tantalum capacitors, where a fast voltage increase during SCT results in much lower breakdown voltages compared to the scintillation testing. However, Klein's model indicates that in the presence of space charges the electrical strength of the dielectric film can change substantially.

Several studies have reported on anomalous decrease of VBR at enhanced rates of voltage increase, and in all cases the anomaly was explained by the electron-trapping effects.

Inuishi [52] observed a significant difference in pulse and DC breakdown fields in KCl crystals with F-centers introduced by gamma radiation. Breakdown fields measured using 10 μs pulses were ~40% lower than those measured at DC conditions. The result was explained by the field distortion caused by electrons trapped at the F-centers, thus changing the probability of electron-impact avalanche breakdown. During DC measurements, electrons trapped on the F-centers at the cathode surface suppressed electron emission and thus increased the breakdown field, whereas step-rise impulse breakdown was not affected by F-centers due to insufficient time for trapping.

A study of electrical characteristics of TiO_2 nanocrystals [53] showed that electrical breakdown under pulsed conditions can occur at lower voltages (up to two times) as compared to quasi-DC biasing. A model used to explain these observations was based on the presence of a high concentration of electron traps (~1E17 cm^{-3}). A fast increase of an external electric field releases electrons from the traps, and at high enough fields the emitted electrons undergo impact ionization and cause breakdown. However, if the voltage changes slowly, then most of the trapped charge would gradually be emitted and drift out of the device before the creation of high electric fields. In such a case breakdown occurs at greater voltages.

As seen in Section II.8, anodic Ta_2O_5 has a high concentration of electron traps, and the observed difference between VBR_CCS and VBR_SCT can be explained using a mechanism similar to the one suggested by Inuishi [52]. At a fast voltage increase, which is typical for SCT, the traps do not have time to change their state substantially, and breakdown is due to impact ionization and avalanching according to Klein's mechanism [27]. Considering the highly developed surface area of the Ta_2O_5 dielectric, the breakdown occurs locally at an asperity where the electric field is high enough to cause repetitive avalanches. When successive avalanches occur at conditions favorable to accelerated multiplications, the breakdown transfers into a thermal runaway and causes destruction of the capacitor due to the exothermic oxidation of tantalum.

At a slow voltage increase, electrons injected at low voltages have enough time to be trapped in the dielectric at the cathode surface and their charge builds up with time. An increase in the

charge enhances the barrier at the cathode, as shown in Figure II.14.c. This reduces emission of electrons, so a higher electric field is necessary to cause conditions for avalanching and a scintillation breakdown.

The concentration and energy levels of electron states most likely depend on the technological history of the dielectric, and their variations from lot to lot might be responsible for the variations in the ratio of VBR_CCS/VBR_SCT.

Long-term operation of a capacitor under high-voltage stresses might cause additional trap generation, charging of slow traps, and/or redistribution of oxygen vacancies in the dielectric. This would cause further changes in the field distribution in the oxide and in breakdown voltages. More study is necessary to analyze possible mechanisms of charge distribution and their effect on reliability of tantalum capacitors. For a preliminary assessment of this effect, the values of VBR_CCS and VBR_SC were measured on 13 different lots after highly accelerated life testing (HALT) at room temperature and voltages varying from 2×VR to 3×VR. Results of these tests are shown in Figure II.16 and confirm a trend of increasing for both surge current and scintillation breakdown voltages. An increase in the scintillation breakdown voltages was more distinct, and on average VBR_CCS rose by 29%, whereas VBR_SCT rose by 11%.

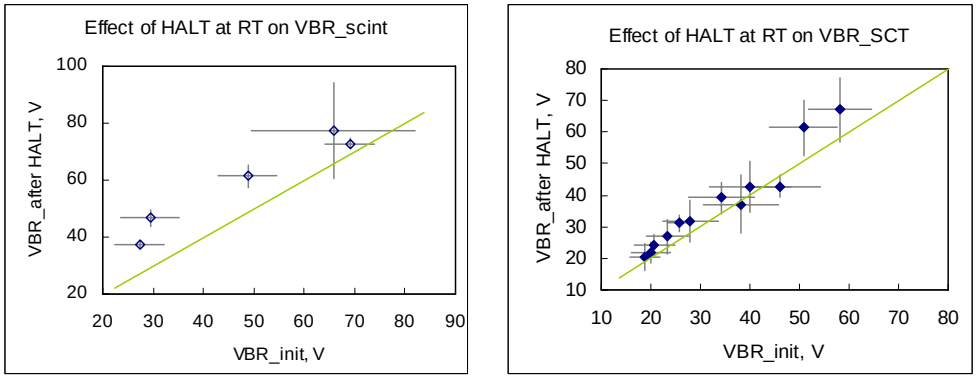

a) b)

Figure II.16. Effect of long-term (~100 to 200 hours) bias at room temperature and high voltages (two to three times VR) on average values of scintillation (a) and surge current (b) breakdown voltages.

II.10. Conclusions.

1. Distributions of scintillation and surge current breakdown voltages were measured on 13 military-grade and 17 commercial lots of solid tantalum capacitors. Analysis of these distributions showed the following:
   - 1.1. In all cases scintillation breakdown voltages significantly exceeded surge current breakdown voltages. On average VBR_CCS exceeded VBR_SCT by 50%.
   - 1.2. The slopes of Weibull distributions for scintillation and surge current breakdown voltages were similar, indicating similarity in the mechanisms of breakdowns.
   - 1.3. Scintillation breakdown voltages are on average 3.5 times greater and surge current breakdown voltages are 2.4 times greater than the rated voltages of the parts. However,

the spread of the ratios VBR_CCS/VR and VBR_SCT/VR was large, so the rated voltage is not a reliable indicator of the electrical strength of tantalum capacitors.

1.4. Breakdown voltages for capacitors rated to the same voltage decrease with the value of capacitance. This is due to a higher probability of having a defect in parts with larger surface areas and indicates the necessity of more thorough quality control for high-CV capacitors. Note also that scintillation breakdown in high-CV parts, similar to surge current events, might result in ignition of capacitors.

1.5. A high probability of failures at VR (more than 1%) during surge current testing was observed in 23% of military-grade and in 47% of commercial lots of tantalum capacitors. This result indicates deficiencies in the existing quality assurance system for both commercial and military parts.

1.6. Breakdown voltages in chip tantalum capacitors are lot related, and parts rated to the same values and voltages but manufactured by different vendors or having different date codes, had significantly different surge current and scintillation breakdown voltages.

2. The quality of tantalum capacitors can be characterized by a breakdown margin, which is calculated using a minimal breakdown voltage in a group of samples from a given lot. Based on analysis of statistical data, the acceptable level of margin for high-quality parts should be 10% for surge current breakdowns and 50% for scintillation breakdowns.

2.1. There is a trend of decreasing of the safety margin for VBR_SCT and VBR_CCS as the rated voltage and/or capacitance increases. This makes employment of the margin verification testing especially important for high-CV parts.

2.2. The surge current and scintillation breakdown margins for military-grade parts were somewhat higher than for commercial parts. However, the spread of the data was large, and also military-grade parts are not available with high CV values, so there might be no substantial difference in the quality of the military and commercial products.

2.3. Utilization of margin verification testing during screening and qualification of tantalum capacitors would guarantee an acceptable level of breakdown voltages in the lot and make voltage derating more effective.

3. Both scintillation and surge current breakdown voltages have similar temperature dependencies, which can be described using an Eyring model. In the operating temperature range from -55 ^{o}C to +85 ^{o}C, the breakdown voltages decrease with temperature on average by 10% to 35%.

4. Electron traps in Ta_2O_5 dielectrics for seven types of tantalum capacitors have been characterized using a polarization/depolarization technique and thermally stimulated depolarization techniques. The results indicate the presence of fast and slow electron states with different energy levels and a high total concentration of the traps (up to 1E19 cm^{-3}) near the manganese/oxide interface.

5. A gradual, controllable increase of the voltage across tantalum capacitors to the “proven” level does not guarantee that the surge current breakdown will not occur at lower voltages. This indicates that the proofing technique might not assure reliable operation of the parts after soldering them onto a board.

6. The physical nature of both scintillation and surge current breakdowns is impact ionization caused by thermal emission of electrons over the barrier at the manganese/oxide interface.

This impact ionization is followed by avalanche and thermal breakdowns with different consequences depending on the availability of the current at the breakdown site. The breakdown occurs locally at an asperity in electrodes or at a defective site of the tantalum pentoxide dielectric with a low electrical strength.

6.1. During surge current breakdown events, the voltage across the capacitor rises rapidly so no trapping of electrons at the energy states in the bandgap of the Ta_2O_5 dielectric occur. This is possible only if a fast delivery of charges, and respectively, high instant currents, can be provided by the power supply system. In this case the post-avalanche thermal breakdown is sustained and the failure develops into an explosion due to exothermic reaction of oxidation of the tantalum pellet.

6.2. When the voltage increases slowly, as occurs during scintillation breakdowns, electrons injected at low fields become trapped at the fast states in the oxide, resulting in a building-up of charges near the surface and raising the energy barrier at the cathode/Ta_2O_5 interface. The increased barrier requires higher voltages to provide the level of electron injection necessary for avalanching. Due to limited current in the system, the thermal breakdown in Ta_2O_5 is not sustained, the voltage at the breakdown site drops momentarily, and the released energy is likely sufficient only for creation of a local overheating in the manganese cathode layer. This local overheating might cause reduction and conversion of the conductive MnO_2 into lower-oxide, high-resistive forms, thus further limiting current at the breakdown site (a self-healing mechanism). Note that during scintillation events in high-CV capacitors, energy stored in the part might be sufficient to sustain local thermal breakdown and cause catastrophic failure.

6.3. In the suggested model, the rate of voltage increase determines the breakdown voltage, and high current spikes that always go along with fast voltage rising are merely by-products of the process rather than the prime cause.

6.4. An anomalous characteristic of the time-dependent breakdown in tantalum capacitors, for which the higher the rate of the voltage increase, the lower the breakdown voltage, is due to the presence of electron traps in anodic Ta_2O_5 dielectrics. A high concentration of fast electron states is a characteristic feature of anodic Ta_2O_5 dielectrics and is the major reason for scintillation breakdown voltages being significantly greater than the surge current breakdown voltages.

7. Long-term high-voltage stresses at room temperature increase surge current and scintillation breakdown voltages in tantalum capacitors by 10% to 30%. This might be due to relatively slow processes of charge trapping at electron states with deeper energy levels in the dielectric.

II.11. References to Part II.

[1] A. Teverovsky, "Effect of surge current testing on reliability of solid tantalum capacitors," The 28th Symposium for Passive Components, CARTS'08, Newport Beach, CA, 2008.

[2] A. Teverovsky, "Scintillation breakdowns in chip tantalum capacitors," Proceedings of IMAPS CZ 2008, 2008, pp. XL-LII.

[3] J. D. Moynihan and A. M. Holladay, "Effectiveness of surge current screening of solid tantalum capacitors," CARTS 1983, Phoenix AZ, 1983.

[4] A. Teverovsky, "Scintillation breakdowns in chip tantalum capacitors," 2008 IMAPS CZ, Brno, Czech Republic, 2008.
[5] R. W. Franklin, "Surge current testing of resin dipped tantalum capacitors," *AVX Technical Information*, 1985.
[6] D. Mattingly, "Increasing reliability of SMD tantalum capacitors in low impedance applications," *AVX Technical Information*, 1995.
[7] H. W. Holland, "Effect of high current transients on solid tantalum capacitors," *Kemet Engineering Bulletin*, 1996.
[8] A. Teverovsky, "Effect of inductance and requirements for surge current testing of tantalum capacitors," CARTS'03, 26th Symposium for Passive Components, Orlando, FL, 2006.
[9] J. Gill, "Surge in solid tantalum capacitors," *AVX Technical Information*, 1995.
[10] B. S. Mogilevsky, "Surge current failure in solid electrolyte tantalum capacitors," *IEEE Transactions on Components, Hybrids, and Manufacturing Technology*, vol. 9, 1986, pp. 475-479.
[11] P. Fagerholt, "A new view on failure phenomena in solid tantalum capacitors," 16th Capacitors and Resistors Technology Symposium, CARTS'96, 1996.
[12] M. J. Cozzolino and R. C. Straessle, "Design, characteristics, and failure mechanisms of tantalum capacitors," 8th CARTS'88, San Diego, CA, 1988.
[13] E. K. Reed, "Tantalum chip capacitor reliability in high surge and ripple current applications," 44th Electronic Components and Technology Conference, 1994.
[14] A. Teverovsky, "Effect of mechanical stresses on characteristics of chip tantalum capacitors," *IEEE Transactions on Device and Materials Reliability*, vol. 7, 2007, pp. 399-407.
[15] J. Marshall and J. Prymak, "Surge step stress testing of tantalum capacitors," 21st Capacitors and Resistors Technology Symposium, CARTS'01, 2001.
[16] K. Lai, E. Chen, P. Blais, P. Lessner, B. Long, A. Mayer, and J. Prymak, "Step surge stress test (SSST) defines dielectric capability," CARTS in Asia, Taiwan, 2007.
[17] J. D. Prymak, "Performance issues for polymer cathodes in Al and Ta capacitors," CARTS USA 2001, 2001.
[18] B. Long, M. Prevallet, and J. D. Prymak, "Reliability effects with proofing of tantalum capacitors," 25th Symposium for Passive Components, CARTS'05, Palm Springs, CA, 2005.
[19] C. R. Sullivan and A. M. Kern, "Capacitors with fast current switching require distributed models," 32nd Annual Power Electronics Specialists Conference. PESC 2001, 2001.
[20] J. W. McPherson, J. Kim, A. Shanware, H. Mogul, and J. Rodriguez, "Trends in the ultimate breakdown strength of high dielectric-constant materials," *IEEE Transactions on Electron Devices*, vol. 50, 2003, pp. 1771-1778.
[21] A. Teverovsky, "Effect of surge current testing on reliability of solid tantalum capacitors," CARTS'08, 28th Symposium for Passive Components, Newport Beach, CA, 2008.
[22] J. Primak, P. Blais, B. Long, A. Ifri, and E. Jones, "Alternate methods of defining dielectric quality using step stress surge testing and scintillation testing," 2008 Components for Military and Space Electronics Conference, San Diego, CA, 2008.
[23] J. Hossick-Schott, "Prospects for ultimate energy density of oxide-based capacitor anodes," CARTS Europe, Barcelona, Spain, 2007.

[24] H. Domingos, J. Scaturro, and L. J. Hayes, "Breakdown voltage of discrete capacitors under single-pulse conditions," *IEEE Transactions on Components, Hybrids, and Manufacturing Technology*, vol. CHMT-4, 1981, pp. 545-552.
[25] D. Qian and D. Dumin, "The electric field, oxide thickness, time and fluence dependences of trap generation in silicon oxides and their support of the E-model of oxide breakdown," Proceedings of the 7th International Symposium on the Physical and Failure Analysis of Integrated Circuits, 1999, pp. 145-150.
[26] L. Howard and A. Smith, "Dielectric breakdown in solid electrolyte tantalum capacitors," *IEEE Transactions on Component Parts,* vol. 11, 1964, pp. 187-193.
[27] N. Klein, "A theory of localized electronic breakdown in insulating films," *Advances in Physics*, vol. 21, 1972, pp. 605-645.
[28] Y. Jeliazova, M. Kayser, B. Mildner, A. Hassel, and D. Diesing, "Temperature stability of thin anodic oxide films in metal/insulator/metal structures: A comparison between tantalum and aluminum oxide," *Thin Solid Films*, vol. 500, 2006, pp. 330-335.
[29] J. Pavelka, J. Sikula, P. Vasina, V. Sedlakova, M. Tacano, and S. Hashiguchi, "Noise and transport characterization of tantalum capacitors," *Microelectronics Reliability*, vol. 42, 2002, pp. 841-847.
[30] S. Ikonopisov, "Theory of electrical breakdown during formation of barrier anodic films," *Electrochemica Acta.*, vol. 22, 1977, pp. 1017-1082.
[31] J. D. Prymak, "New tantalum capacitors in power supply applications," 1998 IEEE Industry Applications Conference, 1998, Thirty-Third IAS Annual Meeting, 1998.
[32] A. Teverovsky, "Performance and reliability of solid tantalum capacitors at cryogenic conditions," 7th International Workshop on Low Temperature Electronics, WOLTE-7, ESTEC, Noordwijk, The Netherlands, 2006.
[33] S. Zednicek, I. Horacek, J. Petrzilek, P. Jacisko, P. Gregorova, and T. Zednicek, "High CV tantalum capacitors – Challenges and limitations," CARTS Europe, Helsinki, Finland, 2008.
[34] E. Reed, "Characterization of tantalum polymer capacitors," Report, NASA Electronic Parts and Packaging Program, 2006.
[35] J. Sikula, V. Sedalkova, H. Navarova, J. Hlavka, M. Tacano, and Z. Sita, "Noibium oxide and tantalum capacitors: Leakage current, restoring voltage and reliability," 28th CARTS, Newport Beach, CA, 2008.
[36] C. Chaneliere, J. Autran, R. Devine, and B. Balland, "Tantalum pentoxide (Ta_2O_5) thin films for advanced dielectric applications," *Material Science and Engineering*, vol. R22, 1998, pp. 269-322.
[37] D. Dumin, J. Maddux, R. Scott, and R. Subramoniam, "A model relating wearout to breakdown in thin oxides," *Electron Devices, IEEE Transactions on*, vol. 41, 1994, pp. 1570-1580.
[38] L. McPherson, J. Kim, A. Shanware, H. Mogul, and J. Rodriguez, "Proposed universal relationship between dielectric breakdown and dielectric constant," Digest International Electron Devices Meeting, IEDM '02, 2002.
[30] E. Loh, "Development of a model for voltage degradation of various dielectric materials," *IEEE Transactions on Components, Packaging, and Manufacturing Technology*, vol. 4, 1981, pp. 536-544.
[40] M. Kimura, "Field and temperature acceleration model for time-dependent dielectric breakdown," *IEEE Transactions on Electron Devices*, vol. 46, 1999, pp. 220-229.

[41] B. Goudswaard and F. J. J. Dreisens, "Failure mechanism of solid tantalum capacitors," *Electrocomponent Science and Technology*, vol. 3, 1976, pp. 171-179.
[42] S. D. Khanin, "Electrical destruction of amorphous tantalum and niobium oxide films," Proceedings of the 4th International Conference on Conduction and Breakdown in Solid Dielectrics, 1992.
[43] E. Atanassova and A. Paskaleva, "Breakdown fields and conduction mechanisms in thin Ta_2O_5 layers on Si for high density DRAMs," *Microelectronics Reliability*, vol. 42, 2002, pp. 157-173.
[44] L. Young, *Anodic Oxide Films,* London and New York: Academic Press, 1961.
[45] T. Tripp and Y. Freeman, *Major Degradation Mechanisms in Tantalum and Niobium Based Capacitors,* Huntsville, AL: Components Technology Institute, 2008.
[46] S. Zednicek, J. Sikula, and H. Leibovitz, "A study of field crystallization in tantalum capacitors and its effect on DCL and reliability," CARTS Europe, Helsinki, Finland, 2008.
[47] S. Whitehead, *Dielectric Breakdown of Solids,* Oxford, Clarendon Press, 1951.
[48] F. Chiu, J. Wang, J. Lee, and S. Wu, "Leakage currents in amorphous Ta_2O_5 thin films," *Journal of Applied Physics*, vol. 81, 1997, pp. 6911-6915.
[49] E. Atanassova and A. Paskaleva, "Conduction mechanisms and reliability of thermal Ta_2O_5-Si structures and the effect of the gate electrode," *Journal of Applied Physics*, vol. 97, 2005, pp. 1-11.
[50] M. Pecovska-Gjorgjevich, N. Novkovski, E. Atanassova, and D. Spasov, "The effect of gate material on dielectric characteristics and conduction mechanism of Ta/sub 2/O/sub 5/ MOS structures," Proceedings of the 2004 IEEE International Conference on Solid Dielectrics, 2004.
[51] S. Ezhilvalavan and T. Tseng, "Conduction mechanisms in amorphous and crystalline Ta_2O_5 thin films," *Journal of Applied Physics*, vol. 83, 1998, pp. 4797-4801.
[52] Y. Inuishi, "Effect of space charge and structure on breakdown of liquid and solid," *IEEE Transactions on Electrical Insulation*, vol. EI-17, 1982, pp. 488-492.
[53] G. Zhao, R. P. Joshi, V. K. Lakdawala, E. Schamiloglu, and H. Hjalmarson, "TiO_2 breakdown under pulsed conditions," *Journal of Applied Physics*, vol. 101, 2007, pp. 1-3.

Part III. Effect of Environmental Stresses on Breakdown Voltages in Chip Tantalum Capacitors

III.1. Introduction.

The major environmental stresses that might cause degradation of chip tantalum capacitors and compromise their reliability are soldering-induced stresses, temperature shocks/cycling, and exposure to high humidity. Requirements for reliability qualification testing reflecting these environmental stresses are described in MIL-PRF-55365. However, the existing test conditions are less severe compared to other electronic components, particularly plastic encapsulated microcircuits. In some cases, commercial tantalum capacitors (e.g., for the automotive industry) are subjected to more stressful testing than their military equivalents.

Obviously, an insufficient level of stress testing might result in potentially unreliable lots passing the test and causing failures during system-level testing or mission life. On the other hand, excessively severe test conditions might initiate wear-out failures and cause rejection of lots that would operate reliably under normal circumstances. Ideally, the level of environmental stresses used should be determined based on application conditions, the required level of reliability, and acceleration factors obtained based on extensive statistical data or through the physics-of-failure methodology. However, this approach cannot be realized in many cases, and the level of stresses during environmental stress testing (EST) is typically chosen based on historical data, industry practice, similarity of test conditions between different part types, and common sense. Clearly, experimental data on the effect of EST on the reliability of the part and statistics of environmentally induced failures are essential for the common sense/historical data approach. Unfortunately, there is a lack of information in relevant literature on the reliability of chip tantalum capacitors under EST, which does not allow for assessment of the effectiveness of tests used for reliability qualification of the parts.

Increased leakage currents and first turn-on failures of chip tantalum capacitors that have been screened by surge current testing (SCT) are often explained by damage of the parts during soldering [1, 2]. It is assumed that damage to a Ta_2O_5 dielectric is caused by thermomechanical stresses developed during soldering due to mismatch of the coefficient of thermal expansions (CTE) between the molding compound and the pellet, and to the pop-corning effect [3]. Soldering the part onto a board may create additional compressive stresses due to CTE mismatch between the printed wiring board (PWB) material and the tantalum capacitor. Considering that compressive stresses might cause degradation of surge current breakdown voltages [4], it is possible that these additional stresses contribute to the post-soldering failures of the parts.

Manual soldering of tantalum capacitors, which is often used during assembly for space projects, might be more stressful compared to solder reflow chamber processes due to significant temperature gradients in the part and direct mechanical pressure caused by inadvertent contact with the soldering iron. However, there is no data in relevant literature on the effect of soldering on breakdown voltages of chip tantalum capacitors and on the effect of manual soldering on reliability in particular.

In our previous work [3], it has been shown that temperature cycling can cause degradation of AC and DC parameters in chip tantalum capacitors, a reduction of surge current breakdown voltages, and an increase of the probability of scintillations. The data indicated the possibility of wear-out

failures during multiple cycling in the military range of temperatures, from -65 ^{o}C to +150 ^{o}C. The results suggested that the number of cycles to wear-out failures, N_w, is likely more than 100. However, more statistical data are necessary to confirm this observation. Reliability qualification testing per MIL-PRF-55365 is performed using 10 cycles from -65 ^{o}C to +125 ^{o}C. This number of cycles is far below possible N_w values, and these test conditions are less severe compared to the requirements for other components. For example, hybrid microcircuits per MIL-PRF-38535 are supposed to demonstrate reliable operation after 100 cycles between -65 ^{o}C and +150 ^{o}C. This means that military-grade chip tantalum capacitors cannot be used in military-grade hybrids (e.g., DC-DC converters) without additional testing. One of the purposes of this work was to demonstrate that normal-quality chip tantalum capacitors could withstand similar conditions without significant degradation, and that N_w is greater than 100.

Another environmental factor that is known to cause failures of tantalum capacitors is humidity. Numerous failures in military-grade solid tantalum capacitors caused by humid environments have been reported by Dobson, Raytheon [5]. It is often assumed that the failure mechanism is related to moisture-induced silver dendrites growing from cathode contacts [6]. However, the effect of moisture on breakdown voltages has not been studied yet. Although humidity testing is not critical for space applications, exposure to high humidity might happen during the ground-phase assembly and testing stages or during pre-launch periods, so the reliability qualification test should demonstrate robustness of the parts against storage in humid environments.

The existing moisture resistance test per MIL-PRF-55365 includes 20 cycles at high humidity (80% RH to 100% RH) between 10 ^{o}C and 65 ^{o}C with a total duration at 65 ^{o}C of 120 hours. These conditions are not adequate for components used for space applications. At 100% RH, the parts cannot be protected from condensation, which might accelerate degradation processes significantly, and the total duration of the high-temperature, high-humidity exposure might not be sufficient for moisture to diffuse to the tantalum pellet [7]. Considering the rate of moisture diffusion through the plastic package, a standard 85 ^{o}C/85% RH unbiased storage test for 240 hours would be much more appropriate for EST of chip tantalum capacitors intended for space applications. Note also that manufacturers of commercial tantalum capacitors routinely use 1,000-hour 85 ^{o}C/85% RH biased test to demonstrate reliability of their products.

In this part of the report, surge current and scintillation breakdown voltages were used as major indicators of reliability of capacitors. The surge current breakdown voltages, VBR_SCT, were measured using a technique compliant to MIL-PRF-55365. To simulate the worst-case conditions, no current-limiting resistors were used. Scintillation breakdowns, VBR_scint, were measured using a constant charging current technique [8]. Distributions of breakdown voltages were measured in 11 different lots of commercial and military-grade chip tantalum capacitors before and after various EST, including soldering simulations, temperature cycling between -65 ^{o}C and 150 ^{o}C, and humidity testing at 85 ^{o}C/85% RH. Results of these tests and statistical analysis of the data are presented.

III.2. Effect of soldering.

Three types of soldering tests were carried out:

1. The first test was manual soldering of the components onto an FR4 board, followed by desoldering. This procedure was repeated three times with a soldering iron set to 300 ^{o}C. Terminals of the parts were intentionally touched during both soldering and desoldering

processes to simulate the worst-case conditions. AC and DC characteristics, as well as surge current breakdown voltages, were measured on loose parts, followed by desoldering after three cycles of resoldering were completed.

2. For the second test the parts were manually soldered onto a 3.1-mm thick FR4 PWB and then reflowed in a temperature chamber at 250 ^{o}C for 1 minute to simulate solder reflow conditions. Estimations showed that this results in compressive stresses in the capacitor of ~10 MPa. Measurements of VBR_SCT were carried out on parts soldered onto the board. The purpose of this test was to assess the effect of mechanical stresses developed due to CTE mismatch between the FR4 board and tantalum capacitors.
3. The third test was solder pot cycling of the parts. The parts were installed in a fixture securing one of the terminals as shown in Figure III.1, and another terminal was brought into contact for 5 seconds with molten solder at 300 ^{o}C. After that the parts were cooled down to room temperature for 5 minutes, and the cycling was repeated until 30 solder pot cycles were completed. Half of the parts were stressed with anode terminals and half with cathode terminals touching the molten solder. AC and DC characteristics were measured after 10 and 30 cycles, and breakdown voltages were measured after 30 cycles.

Typically, from 15 to 20 samples were used for each test. Part types used and the test matrix are shown in Table III.1.

a) b)

Figure III.1. An overall view (a) and a close-up view (b) of the solder pot cycling test. During this test, terminals of tantalum capacitors were brought into contact with molten solder at 300 ^{o}C for 5 seconds.

Table III.1. Test matrix for soldering test.

Part Number	C, μF	VR, V	Comment	Test 1 Resoldering	Test 2 SCT on FR4	Test 3 30 Solder Pot Cycles
CWR11DH226KD	22	6	Case C		X	X
T495D226K015DS	22	15	Case D	X		X
CWR11FH156KB	15	10	Case C, DC0017			X
CWR11FH156KB	15	10	Case C, DC0038	X	X	X
T495X107K016AS	100	16	Case D	X		
CWR09KC106KBA	10	25	Case G	X		
CWR09FC335KBA	3.3	10	Case C	X		X
T495X336K035AS	33	35	Case D		X	X
TAJC476M010XNJ	47	10	Case D		X	
CWR06HC225KBA	2.2	15	Coated			X
T495X227K006ASE100	220	6	Case D	X		X

III.2.1. Manual resoldering.

Weibull distributions of surge current breakdown voltages for 15 μF 10 V and 3.3 μF 10 V capacitors are shown in Figure III.2. Similar plots were obtained for all parts presented in Table III.1. The difference between initial and post-resoldering distributions was estimated using two-sided confidence bounds calculated at a 90% confidence level using ReliaSoft Weibull-7 software. Overlapping of the bounds indicated no significant changes in the distributions, and in this case the effect of soldering was considered as negligible. Analysis of the data presented in Figure III.2 showed that only 3.3 μF 10 V capacitors degraded significantly as a result of resoldering stresses.

Figure III.3 shows correlation between initial and post-resoldering surge current breakdown voltages. To assess an overall effect of resoldering, Figure III.3.a displays correlation between average values of VBR_SCT. The error bars correspond to the respective standard deviations of the distributions. Only one lot, 10 μF 25 V, had a relatively small (~10%) but statistically significant decrease in average breakdown voltages, whereas no substantial variations occurred for other parts.

Variations of average values indicate only a general effect on the whole population, and are not sensitive to cases in which just one sample or a few samples would decrease their breakdown voltages substantially. To check whether resoldering caused an increase of the proportion of low-breakdown-voltage parts, 1-percentile values of the distributions were calculated and their correlation was analyzed (see Figure III.3.b). The data show that three part types, 3.3 μF 10 V, 22 μF 15 V, and 10 μF 25 V, decreased minimal breakdown voltages significantly (from 15% to 50%). Note, however, that after resoldering test all parts still had VBR_SCT exceeding the rated voltages, so no formal failures occurred, but the observed degradation indicates an increased probability of failures caused by the resoldering of these three part types.

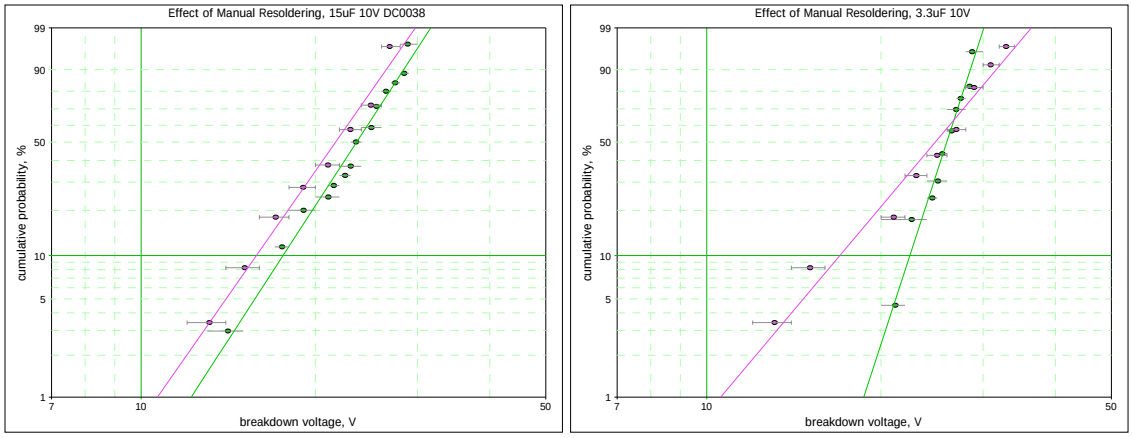

a) b)

Figure III.2. Distributions of surge current breakdown voltages for 15 µF 10 V DC0038 (a) and 3.3 µF 10 V (b) capacitors. Green indicates initial distributions, and red indicates post-three-resoldering data. Analysis using the 90% confidence bounds showed no difference in distributions for 15 µF 10 V parts and a significant difference for 3.3 µF 10 V parts.

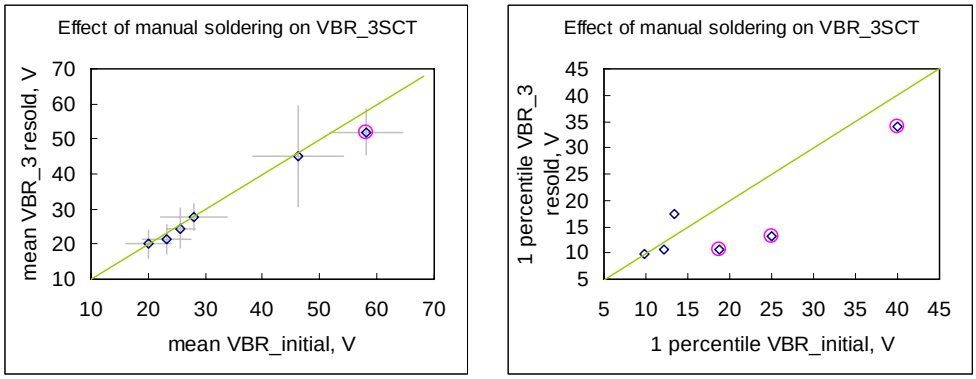

a) b)

Figure III.3. Correlation between average (a) and 1-percentile (b) values of surge current breakdown voltages measured on virgin parts and after three resoldering tests (part types are shown in Table III.1). Red circles indicate parts with significant degradation after resoldering. Only 10 µF 25 V capacitors had an overall decrease in VBR_SCT on ~10% (a). Two more part types, 3.3 µF 10 V and 22 µF 15 V, had an increased proportion of low-voltage devices (b).

Variations of leakage currents during resoldering testing are shown in Figure III.4. To increase the sensitivity of measurements to possible soldering-induced damage, the values of DCL were taken after 1,000 seconds of electrification. The results show that five out of six tested part types did not show significant degradation of leakage currents. The only part type with a noticeable degradation of DCL was 3.3 µF 10 V capacitors; five out of 20 parts increased DCL more than an order of magnitude. Although scintillation breakdowns were not measured for this group, an increase in leakage currents might be an indicator of possible decrease in VBR_scint. The results show that the susceptibility of tantalum capacitors to degradation of SCT is lot related.

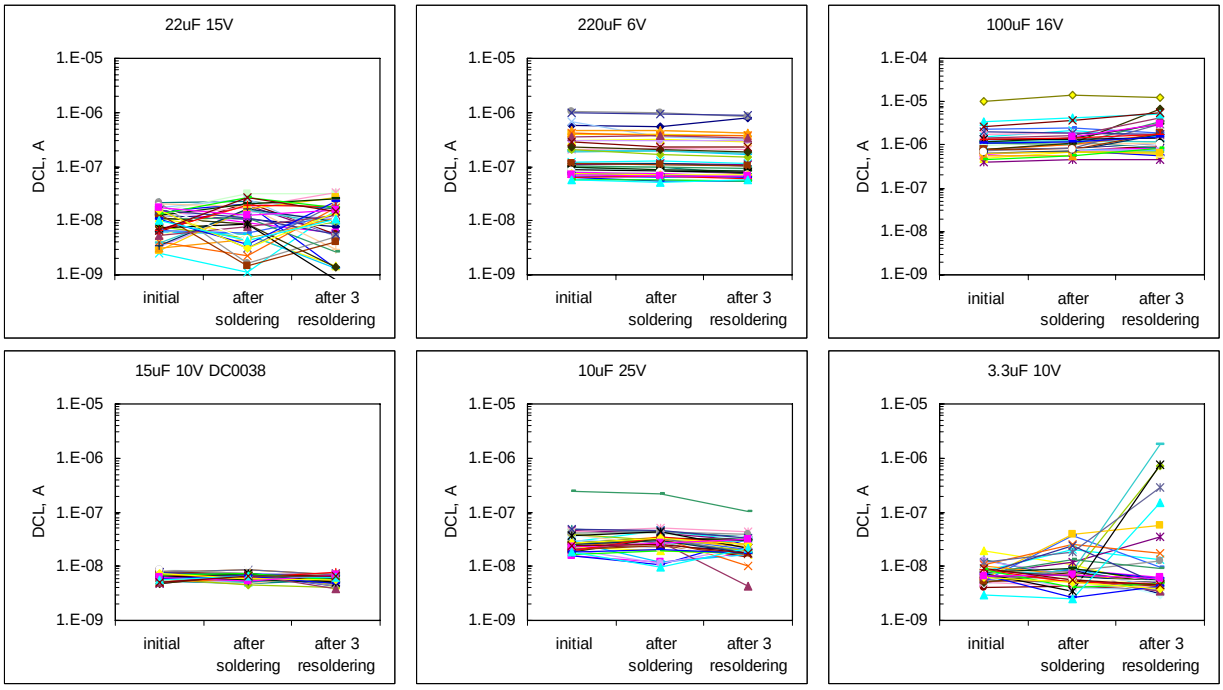

Figure III.4. Variation of leakage currents during manual resoldering test of 20 samples for six part types.

III.2.2. Surge current breakdowns after soldering onto an FR4 board.

Step stress surge current testing was carried out on 20 samples of four part types after soldering them onto an FR4 board. The part types are indicated in Table III.1. Figures III.5 and III.6 show distributions of VBR_SCT values measured on loose parts and on parts soldered onto a 3.1-mm-thick FR4 PWB. Comparative analysis showed no substantial difference between the test results in the four tested part types. This means that mechanical stresses caused by CTE mismatch between tantalum capacitors and the FR4 board normally do not affect surge current breakdown voltages.

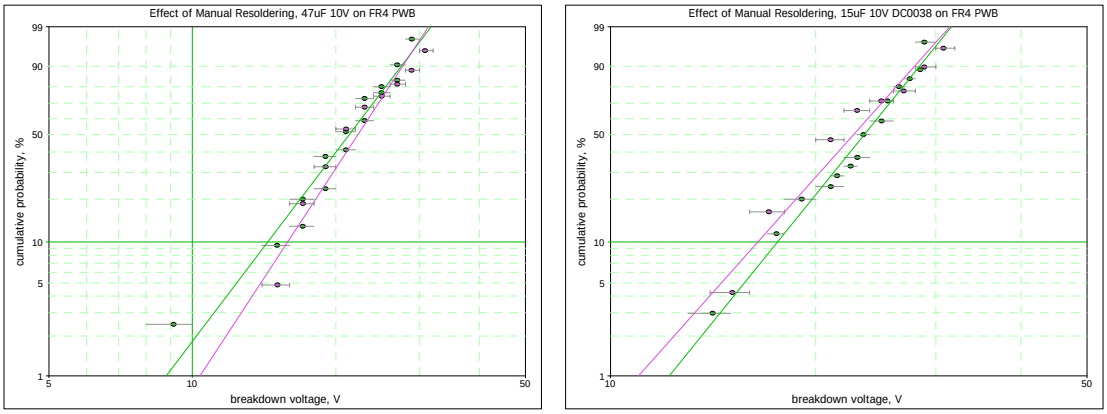

a) b)

Figure III.5. Distributions of surge current breakdown voltages for 47 µF 10 V (a) and 15 µF 10 V DC0038 (b) capacitors in loose condition (green) and after soldering onto an FR4 board (red). Distributions had no significant difference at the 90% confidence level.

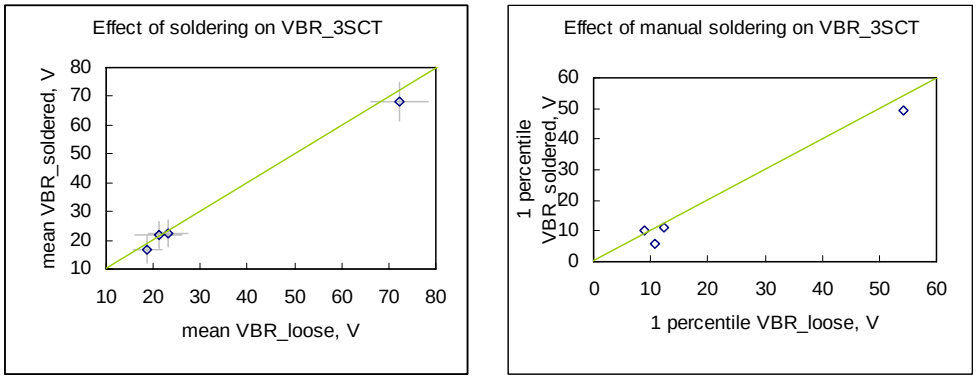

a) b)

Figure III.6. Correlation between average (a) and 1-percentile (b) values of surge current breakdown voltages measured on loose parts and parts soldered onto the FR4 board shown in Table III.1. Analysis showed no significant differences in the breakdown voltages.

III.2.3. Solder pot cycling.

Distributions of surge current and scintillation breakdown voltages for 2.2 µF 15 V and 3.3 µF 10 V capacitors measured before and after 30 solder pot cycles are shown in Figure III.7. Note that similar to these parts, in all cases scintillation breakdowns occurred at significantly greater voltages than the surge current breakdowns. Analysis of data for 2.2 µF 15 V capacitors shows no significant difference in both distributions. However, data for 3.3 µF 10 V capacitors suggest degradation of surge current breakdowns, while scintillation breakdowns did not change significantly.

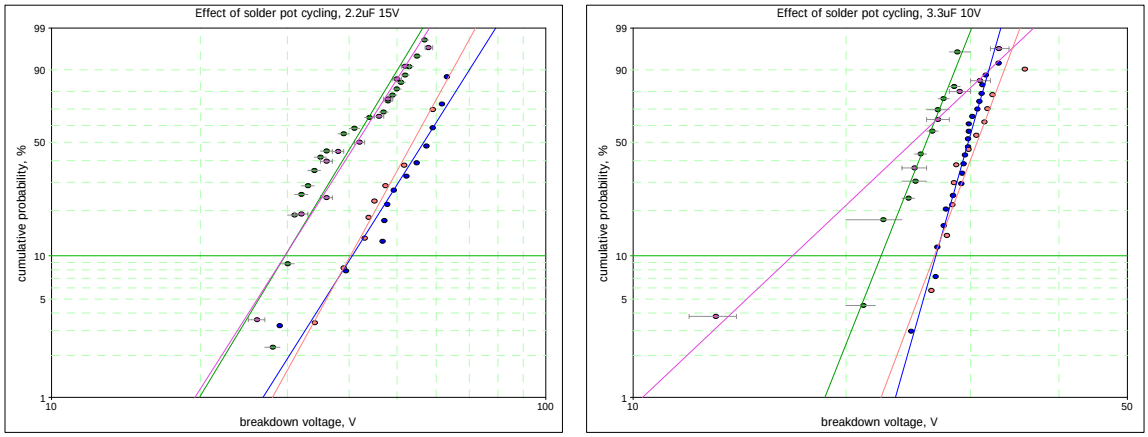

a) b)

Figure III.7. Effect of 30 solder pot cycles on distributions of surge current (data with error bars) and scintillation breakdown voltages for 2.2 µF 15 V (a) and 3.3 µF 10 V (b) capacitors. Green and blue indicate initial conditions for surge current and scintillation breakdowns, respectively, and red indicates post-solder-cycling distributions. All distributions, except for surge current testing of 3.3 µF 10 V capacitors, had no significant difference at the 90% confidence level.

Correlations between surge current and scintillation breakdown voltages for eight tested part types are shown in Figure III.8. No significant changes were observed in average values of surge

current and/or scintillation breakdown voltages. Only one part type, 3.3 µF 10 V capacitors, had a significant decrease of 1-percentile of VBR_SCT. Note that this is the same part type that behaved poorly under manual resoldering test.

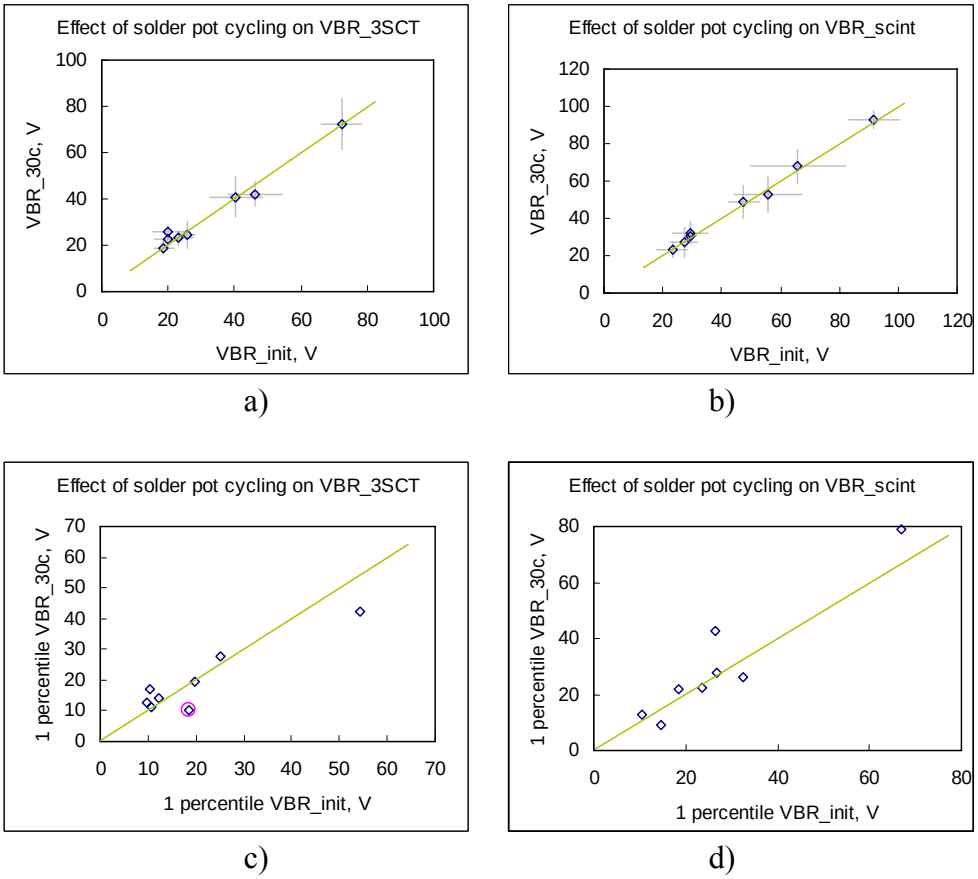

Figure III.8. Correlation between average surge current (a) and scintillation (b) breakdown voltages for eight part types shown in Table III.1. Correlations between 1-percentile values are shown in Figures c) and d) for surge current and scintillation breakdowns, respectively. Analysis showed a significant degradation for 3.3 µF 10 V parts only, where 1-percentile VBR_SCT values decreased by 45%.

Variations of leakage currents in capacitors during solder pot cycling are shown in Figure III.9. No degradation was observed in all capacitors except for one sample out of 20 parts from 3.3 µF 10 V group that failed DCL measurements after 30 cycles. Interestingly, the value of scintillation breakdown voltage for this sample was not determined because it did not break during measurements at 30 µA of charging current, and the voltage could not be increased above 22.1 V. This indicates that both parameters, VBR_scint and leakage current, should be estimated and used for screening during scintillation testing.

Results of the solder pot cycling test confirm that the 3.3 µF 10 V lot of CWR09 devices has a high susceptibility to soldering-induced failures. No failures of DCL or AC characteristics were observed for parts in the other seven lots.

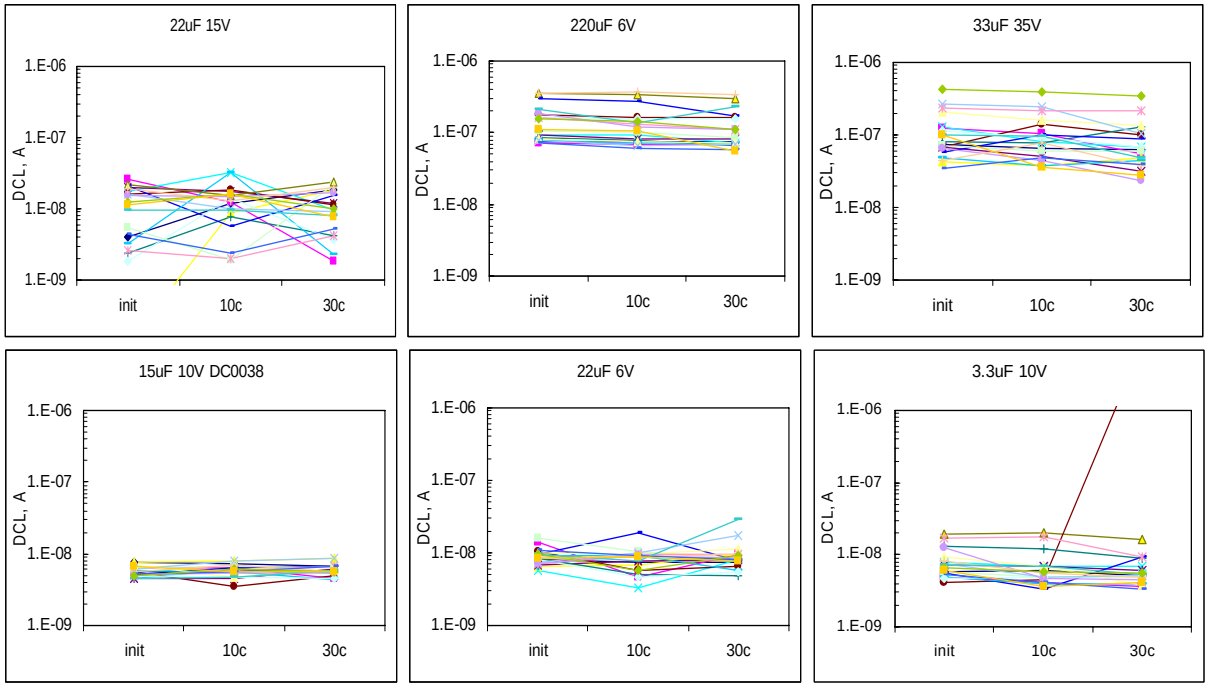

Figure III.9. Variations of leakage currents during solder pot cycling test.

The three techniques used to assess the effect of soldering on breakdown voltages of tantalum capacitors indicated that the majority of the parts can withstand multiple soldering cycle conditions without significant degradation. Considering the level of thermomechanical stresses in the parts under solder pot testing conditions, the observed stability of AC parameters, DCL, and breakdown voltages was surprisingly good. Manual resoldering resulted in more significant degradation in the parts, indicating a high probability of damage by direct contact of the parts with a soldering iron.

Test results indicate also that there is no reason to limit the number of solder reflow cycles before reliability qualification testing of capacitors to one cycle only, as is required currently per MIL-PRF-55365. Similar to what is required for plastic encapsulated microcircuits per JESD22-A113, and generally for solder reflow simulation per MIL-STD-202, preconditioning for reliability qualification testing should include three reflow cycles minimum. To assure the necessary robustness of capacitors to soldering stress, it is important not only to verify standard AC and DC characteristics of the capacitors, but also to make sure that the breakdown voltages remain within the acceptable limits.

III.3. Effect of temperature cycling.

Temperature cycling (TC) in the range from -65 ^{o}C to +150 ^{o}C was carried out on five types of commercial and five types of military-grade chip tantalum capacitors. Table III.2 displays part types and tests used in our experiments. The dwell time at the temperature extremes was 15 minutes, and the transfer time was 10 minutes. AC and DC characteristics of the parts were measured after 100 and 300 cycles, and breakdown voltages were measured after 300 cycles.

Table III.2. Test matrix for temperature cycling test.

Part Number	C, μF	VR, V	Comment	3SCT	Scintillation
CWR11FH156KB	15	10	Case C, DC0017	X	X
CWR11FH156KB	15	10	Case C, DC0038	X	X
CWR06HC225KBA	2.2	15	Coated	X	X
CWR11DH226KD	22	6	Case C	X	X
CWR09FC335KBA	3.3	10	Case C	X	X
T495X227K006ASE100	220	6	Case D	X	
T495156M035AHE225	15	35	Case D	X	
T495X476K020ASE150	47	20	Case D, Mfr. K	X	
TPSD336K035R0200	33	35	Case D, Mfr. A	X	
T495X336K035AS	33	35	Case D, Mfr. K	X	

Figure III.10 shows distributions of breakdown voltages measured before and after 300 TC for two lots of the same CWR11 part type, 15 μF 10 V capacitors manufactured several months apart (date codes 0017 and 0038). The following observations can be made based on analysis of these results:

1. Initial breakdown characteristics of the parts from different lots of military-grade parts can be substantially different (average surge current breakdown voltages differed by ~30% and scintillation breakdown voltages by ~60%).
2. Distributions of scintillation breakdown voltages for lot DC0017 were bimodal, suggesting the presence in this batch of two subgroups with different qualities.
3. The probability of scintillation breakdown in lot DC0017 increased after TC, whereas variations of breakdown voltages in lot DC0038 were negligibly small.
4. Thermal cycling caused a relatively minor degradation of VBR_SCT in both lots.

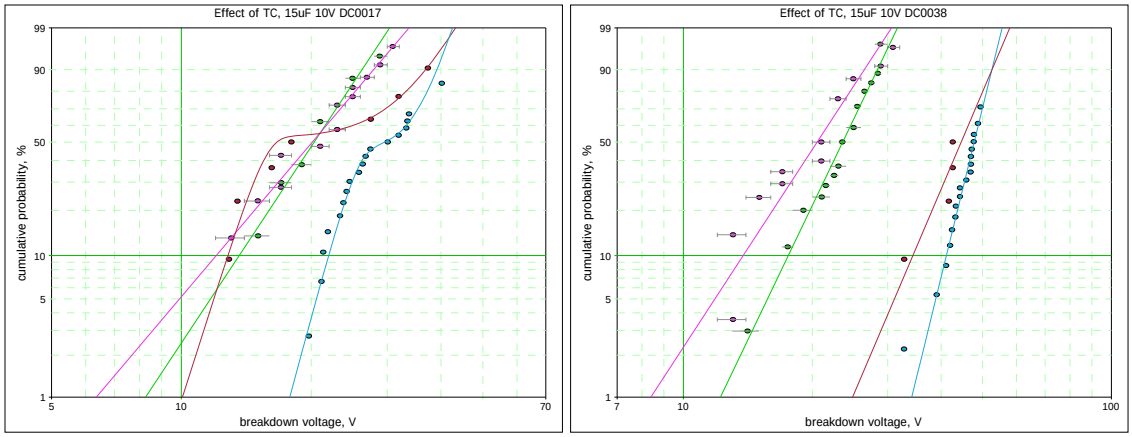

a) b)

Figure III.10. Effect of 300 TC between -65 °C and +150 °C on distributions of surge current (data with error bars) and scintillation breakdown voltages for 15 µF 10 V capacitors with different date codes, DC0017 (a) and DC0038 (b). Green and blue indicate initial conditions for surge current and scintillation breakdowns, respectively, and red indicates post-TC distributions. Note that at the 90% confidence level, a significant degradation of scintillation breakdowns occurred for DC0017 parts only.

Variations of leakage currents for two lots of 15 µF 10 V capacitors are shown in Figure III.11. Leakage currents in lot DC0017 degraded substantially after 100 TC, and approximately half of the samples increased DCL by one to three orders of magnitude. Interestingly, an additional 200 thermal cycles did not degrade leakage currents further. In lot DC0038, leakage currents remained stable even after 300 cycles. These data are consistent with the results of measurements of scintillation breakdown voltages.

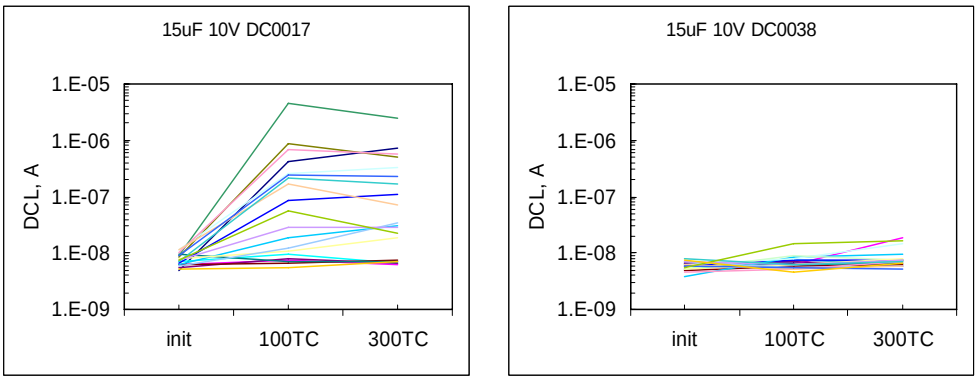

Figure III.11. Variations of leakage currents with the number of thermal cycles between -65 °C and +150 °C for two lots of 15 µF 10 V CWR11-type capacitors.

Correlations between initial and post-TC average and 1-percentile values of the breakdown voltages for all tested lots are shown in Figure III.12. Based on average values of breakdown voltages, no substantial degradation occurred. However, analysis of variations of the 1-percentile data showed some degradation of VBR_SCT in one out of five commercial (220 µF 6 V) and one

out of five military (3.3 µF 10 V) capacitors. Scintillation breakdown voltages decreased in three out of five military lots (22 µF 6 V, 15 µF 10 V DC0017, and 3.3 µF 10 V capacitors). Note that no catastrophic surge current failures occurred, and even reduced breakdown voltages in the two part types exceeded rated voltages. This means that all batches would likely pass the surge current breakdown screening if performed after TC testing.

Analysis of the data presented in Figure III.12.d shows that three out of five lots had decreased 1-percentile breakdown voltages, and although all VBR_scint exceeded the rated voltage, they would fail the 50% safety margin criterion. This means that more than 300 cycles in the military temperature range might cause degradation of scintillation breakdowns in some lots and thus compromise their long-term reliability. It seems reasonable, however, to require that the space-quality parts would withstand 100 thermal cycles in the military range of temperatures without substantial degradation of VBR_scint and remain above the 50% safety margin.

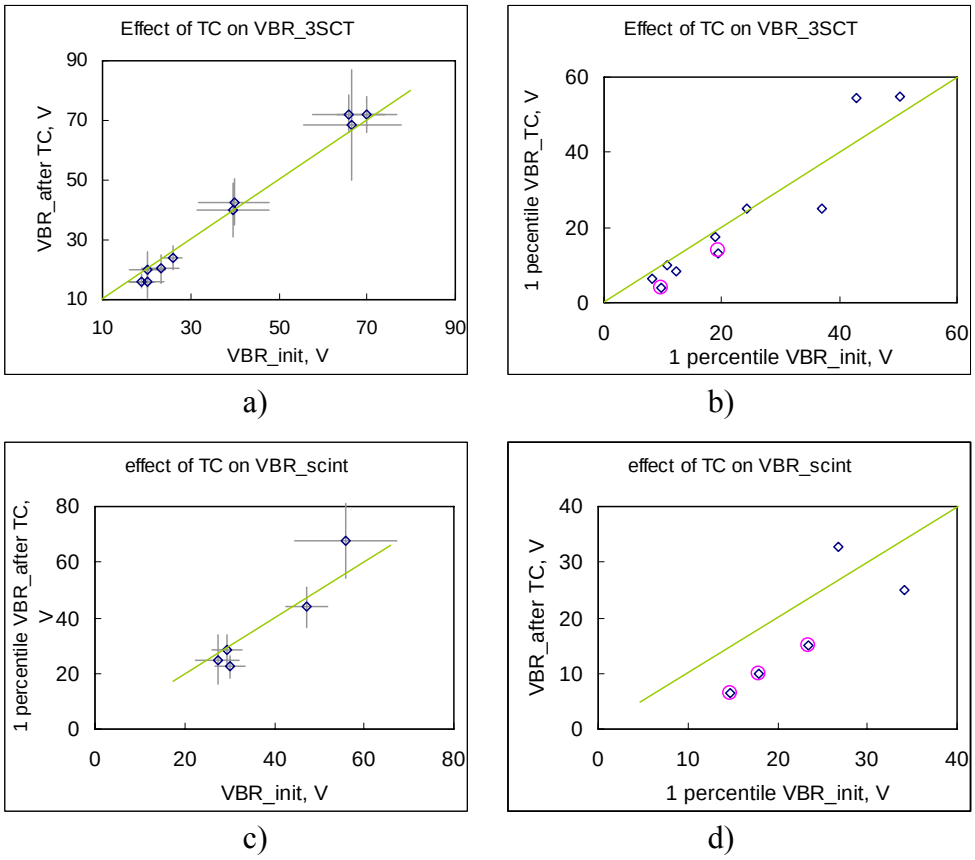

Figure III.12. Correlation between average surge current (a) and scintillation (b) breakdown voltages before and after TC. Correlations between 1-percentile values are shown in Figures c) and d) for surge current and scintillation breakdowns, respectively. Red circles indicate lots with an increased proportion of low-voltage devices.

III.4. Effect of humidity.

Five military-grade and five commercial lots (see Table III.3) with 20 samples each were stored in a humidity chamber at 85 ^{o}C/85% RH for 240 hours. Characteristics of the parts, including

capacitance (C), dissipation factor (DF), effective series resistance (ESR), DCL, and breakdown voltages were measured initially and after humidity testing. Both scintillation and surge current breakdown voltages were measured for military-grade parts, and only surge current breakdown voltages were measured for commercial lots.

Examples of distributions of breakdown voltages for four part types before and after humidity testing are shown in Figure III.13. All distributions, except for surge current testing of 2.2 μF 15 V and 15 μF 10 V DC0017 capacitors, had no significant difference at the 90% confidence level.

For 2.2 μF 15 V capacitors, VBR_SCT had bimodal distributions, and apparently humidity testing resulted in a decrease of breakdowns mostly for the first, low-voltage subgroup. The characteristic breakdown voltage for this group decreased from 34 V initially to 15.6 V after testing, whereas no changes occurred for the second, high-voltage subgroup. This result can be explained assuming that the low-voltage subgroup of this lot was formed by defective parts or parts with partially self-healed breakdowns. Considering that moisture can oxidize manganese oxides and increase their conductivity [7], it is possible that activation of the originally inaccessible defective areas of Ta_2O_5 dielectric resulted in decreasing breakdown voltages.

Table III.3. Test matrix for 85% RH/85 ^{o}C test.

Part Number	C, μF	VR, V	Comment	3SCT	Scintillation
CWR11FH156KB	15	10	Case C, DC0017	X	X
CWR11FH156KB	15	10	Case C, DC0038	X	X
CWR06HC225KBA	2.2	15	Coated	X	X
CWR09FC335KBA	3.3	10	Case C	X	X
CWR11DH226KD	22	6	Case C	X	X
TPSD476K020R0100	47	20	Case D, Mfr. A	X	
T495X476K020ASE150	47	20	Case D, Mfr. K	X	
T495X107K016AS	100	16	Case D	X	
T495X227K006ASE100	220	6	Case D	X	
T510X337K010AS	330	10	Case D	X	

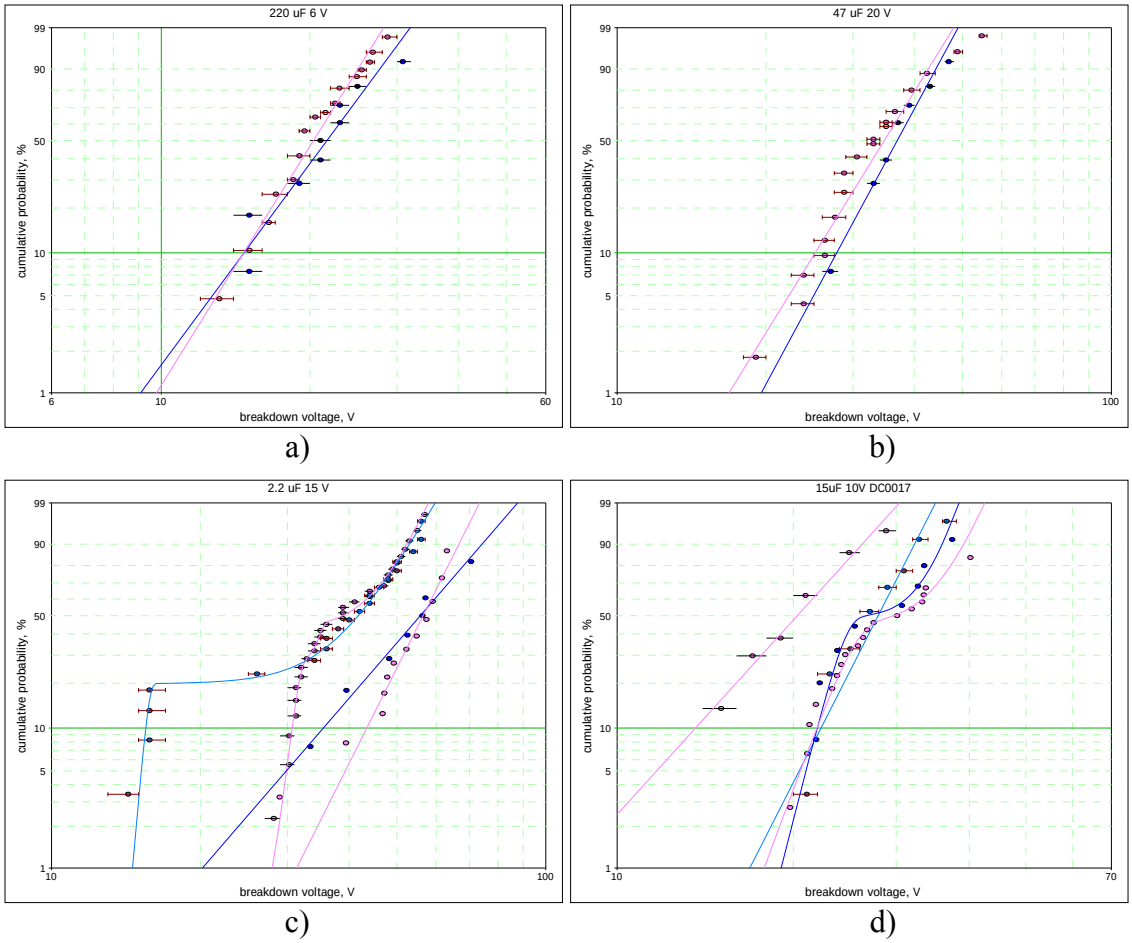

Figure III.13. Effect of humidity testing (85 ^{o}C/85% RH/240 hours) on distributions of surge current (data with error bars) and scintillation breakdown voltages for 220 µF 6 V (a), 47 µF 20 V Mfr. A (b), 2.2 µF 15 V (c), and 15 µF 10 V DC0017 (d) capacitors. On these charts, red indicates initial conditions, and blue indicates post-humidity distributions. Note that after humidity testing 2.2 µF 15 V capacitors had decreased, whereas 15 µF 10 V DC0017 capacitors had significantly increased surge current breakdown voltages.

Correlations between characteristics of distributions of breakdown voltages measured before and after humidity testing are shown in Figure III.14. Eight out of 10 tested part types did not decrease significantly in surge current breakdown voltages, and degradation was observed in 2.2 µF 15 V capacitors only. Scintillation breakdown voltages decreased in two out of five tested lots. For 22 µF 6 V capacitors, both average and 1-percentile scintillation breakdown voltages decreased, whereas only 1-percentile scintillation breakdown reduced in 2.2 µF 15 V capacitors.

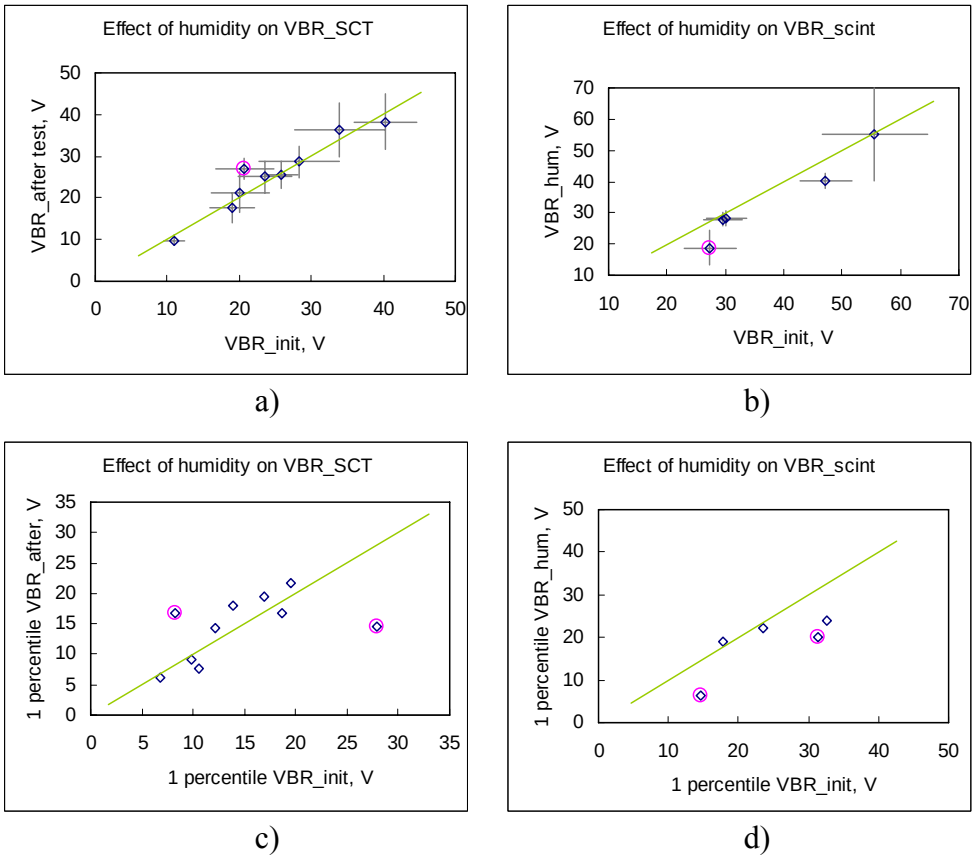

Figure III.14. Correlation between average surge current (a) and scintillation (b) breakdown voltages before and after humidity testing. Correlations between 1-percentile values are shown in Figures c) and d) for surge current and scintillation breakdowns, respectively. Red circles indicate significant variations of the characteristics.

Surprisingly, after humidity testing, average and 1-percentile surge current breakdown voltages increased in 15 µF 10 V DC0017 capacitors, while no changes in scintillation breakdowns were observed (see Figure III.13.c). This result is likely due to a significant increase in ESR values, on average from 0.44 Ohm initially to 0.88 Ohm after humidity testing. This increase in ESR is equivalent to the addition of approximately a 0.45 Ohm resistor in series with capacitors during SCT. It has been shown by Reed [9] that addition of resistors in the range from 0.1 Ohm to 10 Ohms sharply decreases surge current breakdown voltages. An increase in the series resistance slows the rate of voltage variations during surge current testing, and as was shown in Part II of this report, reduces the probability of breakdown.

On average, ESR values for five commercial parts and one military part decreased by 2.5% to 15%, which can be explained by increased conductivity of the MnO_2 layer. A substantial increase in ESR (30% to 200%) was observed for four other military parts. The mechanism of this increase is not clear. A possible reason might be swelling-induced delamination between some of the conductive layers (manganese/graphite/silver epoxy/metal) or corrosion of silver flakes at the silver epoxy/metal interface [10]. Because an increase in VBR_SCT was observed in one lot only, these data show that ESR variations do not correlate directly with the breakdown characteristics of the capacitors.

Post-humidity-testing of leakage currents was measured first at a low voltage of 3 V, and then at the rated voltage. One out of 10 tested lots, 47 µF 20 V Mfr. K, had two samples with leakage currents exceeding 10 µA when measured at 3 V, but all parts had DCL below this value when measured at 20 V. This indicates the possibility of a low-voltage degradation mechanism similar to the one known for ceramic capacitors [11, 12] and likely related to the silver dendrite growth.

Two out of 10 tested lots, 47 µF 20 V Mfr. K and 330 µF 10 V capacitors, had unstable leakage currents at the rated voltages after humidity testing as shown in Figure III.15. The results indicate multiple scintillations and, although the scintillation breakdown voltages were not measured for these lots, they obviously decreased after testing. This erratic behavior of leakage currents might be due to formation and "burning out" of tiny conductive areas shorting the dielectric or significantly increasing the electric field across the tantalum pentoxide layer. Electrolytic conductivity of condensed moisture or silver dendrites are likely periodically formed in these areas and destroyed by high-density currents due to local overheating.

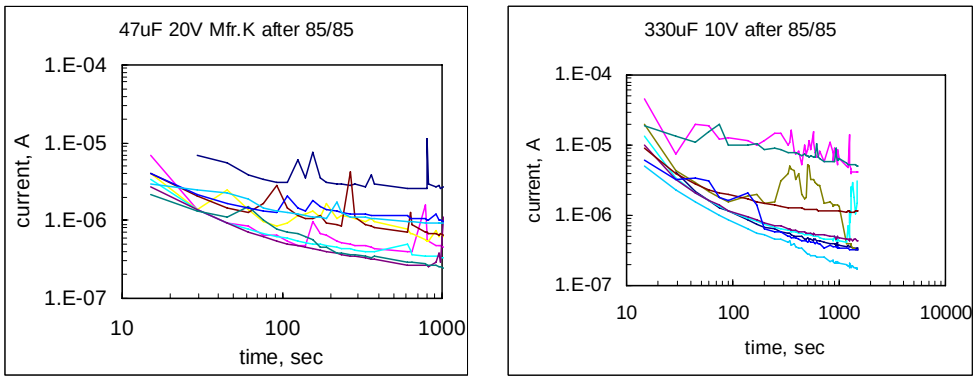

a) b)

Figure III.15. Erratic behavior of leakage currents in 47 µF 20 V (a) and 330 µF 10 V (b) capacitors with time under rated voltage after unbiased humidity testing at 85 °C/85% RH for 240 hours.

These results indicate the necessity of using scintillation breakdown testing and low-voltage current measurements to properly evaluate robustness of tantalum capacitors to exposure to humid environments.

III.5. Summary.

1. Six military-grade and 10 commercial types of chip tantalum capacitors were subjected to soldering simulation stresses, temperature cycling between -65 °C and +150 °C, and humidity testing at 85 °C/85% RH. Degradation of surge current and scintillation breakdown voltages was observed in four military and two commercial lots, indicating that quality of chip tantalum capacitors is lot related, and under environmental stress testing reliability of military parts is not greater than that of commercial parts.
2. Three instances of manual resoldering resulted in degradation of breakdown voltages in three out of six tested lots, whereas only one capacitor out of 20 tested parts failed in one out of 10

lots after 30 solder pot (300 ^{o}C) cycles. This suggests that touching the part with a soldering iron can cause more damage than temperature gradients developed during solder pot cycling.

3. Four lots with 20 samples each had similar surge current breakdown voltages when measured on loose parts and on parts soldered onto an FR4 board. This indicates that mechanical stresses developed after soldering are likely not sufficient to cause degradation of VBR_SCT.
4. Two lots out of 10 noticeably decreased surge current breakdown voltages after 300 TC between -65 ^{o}C to +150 ^{o}C. At this test condition, three out of five lots had decreased scintillation breakdown voltages, suggesting that scintillation breakdowns are more susceptible to TC-induced degradation.
5. Only one out of 10 lots tested at 85 ^{o}C/85% RH conditions for 240 hours had degradation of VBR_SCT, but four lots had increased probability of scintillations. In one lot two parts had anomalously high leakage currents at low voltages, which cleared when the measurements were repeated at the rated voltage.
6. Test results show that normal-quality lots can withstand three solder reflow cycles, 100 temperature cycles between -65 ^{o}C and +150 ^{o}C, and 10 days of unbiased humidity test at 85 ^{o}C/85% RH without significant degradation of breakdown voltages. These environmental tests should be used for reliability qualification testing of chip tantalum capacitors.

III.6. References to Part III.

[1] D. M. Edson and J. B. Fortin, "Improving thermal shock resistance of surface mount tantalum capacitors," 14th Capacitors and Resistors Technology Symposium, Jupiter, FL, 1994, pp. 169-176.

[2] J. Marshall and J. Prymak, "Surge step stress testing of tantalum capacitors," 21st Capacitors and Resistors Technology Symposium, CARTS'01, 2001, pp. 181-187.

[3] A. Teverovsky, "Effect of temperature cycling and exposure to extreme temperatures on reliability of solid tantalum capacitors," CARTS'07, 27th Symposium for Passive Components, Albuquerque, NM, 2007, pp. 279-306.

[4] A. Teverovsky, "Effect of mechanical stresses on characteristics of chip tantalum capacitors," *IEEE Transactions on Device and Materials Reliability*, vol. 7, 2007, pp. 399-407.

[5] R. Dobson, "Surface mount solid tantalum capacitor new wear-out mechanism," CARTS'03, 23rd Capacitor and Resistor Technology Symposium, Scottsdale, AZ, 2003, pp. 141-148.

[6] J. Devaney, "Report on a new failure mechanism for surface mount solid tantalum capacitors," CARTS USA, 1998, pp. 183-187.

[7] A. Teverovsky, "Effect of moisture on characteristics of surface mount solid tantalum capacitors," CARTS'03, 23rd Capacitor and Resistor Technology Symposium, Scottsdale, AZ, 2003, pp. 96-111.

[8] J. Primak, P. Blais, B. Long, A. Ifri, and E. Jones, "Alternate methods of defining dielectric quality using step stress surge testing and scintillation testing," 2008 Components for Military and Space Electronics Conference, San Diego, CA, 2008, pp. 323-347.

[9] E. K. Reed and J. L. Paulsen, "Impact of circuit resistance on the breakdown voltage of tantalum chip capacitors," CARTS, 2001, pp. 150-156.

[10] Y. Li and C. P. Wong, "Recent advances of conductive adhesives as a lead-free alternative in electronic packaging: Materials, processing, reliability and applications," *Materials Science and Engineering*, vol. R 51, 2006, pp. 1-35.
[11] R. Chittick, E. Gray, J. Alexander, M. Drake, and E. Bush, "Non-destructive screening for low-voltage failure in multilayer ceramic capacitors," 3rd Capacitor and Resistor Technology Symposium, CARTS'83, Phoenix, AZ, 1983, pp. 61-69.
[12] R. Straessle and G. Ewell, "The 85C-85% RH -1.5 VDC bias test: Can ceramic capacitors pass this new screen?," 3rd Capacitor and Resistor Technology Symposium, CARTS'83, Phoenix, AZ, 1983, pp. 70-82.

Part IV. Screening and Qualification Testing of Chip Tantalum Capacitors for Space Applications

IV.1. Introduction.

Tantalum capacitors manufactured per MIL-PRF-55365 are established reliability components, and parts used for space applications are supposed to have failure rates of less than 100 FIT. However, although rarely, failures of tantalum capacitors do happen, and several such failures have occurred over the last few years in the space industry during ground-phase testing of assemblies. Due to the specifics of the applications (typically in power supply lines) and of short-circuit failure mode with the possibility of ignition, each instance of such failures might cause catastrophic consequences for the system. This indicates the need for analysis of possible deficiencies in the screening and qualification (S&Q) system currently used to assure adequate reliability of tantalum capacitors for space applications.

In the most recent version of MIL-PRF-55365, released in March 2008, a new grade of capacitors was introduced. These capacitors are supposed to have the highest quality and are recommended for space applications. Batches of grade T parts should be traceable down to lots of tantalum powders, have Weibull failure rates equal to or better than 100 FIT, have mandatory three-temperature surge current testing (SCT), have destructive physical analysis (DPA) and radiographic inspections, and have dielectric leakage currents (DCL) and equivalent series resistances (ESR) within three standard deviations from the mean values. These requirements are aligned with common needs of the space community, provide tighter quality control over the production, and offer better traceability of the lot. However, test conditions and procedures of the existing S&Q system were not revised, and if currently used tests and procedures have deficiencies, these additional measures might not assure the necessary improvement in the product's quality.

Possible reasons for which parts that have passed screening and qualification testing still fail during applications can be classified into three groups:

1. Poor control over the implementation of the existing S&Q requirements. Defective capacitors might escape screening due to operator mistakes, equipment problems, or defective fixtures.
2. Inadequate screening procedures and requirements. Test conditions described in MIL-PRF-55365 might be not sufficient to identify and remove all potentially unreliable capacitors.
3. Inadequate reliability qualification test conditions and requirements. The level of stresses applied during qualification testing per MIL-PRF-55365 might be not high enough, and might not guarantee long-term operation of capacitors under environmental stresses.

Environmental testing is supposed to demonstrate that parts have a sufficient reliability margin to withstand stresses during typical application conditions, particularly under a combination of environmental stresses. This is especially important for surface mount technology (SMT) parts, including chip tantalum capacitors that experience significant stresses during soldering [1]. These stresses might damage the tantalum pentoxide dielectric or create cracks and delaminations in internal conductive layers, and thus aggravate the effect of environment and impair reliability of the parts.

Designing a reasonable and justified system for qualification testing of high-reliability products is quite a challenge because of the diversity of application conditions and the lack of sufficient knowledge about the relationship between reliability of the part and stress parameters (e.g. temperature, voltage, humidity, etc.). An approach for development of such a system for electronic components, and tantalum capacitors in particular, should be based on the existing S&Q system, history of the part application, studies of its reliability, and comparison with the requirements used for other types of components. A variety of part types used in an electronic assembly unit experience the same environmental stresses during applications, and it is reasonable to require that environmental stresses used for S&Q of tantalum capacitors and, for example, microcircuits or ceramic capacitors, would be similar.

It has been shown that failures of tantalum capacitors can be considered as time-dependent dielectric breakdowns (TDDB), and the time to failure is an exponential function of the ratio between the operational voltage and breakdown voltage (VBR) of the Ta_2O_5 dielectric. For this reason it is important that the S&Q system would be able to assure that a sufficient margin between the rated voltage and breakdown voltages of the capacitors exists and remains within the required limits after various environmental stresses.

In this work, analysis of MIL-PRF-55365 requirements is made based on data from relevant literature and extensive testing of chip tantalum capacitors carried out under the NASA Electronic Parts and Packaging (NEPP) Program over the last few years. Recommendations for improving MIL-PRF-55365 specifications and suggestions for S&Q of commercial tantalum capacitors for space applications are discussed.

IV.2. Deficiencies of screening procedures per MIL-PRF-55365.

Definitions of screening and qualification testing procedures are not well established, and a variety of terms including quality assurance, qualification inspection, verification of qualification, conformance inspection, periodic inspection, etc., are used in military documents. In our work we assume that all procedures performed on 100% of the parts to reduce the probability of infant mortality failures are screening procedures, and that all tests performed on a sample basis to demonstrate the necessary level of long-term reliability of the parts under environmental stresses are qualification procedures.

Below, major screening test procedures are analyzed, including measurements of the equivalent series resistance, dielectric leakage current, surge current testing, and Weibull grading. Also discussed is the necessity of a new test, safety margin verification, which has the purpose of assuring that the breakdown voltages in the lot have a certain margin to the rated voltage.

IV.2.1. ESR measurements.

ESR is a critical parameter of tantalum capacitors that affects the value of ripple currents and power losses directly when capacitors are used for filtering in power supply lines [2]. This parameter is related mostly to the resistance of the manganese cathode layer, but depends also on the graphite and silver epoxy coatings and on the quality of silver epoxy attachment to the cathode terminal. In spite of its importance, this parameter is measured per MIL-PRF-55365 only when specified. Also, ESR measurements are not required after surge current testing.

Our experiments showed that in some cases SCT can degrade ESR in tantalum capacitors. Figure IV.1 shows examples of variations of current spikes during step stress surge current testing for 22

µF 15 V and 3.3 µF 10 V CWR06-style capacitors. In both cases, a linear relationship between the current amplitude and voltage that is typical for the majority of the parts changes after a certain voltage to a linear relationship with a lower slope. This behavior indicates an increase in the effective resistance of the circuit, which in turn indicates changes in ESR values [3]. The SCT-induced increase of the ESR phenomenon was observed mostly in small-sized CWR06-type capacitors, and is likely due to development of delaminations and cracking in the cathode attachment caused by significant mechanical stresses in the part associated with the surge current testing.

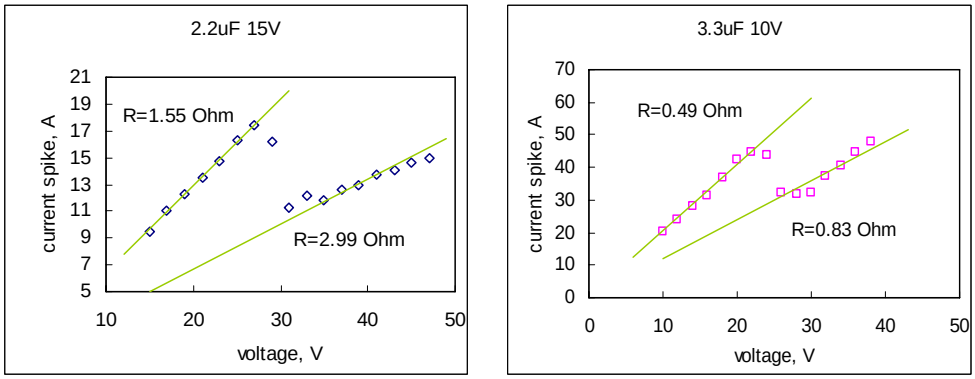

a) b)

Figure IV.1. Anomalies in variations of current spike amplitudes during step stress surge current testing of 2.2 µF 15 V (a) and 3.3 µF 10 V (b) CWR06-style capacitors.

Direct measurements of parts exhibiting anomalous variations of $I_{sp}(V)$ that were removed from the test before destruction confirmed a significant increase in the equivalent series resistance. Although the observed anomalies occurred at voltages exceeding the rated voltage (VR), it shows that this test can potentially cause degradation of ESR values. Respectively, the post-SCT ESR measurements are necessary to assure that this testing does not introduce any internal mechanical damage to the parts.

Analysis of ESR distributions was carried out for 14 lots of tantalum capacitors with 9 to 80 samples in each lot (see Table IV.1). In all cases, the normal function described experimental data adequately, thus justifying the applicability of the 3-sigma test to identify the best-quality parts. Figure IV.2 shows examples of ESR distributions for four types of capacitors. Parameters of distributions together with the number of samples exceeding the 3-sigma limits are tabulated in Table IV.1 for all part types. Using the 3-sigma criterion, a few failures (on average ~0.75%) were observed for both military-grade and commercial products. Note that all ESR values, even those outside the 3-sigma limits, were within the data sheet requirements.

Table IV.1. Parameters of ESR distributions.

Part	Qty.	Mean	STD	M-3S	M+3S	Failures, %
100 µF 16 V	45	0.12	0.01	0.10	0.14	2.22
3.3 µF 10 V	68	0.49	0.11	0.16	0.83	1.47
10 µF 25 V	56	0.16	0.03	0.07	0.25	0
22 µF 6 V	40	0.32	0.02	0.27	0.38	0
15 µF 10 V DC0017	40	0.45	0.04	0.35	0.56	2.50
15 µF 10 V DC0038	80	0.42	0.03	0.33	0.50	0
47 µF 20 V	48	0.09	0.01	0.07	0.12	2.08
220 µF 6 V	40	0.12	0.01	0.10	0.15	0
330 µF 10 V	17	0.04	0.01	0.01	0.08	0
15 µF 35 V	9	0.11	0.00	0.10	0.12	0
33 µF 35 V	45	0.13	0.01	0.10	0.16	2.22
22 µF 15 V	40	0.33	0.05	0.19	0.48	0
2.2 µF 15 V	60	1.75	0.33	0.77	2.74	0
1 µF 50 V	15	2.60	0.45	1.26	3.94	0

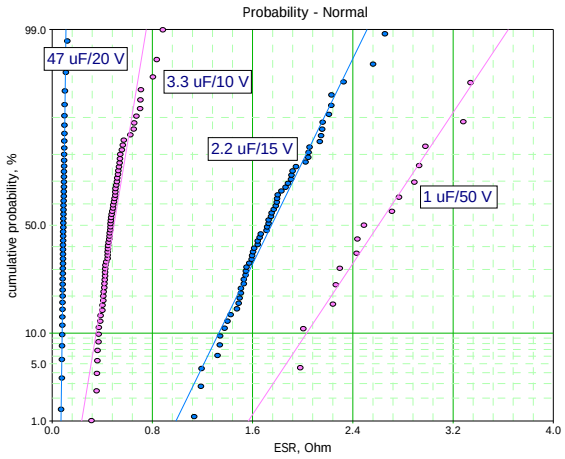

Figure IV.2. Normal plots of ESR distributions for four types of capacitors indicating that the distributions can be adequately approximated with normal functions.

IV.2.2. Leakage current measurements.

Excessive leakage currents in tantalum capacitors are typically attributed to defects in the Ta_2O_5 dielectric and considered to be indicative of the quality of the part. The maximum allowable level of DCL is specified based on the value of capacitance and rated voltage according to an empirical rule: $DCL_{max} = 0.01 \times C \times VR$, where C is in microfarads, VR is in volts, and DCL is in microamperes. Assuming that the thickness of the dielectric is proportional to the formation voltage (VF), and VF is proportional to VR, the thickness can be expressed as $d = m \times VR$, where $5 < m < 9$, d is in nanometers, and VR is in volts. Using a $d(VR)$ relationship, the equation for DCL_{max} can be expressed as a function of surface area of the dielectric, S: $DCL = \varepsilon \times \varepsilon_0 \times S/m$. A

relationship between DCL_{max} and S indicates that the probability of having a defect in the dielectric is proportional to the surface area of the electrode.

Distributions of leakage currents were analyzed for 14 different lots of tantalum capacitors (see Table IV.2). In most cases a log-normal distribution provided the best fit as is shown for four part types in Figure IV.3.a. However, some lots showed significant deviations from the unimodal log-normal distribution (see Figure 3.b), and bimodal distributions would provide a better fit. This indicates that analysis of DCL distributions might be effective in assuring the homogeneity of capacitors in the lot.

Table IV.2. Parameters of DCL distributions.

Part	Qty.	LogMean	LogStd	LK Value LN	Mean	STD	LK Value N
100 µF 16 V	56	-13.6	0.8	684.9	1.89E-06	8.66E-07	392.2
15 µF 10 V DC0017	40	-18.7	0.3	747.6	7.59E-09	2.06E-09	742.5
15 µF 10 V DC0038	80	-18.9	0.2	1543.0	6.04E-09	9.98E-10	773.6
100 µF 10 V	30	-16.5	1.2	443.5	1.90E-07	2.47E-07	405.9
3.3 µF 10 V	40	-18.5	0.8	687.8	1.89E-08	2.58E-08	609.1
2.2 µF 6 V	40	-18.4	0.3	722.5	1.12E-08	4.08E-09	708.2
2.2 µF 15 V	40	-18.6	1.4	673.1	1.54E-08	1.19E-08	673.7
47 µF 20 V	25	-14.9	0.5	356.0	3.70E-07	1.93E-07	350.6
10 µF 25 V	40	-17.4	0.4	669.1	3.32E-08	2.10E-08	613.7
220 µF 6 V	60	-15.7	0.7	874.0	2.10E-07	1.76E-07	837.5
22 µF 15 V	40	-18.6	0.8	695.6	1.06E-08	5.85E-09	702.6
33 µF 35 V Mfr. A	27	-15.6	0.3	418.0	1.71E-07	5.11E-08	413.2
33 µF 35 V Mfr. K	27	-15.3	0.4	397.2	2.54E-07	1.37E-07	381.1
15 µF 35 V	27	-16.0	0.5	411.2	1.30E-07	8.44E-08	396.2

In cases with bimodal distributions, the lot apparently has two subgroups, and if their mean values differ substantially, removal of the high-DCL subgroup would likely improve the quality of the batch. Nevertheless, analysis shows that even in such cases, application of the 3-sigma rule still allows for screening out parts with the highest levels of leakage currents. Note that similar values of the likelihood (LK) calculated for log-normal and normal distributions (see Table IV.2) were observed when a substantial proportion of the parts was out-of-family.

Using parameters of normal distributions shown in Table IV.2 and the 3-sigma criterion, the number of failures for each lot was calculated and is presented in Table IV.3. The proportion of failures averaged at 0.31% and varied from 0.33% to 0.67% for commercial parts and from 0% to 0.5% for military-grade parts. A similar range of DCL failures for military and commercial parts indicates that their quality might be not as different as is usually assumed. This result is in agreement with the analysis of breakdown voltages in military and commercial parts described in Parts I and II of this report.

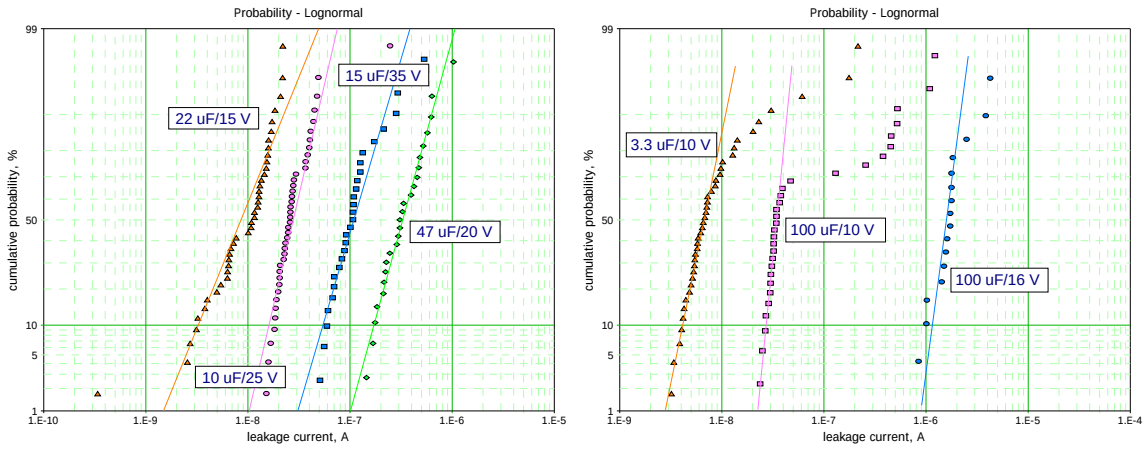

a) b)

Figure IV.3. Distributions of DCL for different part types showing good (a) and poor (b) approximation with the log-normal functions.

Table IV.3 shows the ratio between the specified leakage current, $DCL_{spec.}$, and the median value, DCL_{50}, of the distributions. Values of the DCL margin, M_{99}, that characterize the difference between DCL of the high-leakage-current parts and the specified value are shown in the last column of Table IV.3. The DCL margin is calculated based on the 99 percentile of the distribution, DCL_{99}:

$$M_{99} = 100 \times (DCL_{spec} - DCL_{99}) / DCL_{spec.}$$

The results suggest that the leakage currents of the majority of the population in the lot are more than one to two orders of magnitude lower than the specified values. (This corresponds to the data presented by NEC Corp.) However, the margin is relatively consistent for most of the lots, averaging at ~80%, and variations of the margin are similar for commercial parts (from 0% to 94%) and for military-grade parts (from 9% to 99%).

Table IV.3. Proportions of parts with DCL exceeding 3-sigma level and 99-percentile margin of distributions.

Part	Mean+3S	Fail 3S	Failures, %	DCL Max., A	DCL_{50}	DCL/ DCL_{50}	99 Percentile	M_{99}, %
100 µF 16 V	4.49E-06	2	0.36	1.6E-05	1.29E-06	1.24E+01	5.00E-06	68.75
15 µF 10 V DC0017	1.38E-08	1	0.25	1.5E-06	7.34E-09	2.04E+02	1.50E-08	99.00
15 µF 10 V DC0038	9.03E-09	0	0.00	1.5E-06	6.12E-09	2.45E+02	9.00E-09	99.40
100 µF 10 V	9.31E-07	2	0.67	1.0E-05	7.11E-08	1.41E+02	1.50E-06	85.00
3.3 µF 10 V	9.63E-08	2	0.50	3.3E-07	8.80E-09	3.75E+01	3.00E-07	9.09
2.2 µF 6 V	2.34E-08	2	0.50	1.3E-07	1.05E-08	1.24E+01	3.00E-08	76.92
2.2 µF 15 V	5.11E-08	0	0.00	3.3E-07	8.40E-09	3.93E+01	5.00E-08	84.85
47 µF 20 V	9.49E-07	1	0.40	1.0E-06	3.28E-07	3.05E+00	1.00E-06	0.00
10 µF 25 V	9.62E-08	1	0.25	2.5E-06	2.78E-08	8.99E+01	4.00E-08	98.40
220 µF 6 V	7.38E-07	2	0.33	1.3E-05	1.51E-07	8.60E+01	1.00E-06	92.31
22 µF 15 V	2.82E-08	0	0.00	3.3E-06	8.57E-09	3.85E+02	2.00E-08	99.39
33 µF 35 V Mfr. A	3.24E-07	1	0.37	1.0E-05	1.64E-07	6.10E+01	4.00E-07	96.00
33 µF 35 V Mfr. K	6.65E-07	1	0.37	1.0E-05	2.24E-07	4.46E+01	7.00E-07	93.00
15 µF 35 V	3.83E-07	1	0.37	5.0E-06	1.09E-07	4.58E+01	3.00E-07	94.00

Forward currents in tantalum capacitors are not constant, but vary with time after voltage application, similar to those shown in Figure IV.4. Generally, these currents are a sum of absorption currents that decrease with time, and leakage currents that do not vary with time. Absorption currents are due to charging of electron traps in the Ta_2O_5 dielectric; they do not depend on the presence of defects, and their decay can continue even after several hours after voltage application. The leakage currents, in turn, are a sum of currents related to the intrinsic conduction mechanisms in the Ta_2O_5 dielectric and currents caused by the presence of defects. The first type of current flows through the defect-free areas of the dielectric and is controlled by the Poole-Frenkel and/or Schottky mechanisms of conductivity. The second, defect-related current, in a simplified form, can be considered as a current flowing through a thinning area of the dielectric layer or at an asperity of the electrode. Considering that the electrical field at the defective sites of the dielectric is much greater than the average field and that the current density increases exponentially with the field, even relatively minor defects might have current density much greater than average. Although the total area of the defects might be relatively small, their contribution into the leakage current might be substantial.

Due to the presence of the high density of electron traps in the dielectric, absorption currents are high and often conceal the presence of the defects. To measure defect-related currents in tantalum capacitors, the time under bias should be great enough. Note that currents in 22 µF 15 V capacitors shown in Figure IV.4 already are below the specified limit of 3.3 µA after 10 seconds, but two out of nine parts that have excessive leakage currents could be revealed only after ~300 seconds.

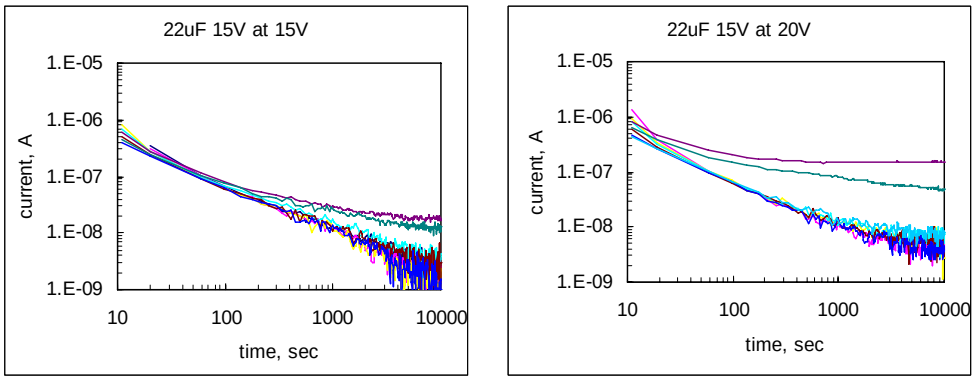

a) b)

Figure IV.4. Decay of leakage currents in nine 22 µF 15 V capacitors with electrification time under rated voltage (a) and at V = 1.33 VR (b).

MIL-PRF-55365 requires measurements of DCL to be taken after a maximum electrification period of 5 minutes. Because leakage currents decay with time, a manufacturer can stop taking readings of a capacitor as soon as it is below $DCL_{spec.}$ (for example, after 10 seconds for the 22 µF 15 V capacitors). However, these measurements would not represent defect-related currents, and at these conditions the presence of defective samples in the lot cannot be revealed. For this reason, DCL measurements should be taken after 5 minutes of electrification minimum (not maximum, as is required per MIL-PRF-55365).

Figure IV.4.b shows that measurements of DCL at V = 1.33 VR make the presence of defective parts in a lot much more apparent and at shorter electrification times. Experiments show that

application of 1.5VR is even more effective in revealing defects in the dielectric. Note that application of voltages exceeding VR is widely used during S&Q procedures and is not damaging for normal-quality parts. For example, surge voltage testing is performed at 85 ^{o}C and 1.3 VR, and up to 1.53 VR is applied at 85 ^{o}C during Weibull grading test.

Early detection and removal of parts with excessive leakage currents is an effective way to improve the quality of the lot during screening. Figure IV.5 displays variations of leakage currents in 47 µF 35V capacitors measured through the screening process. This process included thermal shock (five cycles from -55 ºC to +125 ºC), voltage aging (96 hours at Ta = 85 ºC, 35 V), and surge current testing. The results demonstrate that two out of 95 tested parts had excessive DCL values initially, and these parts degraded significantly through the screening process. Although all leakage currents remained within the specified limits, the two parts clearly demonstrated degradation with time, and their removal from the lot would increase its quality.

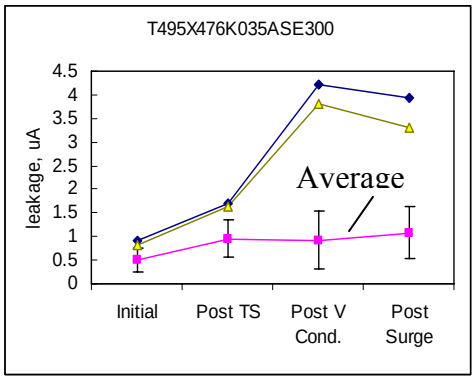

Figure IV.5. Variations of average leakage currents for 94 samples of 47 µF 35 V capacitors measured through screening compared to two samples having excessive DCL initially.

IV.2.3. Surge current testing (SCT).

Surge current testing is a stress test having the purpose of assuring that no first turn-on failures will occur in capacitors used in low-impedance circuits. This test per MIL-PRF-55365 is performed at the rated voltage, and hence provides a zero safety margin for the parts used at the rated conditions. For this reason, all manufacturers of chip tantalum capacitors are warning users against using their parts at the rated conditions and suggest voltage derating. This situation is probably specific to tantalum capacitors only. Normally, manufacturers of high-reliability electronic components guarantee reliable application of their products at the rated conditions, and derating is a means for a user to further increase reliability of the parts during applications.

In addition to the absence of safety margin, SCT has other deficiencies related to the test conditions and setup used. These deficiencies have been discussed in [3-5] and in NEPP Report 2007, and can be summarized as follows:

1. Results of SCT depend on the rate of voltage changes that is controlled by the value of limiting resistors, the inductance of the circuit (length of the connecting wires), and the type of switches used. The most stressful conditions of testing can be achieved by using no limiting resistors, short connecting wires, and power field-effect transistors (FETs) as switches operating under sharp gate pulses. Measurement of the current spike amplitudes allows for an estimation of the effective resistance in the circuit, R_c, and should be used to control the

correctness and reproducibility of test results. Acceptable test conditions can be determined as $R_c \leq 0.3 + ESR$.

2. SCT failures at the rated voltage can occur at any number of cycles, so the parts that passed 10 cycles at VR, as is currently required per MIL-PRF-55365, have a certain probability of failures after screening. To reduce this probability substantially, SCT should be performed at 1.1 VR. This also would provide a 10% safety margin for surge current events at the rated voltage.
3. As SCT does not affect results of life testing at steady-state conditions, and conversely, life testing does not affect results of SCT, this test can be carried out at any step during the screening.

IV.2.4. Weibull grading test (burn-in).

All high-reliability components are screened by a burn-in (BI) test to eliminate marginal devices and reduce the probability of infant mortality failures. This test is considered as a most critical procedure in the screening process and is typically performed at or above maximum rated operating conditions (MIL-STD-883, TM 1015). As was shown in Part I, a specific of tantalum capacitors is that infant mortality failures continue with time of operation until most of the parts in a group fail. For this reason, the purpose of BI for tantalum capacitors should be a reduction of the failure rate below the acceptable level as it performed during Weibull grading test.

Two BI procedures are known for tantalum capacitors: voltage aging and Weibull grading test. Both tests are performed at 85 ^{o}C and 40 hours or more (for Weibull test). The voltage aging test is carried out at the rated voltage and the Weibull grading test at voltages varying from 1.1 VR to 1.53 VR depending on the required level of reliability. Obviously, the voltage aging test provides much less stress to the part and likely for this reason it was replaced after 1990 with the Weibull grading test. Nevertheless, voltage aging is still used in the GSFC guidelines, EEE-INST-002, to select space-grade tantalum capacitors.

Calculations of the test conditions and reliability grading are based on the validity of the expression for the voltage acceleration factor used in MIL-PRF-55365:

$$AF = 7.03412025 \times 10^{-9} \times \exp\left(18.77249321 \frac{V}{V_R}\right) \quad (1)$$

This formula was obtained by Navy Crane in the late 1970s for hermetically sealed solid tantalum capacitors [6], and its applicability for contemporary chip tantalum capacitors is questionable [7]. Our analysis in Part I of this report has shown that this equation might be valid at specific conditions only. In particular, VR should be proportional to the breakdown voltage of the capacitor. However, the coefficient of proportionality between VBR and VR varies from manufacturer to manufacturer and from lot to lot, thus indicating that reliance on this equation might produce erroneous results.

Figure IV.6 displays variations of acceleration factors (AF) with V/VR calculated per Eq. (1) in the assumption that the real values of the rated voltage (VR_{real}) vary ±10% from the nominal value (VR). Even these relatively minor changes of VR produce significant errors in the acceleration factors. The AF calculated for VR_{real} = 0.9 VR and VR_{real} = 1.1 VR changed by 65 times at V/VR = 1.1, and in 300 times at V/VR = 1.5.

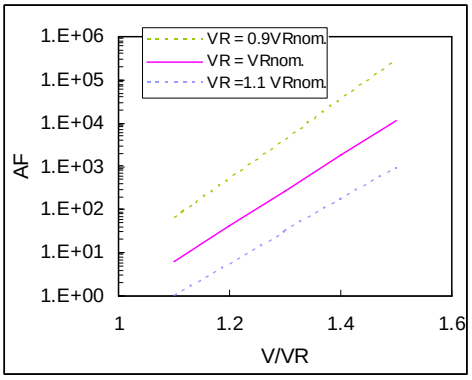

Figure IV.6. Acceleration factors calculated per Eq. (1). The dashed lines show AF for cases in which the real, breakdown-related VR value deviated by ±10% from the nominal value.

In spite of obvious errors in calculating failure rates based on the Weibull grading test results, stressing of tantalum capacitors at high temperatures and voltages exceeding VR is aligned with the philosophy of burning-in of high-reliability components and was proven to be effective. For this reason, BI testing at 85 ^{o}C and 1.5 VR for 40 hours seems to be a reasonable screening procedure for the space-grade capacitors.

Another problem with using the Weibull grading test is related to the method of detecting failures. During the test, capacitors are connected to a power supply through 1 A or 2 A fuses (or an equivalent electronic circuit) with cold resistance of not more than 1 Ohm. A failure is defined as a blown fuse or equivalent, and the failed parts are removed from the lot. One obvious problem with this test is that results of screening with 1 A fuses might be not equivalent to the results of testing with 2 A fuses.

To blow a 1 A fuse, the part should either fail short circuit permanently, or experience a current spike of more than a dozen amperes during a few milliseconds. Clearly, parts that exhibit scintillations or current spiking should not be acceptable even if their characteristics remain within the specification limits after testing. An apparently anomalous recovery of capacitors after failures during BI is observed sometimes and can be explained assuming that scintillations that had caused the fuse to blow open resulted in self-healing and did not destroy the part. However, relatively low-current scintillations (below a few amperes) would remain undetected. Such scintillations might damage the part and degrade its reliability, but if the post-Weibull-grading leakage current is within the specified limits, the degraded part would not be screened out.

To reduce the probability of parts that exhibit scintillation spikes of a few amperes or less, the amplitude of detectable current spikes should be reduced by at least an order of magnitude. For this, the BI testing is recommended to be carried out using 200 mA fast-acting fuses (or an equivalent electronic circuit) with a cold resistance of 1 Ohm or less.

IV.2.5. Margin verification test.

The rated voltage of tantalum capacitors is a major parameter of the part that is directly related to its reliability. All models used to calculate acceleration factors of the test conditions compared to operation conditions, and respectively to predict reliability of capacitors, employ a ratio between the operational voltage and VR.

It has been shown before that the physical model of failures of tantalum capacitors employs breakdown voltages rather than rated voltages, and calculations of the acceleration factors of the time-to-failure employ a ratio V/VBR. Obviously, the rated voltage can be used to calculate AF if it is a fixed portion of VBR only. However, experiments described in Parts I and II of this report showed that the correlation between VBR and VR is poor. This might explain a significant difference in AF used by different manufacturers of tantalum capacitors (see Figure IV.7). At a 50% derating (V/VR = 0.5), the values of AF suggested by different manufacturers vary by almost four orders of magnitude. Considering that materials and technological processes employed by different vendors do not vary substantially, one of the major reasons for these variations is likely the difference in the methodology of determining VR employed by different vendors and the lack of control over the breakdown voltages.

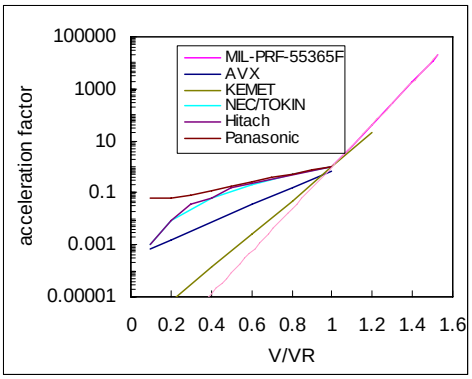

Figure IV.7. Acceleration factors suggested by different manufacturers of tantalum capacitors compared to MIL-PRF-55365.

The best method of establishing a relationship between VBR and VR would be by analysis of the distributions of VBR for each lot of parts as was made in Parts I and II of this report. This method is rather time- and cost-consuming and might be not practical for mass-production conditions. A simpler test that would assure that VBR values have the necessary safety margin towards VR can be suggested.

It has been shown that 50% minimum is a reasonable requirement for the margin that is determined as M = (V1-VR)/VR*100, where V1 is the 1-percentile voltage of the distribution of VBR. The margin verification test should assure that all parts in the lot have a minimum of a 50% margin between the scintillation breakdown voltages and the rated voltage. This test is similar to the constant charge current scintillation breakdown test described in Part I of this report, but the maximum voltage is limited to 1.5*VR. The charging current during the test, I_{ch}, is calculated based on the requirement that the maximum voltage is reached in 10 ±2 seconds: $I_{ch} = 1.5 \times C \times VR/10$. This test is carried out at room temperature, and only capacitors that did not have scintillations below 1.5 VR shall be considered as passing the test.

IV.3. Deficiencies of qualification testing per MIL-PRF-55365.

Temperature cycling, humidity, and life testing are major reliability qualification tests commonly used for all high-reliability electronic components encapsulated in plastics. Being soldered onto a board is one of the most stressful events that all SMT components, including tantalum capacitors, can experience before applications, and this stress might affect results of all qualification tests

substantially. For this reason, the effect of soldering is considered below along with analysis of environmental and life testing.

IV.3.1. Effect of soldering.

MIL-PRF-55365 addresses the effect of soldering twice: the first time during screening by implementing reflow conditioning, and the second time during the resistance-to-soldering heat test employed as qualification testing. During reflow conditioning all parts are exposed one time to 230 ^{o}C for 5 seconds, and post-conditioning measurements are not required. During the resistance-to-soldering-heat test, 18 capacitors are also exposed one time also to 235 ^{o}C for 30 seconds. The latter test is performed within group II testing and is followed by the moisture resistance test. One failure during the post-soldering-heat test electrical measurements is considered acceptable if no other failures have occurred during group II to group V tests. Note that only C, DF, and DCL are measured after testing and ESR measurements are not required, so possible degradation in anode or cathode attachment might remain unnoticed. Potentially up to 5% of parts might fail after soldering, but the lot is still considered acceptable for space applications.

Flux application and three cycles of solder reflow simulation are required during qualification testing per MIL-STD-202, TM210, to evaluate robustness of the parts to the soldering-induced stresses. Relaxing these requirements to one cycle only might not reveal potential problems with the lot. This stress might affect reliability of the parts not only under high-humidity environments, but also during temperature cycling and operating life, and it should be used as a preconditioning for all reliability qualification tests. This would also mimic the real-life situation in which all parts before applications are soldered onto printed wiring boards (PWBs).

It has been shown that the pop-corning effect might occur in chip tantalum capacitors similar to that effect in plastic encapsulated microcircuits (PEMs) [8]. For this reason preconditioning of tantalum capacitors should be carried out in a manner similar to PEMs, and it should include moisture soaking (168 hours, 85 ^{o}C, 60% RH); flux application and cleaning; and three reflow simulation cycles per MIL-STD-202, TM210, condition J. Post-reflow-simulation electrical tests should include measurements of C, DF, DCL, ESR, surge current, and margin verification testing. This test should be performed on all space-grade parts intended for qualification testing, and no failures should be allowed.

IV.3.2. Effect of temperature cycling.

Tantalum capacitors manufactured according to MIL-PRF-55365 are subjected to five thermal shocks (TS) between -55 ^{o}C and +125 ^{o}C (unmounted parts) during screening and to 10 TS (mounted parts) during qualification inspection. The temperature range of TS testing during screening can be extended to -65 ^{o}C to +15 ^{o}C, but at the option of the manufacturer only. It is not clear what might force the manufacturer to extend the temperature range during the testing.

Contrary to tantalum capacitors, military-grade chip ceramic capacitors manufactured per MIL-PRF-123 and microcircuits manufactured per MIL-PRF-38535 have much more stringent requirements for temperature cycling (TC) or TS testing. Ceramic capacitors should demonstrate the capability to withstand 100 TS between -55 ^{o}C and +125 ^{o}C, and the microcircuits during qualification testing are stressed with 100 TC between -65 ^{o}C and +150 ^{o}C. This means that the existing S&Q system does not guarantee that tantalum capacitors can withstand multiple cycling, even within a relatively narrow operating temperature range.

Our tests described in Part III of this report have demonstrated that normal-quality lots of tantalum chip capacitors are capable of withstanding 100 TC between -65 ^{o}C and +150 ^{o}C in a loose condition. This justifies the requirement according to which high-quality parts should demonstrate the capability to withstand F-3 test conditions per MIL-STD-202 (100 TS between -65 ^{o}C and +150 ^{o}C). This would also allow using such capacitors in MIL-PRF-38534 hybrid microcircuits without re-screening and re-qualification.

Note that contrary to ceramic capacitors, in which mechanical stresses change substantially after being soldered onto a board, in tantalum capacitors, due to the presence of some stress relief provided by terminals, the stresses developed during TS might not vary substantially for loose and soldered parts. This makes TS testing of loose tantalum capacitors more effective and important compared to the ceramic parts.

IV.3.3. Effect of humidity.

Military specification MIL-PRF-55365 requires moisture resistance testing of chip tantalum capacitors in accordance with test method 106 of MIL-STD-202. According to this method the parts are subjected to 20 24-hour cycles in a humidity chamber without bias. During each of the cycles the relative humidity and temperature varies several times, from 80% to 100% RH at 25 ^{o}C to 90% to 100% RH at 65 ^{o}C. Note that at 100% RH moisture condensation is difficult to avoid, so it is quite possible that some parts are immersed into water during this testing.

The purpose of the test per MIL-STD-202 is the evaluation of resistance of parts to deteriorative effects of high humidity and heat conditions typical in tropical environments where direct surface wetting of metals and insulation might happen. It is assumed that this test is especially effective due to employment of temperature cycling, which provides alternate periods of condensation and drying essential to the development of the corrosion processes.

Obviously, these test conditions are not adequate for capacitors used for space applications where parts can be exposed to moisture during ground-phase testing and integration periods only, and typically humidity of the environment does not exceed 85%. For this reason, a commonly used 85 ^{o}C/85% RH test condition for 100 hours should be sufficient to assure the necessary moisture resistance of the parts. Our experiments described in [9] and Part III of this report showed that most of the lots can withstand 240 hours at 85 ^{o}C/85% RH without degradation. Note also that many commercial tantalum capacitors, in particular those used in the automobile industry, are subjected to 85 ^{o}C/85% RH test for 1,000 hours under bias during qualification testing.

According to the existing requirements, after the testing C, DCL, DF, and ESR (when specified) are measured. Variations of the capacitance after the test shall not exceed ±15% of the initially measured values, and DCL changes should not exceed 200% of the rated value. However, our experiments showed that changes of C depend on the previous history of exposure of the parts to high humidity or dry conditions; changes in capacitance up to 15% are rather common and are due to the presence of microvoids at the manganese/Ta_2O_5 interface [9]. Therefore, changes of the capacitance after testing might vary depending on the initial condition of the parts, and in most cases these changes are not related to moisture-induced degradation. On the other hand, it was shown in Part III of this report that measurements of DCL, both at low voltages (1.5 V) and at the rated voltage, as well as margin verification test, are informative and can reveal lots that degrade under humid conditions.

IV.3.4. Life test.

According to MIL-PRF-55365, life testing is performed for 2,000 hours either at 85 °C and V = VR, or at 125 °C and V = 0.67 VR. In the first case, 102 parts are used with one failure allowed. In the second case, 24 parts are used and one failure is allowed if no failures occurred during group II to group V testing. It is assumed that both test conditions are equivalent. Calculations of the voltage acceleration factor per Eq. (1) for these conditions yield AF = 0.002. Assuming that the temperature-related acceleration factor follows Arrhenius law, the corresponding activation energy should be 1.9 eV. This is a relatively large value, and estimations made based on the guidelines offered by different manufacturers indicate much lower values of Ea, in a range from 0.2 eV to 1.2 eV. This indicates that the equivalency of the two test conditions is doubtful and likely explains several cases in which employment of both tests showed different results.

Life test at 85 °C is performed at the same temperature as the Weibull grading test, thus allowing for comparison of the test results. Assuming that one out of 102 parts failed life testing, the failure rate at 85 °C and confidence level of 60% can be calculated as follows:

$$\lambda_{85C} = \frac{\chi^2\left[(1-c.l.),(2n+2)\right]}{2} \times \frac{1}{AF} \times \frac{1}{N \times t} = \frac{\chi^2\left[(1-0.6),(4)\right]}{2} \times \frac{1}{102 \times 2000} = 9.8 \times 10^{-6} \approx 1\%/1000hr\,,$$

where χ^2 is the chi-square function, *c.l.* is the confidence level, *n* is the number of failures, *N* is the number of samples, and *t* is the duration of the test; AF = 1 because the test is performed within the operational conditions of the part.

Considering that the parts after Weibull testing are supposed to have a failure rate of below 0.01% per 1,000 hours, the calculated value of λ_{85} = 1%/1,000 1/hr. is rather high. This indicates that the life-test conditions are not stressful enough to demonstrate long-term reliability of tantalum capacitors screened to level T.

Assuming that a typical operational temperature of the part is 55 °C and "standard" activation energy E_a = 0.7 eV, the 2,000-hour life test at 85 °C would be equivalent to 1.8 years of operation only. By raising the test temperature to 105 °C, the equivalent operational time would increase to 6 years. Further increase of the stress level by raising voltage to 1.1 VR would raise the equivalent time to 36 years. Considering that the expected life of high-reliability parts is 10 to 20 years, it seems reasonable to require life testing to be performed at 105 °C, 1.1 VR for 1,000 hours.

IV.4. Recommendations for screening and qualification of commercial tantalum capacitors.

The quality assurance system designed to provide high-reliability parts for military applications is based on a detailed and verifiable control of all process steps, traceability of materials used, and thorough examination and testing during manufacturing. The S&Q procedures described in military specifications present a sophisticated system of time-related (periodical), lot-related, and sample-related tests designed to assure consistency in the quality of the product. Those procedures have a proven record of successful use for mature products that are manufactured in large quantities and for a long period of time. However, military-grade products have an increased cost, and what is more important for space projects, longer delivery time. Also, the procedures cannot be adjusted easily for advanced technology, high-performance commercial-off-the-shelf (COTS) products that are coming to the market with an increasing speed.

Typically, space projects use a relatively small number of samples that are purchased for a specific project only, and they require fast delivery. Distributions of the lot sizes for four part types used in GSFC projects over the last several years are shown in Figure IV.8. An average lot size was from 6 to 15 pieces, and most of the lots had less than 100 samples.

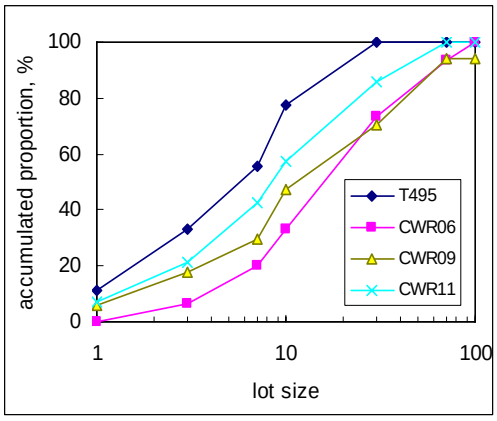

Figure IV.8. Distributions of lot sizes for four types of tantalum capacitors used in GSFC projects.

For space projects there is a need for screening and qualification procedures to be capable of assuring the necessary quality and reliability for specific, small-sized lots of commercial tantalum capacitors. Considering that materials and manufacturing processes used for military-grade and commercial parts are similar, and the difference in their manufacturing is mostly related to the level of testing, it seems that by employing a proper S&Q system for commercial parts, the quality required for space applications can be achieved. Note also that the results of testing of military and commercial capacitors reported in Parts I to III of this report showed that their quality does not differ substantially; hence, improvements in S&Q system might be effective in both cases.

IV.4.1. Screening test flow.

Based on the discussions above, Table IV.4 displays a screening test flow for commercial chip tantalum capacitors. It is based on the current MIL-PRF-55365 requirements with some variations described in the comments column. This test flow is applicable to level 1 projects per GSFC EEE-INST-002 classification. For level 2 projects, SCT can be performed at room temperature only. For level 3 projects, the radiographic inspection and margin-verification testing can be omitted, and stability at low- and high-temperature test can be replaced with electrical measurements of C, DF, ESR, and DCL at room temperature only.

Note that log-normal function provides the best fit for distributions of DCL, and analysis of these distributions, as well as distributions of breakdown voltages, can be used to assure the homogeneity of the lot. The homogeneity analysis might be useful for selection of tantalum capacitors for level 2+ projects.

Table IV.4. Screening process for commercial solid tantalum capacitors.

Test	Method	Comments
Visual inspection	MIL-PRF-55365	
Reflow conditioning	MIL-PRF-55365	
Thermal shock	MIL-PRF-55365	
Electrical measurements	MIL-PRF-55365	Measurements of C, DF, ESR, and DCL. ESR measurements are mandatory. DCL is measured at 1.5 VR after 5 min. electrification minimum. Analysis of DCL and ESR distributions to assure homogeneity of the lot.
Margin verification	GSFC Test Method	The test verifies that VBR_scint exceeds 1.5 VR.
Radiographic inspection	MIL-PRF-55365	
Burn-in (voltage aging)	MIL-PRF-55365	Except for V = 1.5 VR, resistance of the circuit does not exceed 1 Ohm and failures are determined using 200 mA fast-acting fuses.
Surge current test	MIL-PRF-55365, Conditions A and B (three temperature measurements)	Except for V = 1.1 VR and effective resistance is below 0.3 Ohm + ESR.
Stability at low and high temperatures	MIL-PRF-55365	ESR measurements are mandatory.
Visual inspection	MIL-PRF-55365	

IV.4.2. Qualification test flow.

Although it is commonly expected that capacitors manufactured per MIL-PRF-55365 are superior compared to commercial devices, our testing showed no substantial difference in degradation under environmental stress testing for commercial and military capacitors. This is understandable considering that both are manufactured using the same materials and processes, and that MIL-PRF-55365 does not address the effect of environment during reliability qualification tests adequately.

Analysis of drawbacks of MIL-PRF-55365 showed that one of the problems is related to the absence of preconditioning and soldering simulation prior to reliability testing. Also, major environmental tests including temperature cycling, moisture resistance, and life testing are not stressful enough to assure long-term reliability of the parts. Space-qualified lots of tantalum capacitors should demonstrate not only stability of their characteristics (C, DF, ESR, and DCL) during post-stress-testing measurements, but also their breakdown safety margins should remain within the specified limits.

A suggested qualification test flow for commercial tantalum capacitors is presented in Figure IV.9. A group of 50 samples is selected after screening for this testing. If results of screening testing are available, no initial measurements are required. After preconditioning that consists of moisture soak, flux application, and three solder reflow simulation cycles (per JESD22-A113/MIL-STD-202, TM210), all parts are electrically tested including measurements of C, DF, ESR, and DCL at rated voltage, SCT, and margin verification. Then the parts are split in three subgroups for life testing (20 samples), temperature cycling (15 samples), and humidity test (15 samples). Conditions of these stress tests are discussed above. Post-stress-testing measurements are performed as shown in Figure IV.9. No failures are allowed.

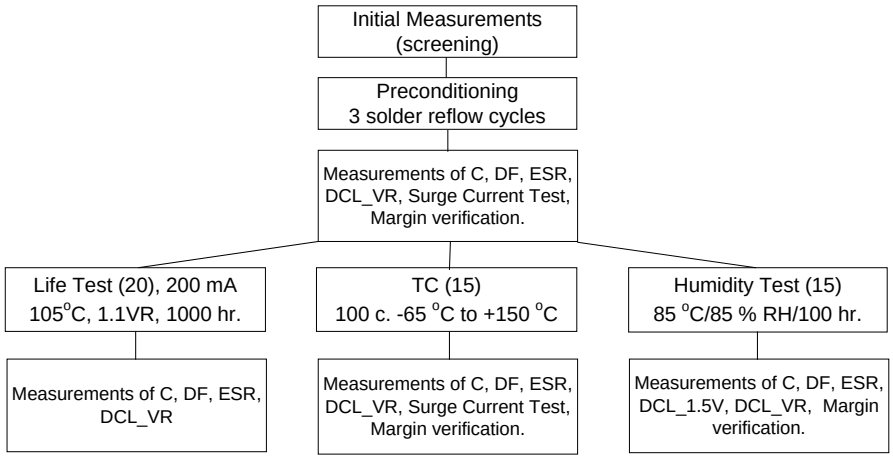

Figure IV.9. A simplified test flow for reliability qualification testing of chip tantalum capacitors. The numbers in brackets show the minimum required quantity of samples.

Figure IV.9 shows a typical test flow for level 2 projects. For level 1 projects, life testing should be performed during 2,000 hours; SCT is also required after humidity test, and the number of temperature cycles might be increased based on the specific requirements of the project. For level 3 projects, humidity test, surge current testing, and margin verification are not necessary.

IV.5. Summary.

1. Deficiencies of MIL-PRF-55365 have been analyzed, and recommendations to change screening and qualification procedures have been discussed.
2. Recommendations for screening can be summarized as follows:
   2.1. Experiments show that surge current testing can cause degradation of ESR, and ESR measurements should be used after SCT. Measurements of ESR during screening and qualification testing should be mandatory, instead of "when specified only."
   2.2. To reveal defects in the Ta_2O_5 dielectric, DCL measurements should be made after five minutes of electrification minimum, but not maximum as is required currently. The effectiveness of revealing defects can be increased substantially if measurements are made at 1.5 VR.

2.3. To prevent first turn-on failures during applications, surge current testing should be performed at 1.1 VR using setups with the effective resistance of the circuit not exceeding 0.3 Ohm + ESR.

2.4. Employment of 1 A to 2 A fuses during the Weibull grading test allows detection of capacitors that have high-current scintillation spikes (dozens of amperes) only. To reveal potentially defective capacitors with lower current spikes, burn-in testing should be performed using 200 mA fast-acting fuses with a cold resistance of not more than 1 Ohm or equivalent electronic circuit. The suggested burn-in test conditions are: T = 85 ^{o}C, V = 1.5 VR, and t = 40 hours.

2.5. A margin verification test should be used during screening to assure that a 50% minimum safety margin exists between the rated voltage and scintillation breakdown voltages for all capacitors in the lot.

3. Recommendations for reliability qualification testing are as follows:

3.1. Preconditioning, including moisture soak, flux application, and three solder reflow simulations cycles, should be used prior to any reliability qualification testing of the parts. Post-solder-reflow simulation testing should include SCT and margin verification tests.

3.2. High-quality tantalum capacitors should demonstrate the capability to withstand 100 thermal shocks between -65 ^{o}C and +150 ^{o}C. TS testing should not degrade surge current and scintillation breakdown voltages below the acceptable levels.

3.3. The space-grade parts should be able to pass a 10-day unbiased humidity test at 85 ^{o}C/85% RH without significant degradation of surge current and scintillation breakdown voltages. Prior to DCL measurements at VR, leakage currents at 1.5 V should be measured to assure that no low-voltage degradation occurred.

3.4. The existing life test conditions (85 ^{o}C, VR, 2,000 hours) are not stressful enough to evaluate long-term reliability of the space-grade capacitors that are supposed to have a failure rate of less than 100 FIT. The suggested life test conditions are 1,000 hours at 105 ^{o}C and 1.1 VR.

4. Test flows recommended for screening and reliability qualification of commercial tantalum capacitors for space applications are shown in Table IV.4 and Figure IV.8.

IV.6. References to Part IV.

[1] R. Hahn, J. Piller, and P. Lessner, "Improved SMT performance of tantalum conductive polymer capacitors with very low ESR," 26th Symposium for Passive Components, CARTS'06, Orlando, FL, 2006.

[2] E. K. Reed, "Tantalum chip capacitor reliability in high surge and ripple current applications," 44th Electronic Components and Technology Conference, 1994.

[3] A. Teverovsky, "Effect of surge current testing on reliability of solid tantalum capacitors," 28th Symposium for Passive Components, CARTS'08, Newport Beach, CA, 2008.

[4] A. Teverovsky, "Effect of inductance and requirements for surge current testing of tantalum capacitors," CARTS'03, 26th Symposium for Passive Components, Orlando, FL, 2006.

[5] E. K. Reed and J. L. Paulsen, "Impact of circuit resistance on the breakdown voltage of tantalum chip capacitors," CARTS, 2001.

[6] J. N. Burkhart, "Use of accelerated testing techniques in military specification MIL-C-39003," CARTS, Phoenix, AZ, 1983.
[7] J. L. Paulsen, E. K. Reed, and J. N. Kelly, "Reliability of tantalum polymer capacitors," CARTS 2004, 24th Annual Capacitor and Resistor Technology Symposium, 2004.
[8] A. Teverovsky, "Effect of temperature cycling and exposure to extreme temperatures on reliability of solid tantalum capacitors," CARTS'07, 27th Symposium for Passive Components, Albuquerque, NM, 2007.
[9] A. Teverovsky, "Effect of moisture on characteristics of surface mount solid tantalum capacitors," CARTS'03, 23rd Capacitor and Resistor Technology Symposium, Scottsdale, AZ, 2003.